THE UNIVERSITY OF MICHIGAN
OCT 25 1963

REACTOR MATERIALS

A Quarterly Technical Progress Review

Prepared for DIVISION OF TECHNICAL INFORMATION, USAEC, by
R. W. DAYTON, E. M. SIMONS, and ASSOCIATES, BATTELLE MEMORIAL INSTITUTE

August 1963

FEATURE ARTICLE:

Nuclear Fuels from Civilian Power Reactors to Space Power

● VOLUME 6

● NUMBER 3

TECHNICAL PROGRESS REVIEWS

To meet the needs of industry for concise summaries of current atomic developments, the Atomic Energy Commission is publishing this series, Technical Progress Reviews. Issued quarterly, each of the reviews digests and evaluates the latest findings in a specific area of nuclear technology and science.

The four journals published in this series are:

Nuclear Safety, Wm. B. Cottrell, W. H. Jordan, and associates, Oak Ridge National Laboratory

Power Reactor Technology, W. H. Zinn and J. R. Dietrich, General Nuclear Engineering Corporation

Reactor Materials, R. W. Dayton, E. M. Simons, and associates, Battelle Memorial Institute

Reactor Fuel Processing, Stephen Lawroski and associates, Chemical Engineering Division, Argonne National Laboratory

Each journal may be purchased ($2.00 per year for subscription and individual issues $0.55) from the Superintendent of Documents, U. S. Government Printing Office, Washington 25, D. C. See back cover for remittance instructions and foreign postage requirements.

The views expressed in this publication do not necessarily represent those of the United States Atomic Energy Commission, its divisions or offices, or of any Commission advisory committee or contractor.

Availability of Reports Cited in This Review

Unclassified AEC reports are available for inspection at AEC depository libraries and are sold by the Office of Technical Services, Department of Commerce, Washington 25, D. C. Some of the reports cited are not available owing to their preliminary nature; however, the information contained in them will eventually be made available in formal progress or topical reports.

Unclassified reports issued by other Government agencies or private organizations should be requested from the originator.

Unclassified British and Canadian reports may be inspected at AEC depository libraries. British reports are sold by the British Information Service, 45 Rockefeller Plaza, New York, N. Y.; Canadian reports (AECL series) are sold by the Scientific Document Distribution Office, Atomic Energy of Canada, Ltd., Chalk River, Ontario, Canada.

Classified U. S. and foreign reports identified in this journal as Classified may be purchased by properly cleared Access Permit Holders from the Division of Technical Information Extension, U. S. Atomic Energy Commission, P. O. Box 1001, Oak Ridge, Tenn. Such reports may be inspected at classified AEC depository libraries.

REACTOR MATERIALS

A REVIEW OF RECENT DEVELOPMENTS

Prepared for DIVISION OF TECHNICAL INFORMATION, USAEC,
by R. W. DAYTON, E. M. SIMONS, and ASSOCIATES,
BATTELLE MEMORIAL INSTITUTE

● AUG. 1963
● VOLUME 6
● NUMBER 3

Foreword

Reactor Materials is one of a series of quarterly technical progress reviews broadly covering the field of nuclear science and technology. Under the auspices of the USAEC Division of Technical Information, *Reactor Materials* is prepared by Battelle personnel from worldwide literature. It covers properties, behavior, and fabrication processes of materials applicable to nuclear reactor components and associated equipment.

The reader will recognize that the scope of this Review is too broad to permit detailed coverage of every topic. Rather, the authors and editors attempt to combine the highlights of significant new developments into an information summary of current research for both management and the technical specialist. As a rule, enough of the results are presented to define the research and summarize the findings. For readers desiring more information on any particular topic, a complete set of references is provided at the end of each section.

Each quarter, a number of bibliographies, monographs, and books appear on subjects within the scope of *Reactor Materials*. Although the main purpose of this Review is to call attention to findings that are new and significant, such publications are noted in the text because they often represent excellent compilations of available information on important materials topics.

R. W. DAYTON
E. M. SIMONS
R. W. ENDEBROCK
Battelle Memorial Institute

Contents

FEATURE ARTICLE

Nuclear Fuels from Civilian Power Reactors to Space Power 1

by M. J. Whitman, Division of Reactor Development, USAEC

I FUEL AND FERTILE MATERIALS . . 11
Uranium Metal and Alloys 11
Plutonium 13
Dispersion Fuels 16
Coated-Particle Fuel Materials 19
Refractory Fuel and Fertile Materials . . 24
Basic Studies of Irradiation Effects on Fuel Materials 27
References 28

II MODERATOR MATERIALS 32
Graphite 32
Beryllium Metal and Alloys 33
Beryllium Oxide 37
Beryllium Compounds 38
Solid Hydrides 38
References 39

III NUCLEAR POISONS 41
Metallic Poisons 41
Dispersion Poison Materials 41
References 42

IV CLADDING AND STRUCTURAL MATERIALS 43
Corrosion 43
Metal-Water Reactions 49
Radiation Effects in Nonfuel Materials . . 49
Selected Mechanical Properties of Cladding and Structural Materials . . . 56
Selected Metallurgical Aspects of Cladding and Structural Materials . . . 57
Diffusion Studies 59
Ceramic Technology 59
References 60

V SPECIAL FABRICATION TECHNIQUES 66
Melting, Hot and Cold Working 66
Cladding 67
Welding and Brazing 71
Explosive Forming 72
Nondestructive Testing 73
References 74

Issued quarterly by the U. S. Atomic Energy Commission. Use of funds for printing this publication approved by the Director of the Bureau of the Budget on November 1, 1960.

DEPOSITED BY THE
UNITED STATES OF AMERICA

FEATURE ARTICLE

Nuclear Fuels from Civilian Power Reactors to Space Power*

By M. J. Whitman†

(Editor's Note: In the Feature Article below, Mr. Whitman points out that AEC-sponsored developments in nuclear fuels for earthbound power reactors are providing a head start toward solving the fuel problems for space power reactors. He discusses the available data on five high-temperature fuel materials that were originally considered for civilian power and now show real potential for space power applications.

In spite of this valuable background, there is much materials-development work to be done before nuclear power for space can become a reality. However, without this head start, achievement of the goal would be perhaps a decade further away.)

Introduction

The Reactor Fuel Development Program of the USAEC's Division of Reactor Development has, for well over a decade, been striving for improved fuels to enhance the economics of stationary and portable nuclear power systems. Some of the specific objectives have been to increase the operating temperature capabilities of the materials, increase allowable fuel burnup, ensure fission-product retention, and solve the compatibility problems that occur when temperatures are increased.

The requirements for nuclear fuel for civilian power reactors and for space-power reactors differ in emphasis rather than in kind. For civilian power reactors very high integrity is needed for very long times, with a less urgent requirement for extracting the maximum amount of heat from a given mass. The space reactor must provide the highest possible power density in order to minimize reactor weight. This leads to a requirement for very high fuel-element surface temperatures. The integrity and lifetime requirements for space reactors are relaxed for the rocket propulsion reactor, but the 10,000 hr of unattended lifetime needed for nuclear SNAP systems certainly requires reliable high-temperature operating characteristics and high burnup capability. It can also be predicted with some certainty that a first-stage nuclear rocket cannot release fission products; therefore the technology developed in this area for civilian power reactors is of value for space nuclear propulsion systems. The high operating temperatures both for space propulsion requirements and auxiliary power needs make compatibility of materials very important, and information derived from the civilian power program is directly applicable in many cases.

Thus the fine background of experience and research findings available from the civilian power program prevents space-reactor designs from being too unreasonable. It also provides for the recognition of problems in materials

*The views expressed in this article do not necessarily represent those of the U. S. Atomic Energy Commission or its appropriate office or division.

†Chief of the Reactor Experiments Branch, Division of Reactor Development, U. S. Atomic Energy Commission, Washington, D. C.

Table 1 PHYSICAL PROPERTIES OF SELECTED HIGH-TEMPERATURE FUEL MATERIALS

	UC	UN	UO_2	80 vol.% UO_2 in Nb	Nb–20 wt.% U
Density, g/cm³	13.6	14.3	10.9	10.5	9.1
Uranium density, g/cm³	13.0	13.6	9.6	9.2	1.8
Thermal conductivity, cal/(sec)(cm)(°C)	0.055 (room temperature)	0.04 (room temperature)	0.027 (70°C); 0.014 (400°C); 0.009 (800°C)	0.026 (room temperature)	0.041 (room temperature)
Melting point, °C	2400	2630	2750	2470	2300

capabilities and, in general, gives a note of realism to planning. As specific examples of the contributions made by civilian power to the space program, those nuclear fuels which were initially studied as possible power-reactor fuels and now show real potential for space power applications will be considered. Table 1 lists five fuels that were developed primarily with civilian power in mind. These are UC, UN, UO_2, a UO_2-niobium cermet, and a niobium-base alloy. Note that in every case the melting point is over 2000°C. In the following paragraphs these materials are discussed in some detail.

Uranium Dioxide [1–8]

The senior member of the uranium-compound fuel group is uranium dioxide. Serious development of this material as a fuel for power reactors began in 1955, when it was decided to fuel the Shippingport Pressurized-Water Reactor with Zircaloy-2-clad fuel rods composed of UO_2 pellets. Since that time it has been chosen as the fuel for all major power reactors now in operation. As would be expected, the research effort that has been expended on UO_2 during the past eight years has resulted in an extensive technological background.

The thermal conductivity of stoichiometric UO_2 decreases with increasing temperature, the conductivity being proportional to $1/T$, where T is the absolute temperature. Thus at room temperature the conductivity is 0.027 cal/(sec)(cm)(°C), whereas at 800°C it is about 0.009 cal/(sec)(cm)(°C). Further decrease occurs with increasing temperature, but there is evidence that an effective increase may occur as a result of the greatly enhanced radiation component of internal heat transmission. It must also be pointed out that there is experimental evidence which indicates that reactor irradiation of UO_2 lowers its thermal conductivity. This effect can, however, be almost completely annealed out by postirradiation heat-treatment. There are still some inconsistencies in thermal-conductivity values which require resolution.

The civilian power program has stimulated extensive work on the determination of mechanical, electrical, magnetic, and optical properties of UO_2, and, as a result, considerable data are available. Most of these data are summarized in Ref. 1.

In low-temperature air or oxygen, UO_2 absorbs oxygen; at temperatures over 100°C it is oxidized to a tetragonal oxide; and at temperatures above 250°C, a second oxidation step occurs in which tetragonal oxide is converted to orthorhombic U_3O_8. This conversion to U_3O_8 results in a volume change that is undesirable (a fourfold increase in surface area results). Therefore considerable effort has been devoted to stabilization of the oxide by additions of yttria for use in high-temperature oxidizing atmospheres. The chemical stability of UO_2 in high-temperature water and steam is good and is, in fact, a major reason for initial consideration of the compound as a reactor fuel. Although data on the high-temperature compatibility of UO_2 with structural materials are meager, it can be said that UO_2 is probably the least reactive of the fuels discussed in this article.

Irradiation studies on UO_2 have been many and varied. The following basic conclusions are repeated from the book, *Uranium Dioxide: Properties and Nuclear Applications*.[1]

1. Oxides having a fluoritelike structure (UO_2) exhibit a maximum stability to fission-fragment damage.
2. Fission-fragment damage appears to conform to theoretical predictions.
3. Fission-gas release from UO_2 occurs by a diffusional mechanism (effects of temperature and density variations are in agreement with such a mechanism).

Transverse cross section of UO_2 fuel pin

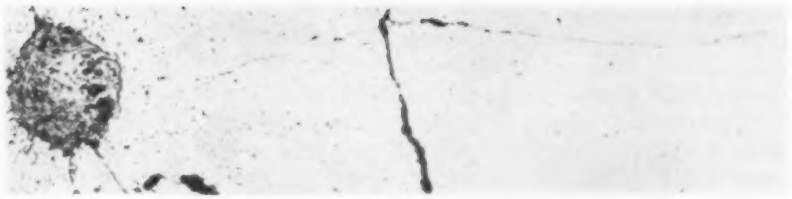

Center Edge

Composite of UO_2 fuel from center to edge with about 3 at.% of total uranium burned up

Typical UO_2 fuel pin

Fig. 1 Typical stainless-steel-clad UO_2 fuel pin.

4. UO_2, when fissioned up to about 5×10^{16} fissions/cm^3 (less than 0.001 per cent of uranium atoms), forms an equilibrium number of point defects and shows no apparent change in dimension or structure.
5. As fissioning progresses to 10×10^{20} fissions/cm^3 (about 4 per cent of uranium atoms fissioned), the stable condition of UO_2 is maintained, with fission fragments being incorporated in the oxide in some manner.
6. As fissioning proceeds beyond 10×10^{20} fissions/cm^3 (about 4 per cent of uranium atoms fissioned), the following happens:
   (*a*) Fission-gas diffusion rates and releases begin to increase in an approximate exponential manner.
   (*b*) Volume changes begin to occur.
   (*c*) Plastic flow of oxide begins.
   (*d*) Porosity begins to be apparent in the microstructure.

It must be emphasized that the conclusions have been based on irradiations performed at fuel-cladding surface temperatures below 1100°F (600°C).

On the other hand, pin type elements that contain sintered high-density UO_2 fuel pellets have been irradiated under thermal conditions that have caused grain growth or central-core melting of the oxide. Center melting of the fuel can be considered as the controlling or limiting feature on thermal rating of UO_2, although a number of experiments have indicated that center melting can occur without damage to the cladding. Figure 1 shows a typical stainless-steel-clad UO_2 fuel pin. A cross section of such a pin after irradiation shows the center melting or sintering. This can occur under high heat ratings.

Since release of fission gas is temperature dependent to a high degree, the use of UO_2 fuel particles in a graphite matrix for a high-temperature gas-cooled system is limited by the allowable release of contamination to the coolant. The development of coatings for the individual fuel particles is a promising technique for control of fission-product release. As discussed in Dr. Oxley's Feature Article in the May issue of *Reactor Materials*, investigations now in progress are designed (1) to improve coatings, (2) to obtain an understanding of coating failures, and (3) to evaluate thoroughly their potential.

Although UO_2 has been studied rather thoroughly under power-reactor conditions, there is a lack of data covering the higher temperatures needed for space power. For example, much work remains to be done to determine the compatibility of UO_2 with applicable structural materials, to look into radiation effects at really high temperatures, and to resolve the reported differences in thermal conductivity.

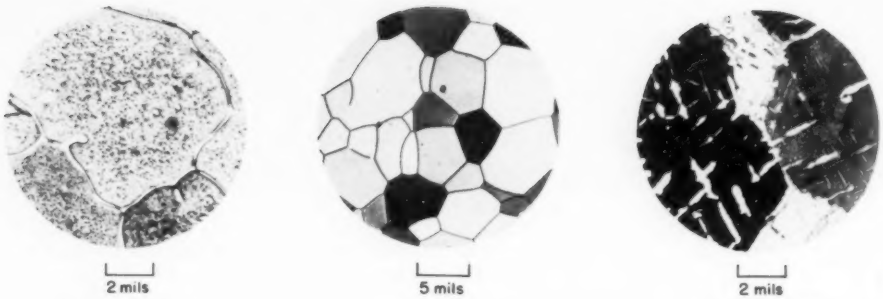

UC (4.6 wt.% C) UC (4.8 wt.% C) UC (5.0 wt.% C)

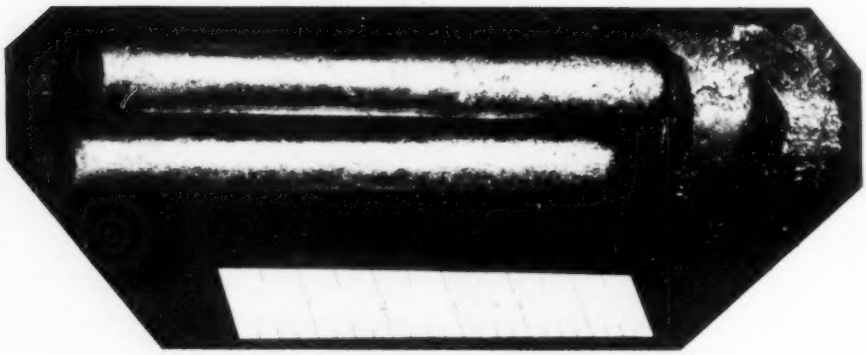

Typical ganged casting of UC

UC pressed and sintered bar

Fig. 2 Uranium carbide bodies and typical microstructures.

Uranium Carbide[9–18]

Uranium carbide as a fuel material was initially developed for sodium- or organic-cooled power reactors, but as more data became available the applicability to compact high-temperature liquid-metal-cooled reactors became apparent. In the five years since serious research and development was initiated on uranium carbide fuels, a large amount of invaluable basic and engineering data has been accumulated. Figure 2 shows examples of massive uranium monocarbide as well as typical microstructures.

The high uranium density of uranium carbide, 13.0 g/cm^3, is attractive whenever system weight is of importance, and the high thermal conductivity, 0.055 cal/(sec)(cm)(°C), makes possible the use of fuel pins with convenient diameters. The uranium carbides are quite hard at room temperature, but above 1000°C (2100°F) this hardness drops off rapidly. This indicates a loss in strength. It is interesting to note, however, that the addition of NbC, ZrC, TaC, or WC increases the high-temperature strength of uranium carbide appreciably.

Uranium carbide is a stable compound up to its melting point of 2400°C (4352°F), but it is a highly reactive material. It is incompatible with moist air at room temperature and fails catastrophically in water at 100°C. At 300°C, bulk pieces oxidize rapidly in oxygen, and powders are pyrophoric at room temperature. The carbides exhibit a low corrosion rate in organic coolants such as terphenyl, and even with water vapor present, corrosion is far from being catastrophic. They also have a negligible reaction rate with liquid metals of low oxygen content at temperatures below 1800°F. Refractory metals (niobium, tantalum, tungsten, and molybdenum) begin to decarburize the material at temperatures above 1200°C (2200°F). Steel will be carburized by hyperstoichiometric carbide (above 4.8 wt.% carbon) at temperatures above 800°C (1475°F), whereas stoichiometric material is relatively inert against iron alloys at 870°C.

Uranium carbides exhibit exceptionally good behavior in irradiation. Material that contains from 4.4 to 6.8 wt.% carbon has been irradiated under various conditions of burnup and temperature. Hyperstoichiometric carbide (5.2 wt.% carbon) has been irradiated in NaK to a burnup of 2.7% of the uranium atoms ($\sim 6.75 \times 10^{20}$ fissions/cm^3) at peak center temperatures of 1250°F (680°C) with a total density decrease of 4.4% and a fission-gas release of only that which could be accounted for by recoil. Stoichiometric fuel (4.8 wt.% carbon), sodium bonded to nickel cladding, has been irradiated to burnups of 1.82% of the uranium atoms ($\sim 4.7 \times 10^{20}$ fissions/cm^3) at peak center temperatures of 2100°F (1140°C) with a density decrease of less than 2% per atomic percent of uranium burnup. The fission-gas release was 0.18% of that produced.

In the case of hypostoichiometric carbide (<4.8 wt.% carbon), the presence of free uranium in the structure would be expected to harm the radiation stability of the material. However, after irradiation to burnups of 0.8% of the uranium atoms present (2.08×10^{20} fissions/cm^3) at peak center temperatures of 1800°F (980°C), only about 1.5% of the fission gas produced was released, and the density decrease was on the order of 2% per atomic percent burnup.

Higher temperature irradiations have been and are being performed with 5.2 and 6.8 wt.% carbon; however, the data have not as yet been fully evaluated. It might be reasonable to assume that, on the basis of hot-hardness data, uranium carbide might be expected to show some swelling with the buildup of fission products at temperatures above 2100°F (1140°C). This problem should be rather easily solved by the addition of other carbides as strengtheners.

The preceding paragraphs deal with massive carbide fuel covered with a cladding to retain fission products. One difficulty with this concept would be the release of fission products from the fuel. The coated-fuel-particle concept mentioned earlier is being investigated as a possible answer to this problem. The pyrolytic carbon coating deposited on the fuel particles shows potential as a barrier for fission-product release.

In order that uranium carbide may be exploited to its full potential, considerable effort is being devoted to determining its burnup and temperature capabilities. This includes determination of the compatibility of carbide fuels with refractory metals and their alloys and with various coolant media. In addition, the development of alloy carbides (uranium carbide plus a refractory-metal carbide) is considered important enough to warrant equal effort. The studies of coated particles will be continued in an attempt to provide particles that ideally will each be a self-sufficient fuel element able to retain fission gases.

Uranium Mononitride[19,20]

About two years ago an investigation was initiated under the Joint U. S.–Euratom Research and Development Program with the objective of studying uranium mononitride as a potential fuel for organic-cooled reactors. The results to date have been promising. Figure 3 illustrates a rod of massive uranium mononitride, typical microstructures, structure of both cast and powder-metallurgy material, and a specimen after being irradiated to a burnup of 2% of the uranium atoms. As is shown in Table 1, this material has the highest density of all uranium compounds (14.3 g/cm^3) and also the highest uranium density (13.6 g/cm^3). It melts at 4766°F (2630°C) and has a thermal conductivity of about 0.04 cal/(sec)(cm)(°C) at room temperature and 0.05 cal/(sec)(cm)(°C) at 800°C. (It will be noted that at 800°C its thermal conductivity is equal to that of uranium carbide.) Hot-hardness data indicate that there

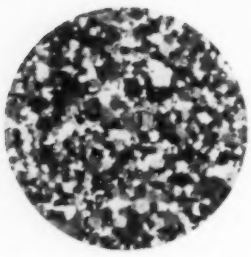

5 mils

UN isostatically hot pressed under 10,000 psi gas pressure at 2700°F in niobium cans

UN produced from uranium metal by arc melting under $^{2}/_{3}$ atm hydrogen–$18^{2}/_{3}$ atm nitrogen mixed gas pressure

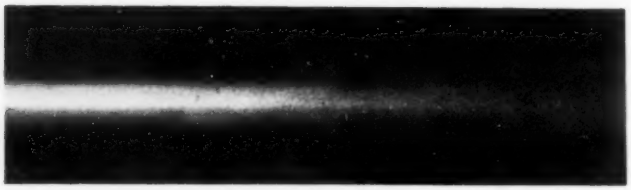

Sintered UN rod

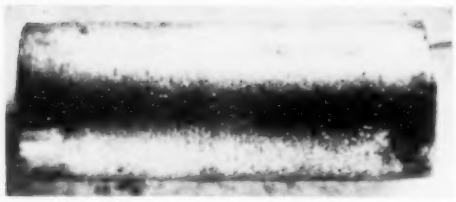

1/4 in.

Irradiated UN specimen; cladding has been removed

Fig. 3 Uranium mononitride bodies and typical microstructures.

is no serious drop in high-temperature strength up to 2000°F (1093°C). (Data above this temperature have not been obtained.)

The material is not pyrophoric as are some other uranium compounds, and it can be handled and stored in moist air with no difficulty. Even after 48 hr in 500°F deoxidized water, the total weight loss is reported as only 3.8 mg/cm^2.

Although no detailed compatibility results are available, studies of UN dispersed in matrices of molybdenum, stainless steel, and chromium indicate some degree of compatibility.

Specimens have been irradiated, unclad in NaK and clad with type 304L stainless steel, to burnups of 3.5% of the uranium atoms ($\sim 9.00 \times 10^{20}$ fissions/cm^3) at peak center temperatures of 2600°F (1425°C). The decrease in density was less than 2% per atomic percent uranium burnup. Although nitrogen undergoes an (n,p) reaction, the hydrogen so produced apparently causes no deleterious effects.

The results of studies to date are definitely encouraging, and therefore additional research is planned. Since the initial radiation tests were promising, immediate emphasis for the

next year should be on further study of basic and engineering properties, determination of the phase relations, and further study of preparation techniques. The emergence of this material as a strong candidate for high-temperature compact-reactor application could warrant a substantial increase in the development effort.

Cermets [21,22]

A relatively new concept in the use of ceramic fuel is represented by the cermet type of element. A composite that contains more than 50 vol.% of ceramic fuel in a metallic matrix is called a cermet. Figure 4 shows cermet fuels fabricated by two different techniques. The microstructure in part *b* of Fig. 4 is that of a fuel containing 80 vol.% UO_2 in a network of niobium, and it is prepared by isostatically hot-pressing niobium-coated UO_2 particles. The photomicrograph in part *a* of Fig. 4 illustrates a chromium-matrix cermet fuel fabricated by premixing and hot-pressing UO_2 and chromium powders.

The principal advantage of a UO_2 cermet, depending on the matrix material and temperature, is that the continuous network of metal improves the overall thermal conductivity of the fuel over that of bulk UO_2 by three to eight times. The metal skeleton or continuous network between the fuel particles provides toughness and strength that a completely ceramic type fuel does not possess. Oxidation tests have shown that, with an oxidation-resistant metal such as chromium as the matrix, oxidation of the UO_2 is only on the order of 8% after 144 hr in air at 1750°F. Ceramic UO_2 exhibited about 60% oxidation after a similar test.

Because of the structure of the body, any cladding compatible with UO_2 and the matrix metal should be suitable. Naturally it would be best to use the same metal for both cladding and matrix. With the metallic network, there are always points of good thermal contact between the cladding and the fuel core. A specimen of 80 vol.% UO_2 in niobium has been irradiated at surface temperatures that exceed 925°C to a burnup of about 3 at.% of the uranium atoms (5.3×10^{20} fissions/cm^3). The specimen exhibited a decrease in density of only 1.4%, which indicates exceptional irradiation stability.

Such a fuel type would seem particularly well adapted for thermionic application where the cladding and the matrix might be a good emitting material and for compact ground-base reactors where system weight is not as critical.

At this time one of the major disadvantages of this fuel type is that there is not enough known about its properties to predict its true potential.

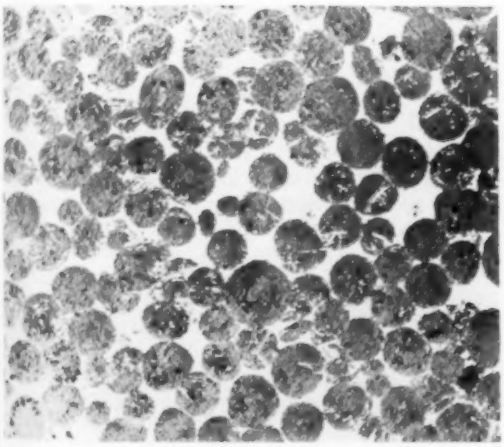

(*a*) UO_2-Cr cermet prepared by blending of metal and ceramic powder

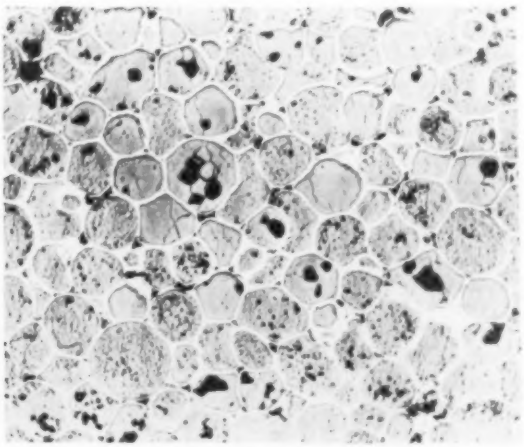

(*b*) UO_2-Nb cermet prepared from vapor-coated powder

Fig. 4 Cermet fuels (80 vol.% UO_2) prepared by two different methods.

Niobium-Base Uranium Alloy[23–27]

Although a metallic fuel is generally not thought of for application at the temperatures that are required for space power, there is one alloy that might be suitable in applications where surface temperatures would be on the order of 1800 to 1900°F. This fuel is a niobium-base alloy containing 20 wt.% uranium. Figure 5 shows graphically some of the excellent high-temperature properties of this alloy, and Fig. 6 shows the exceptional quality of a fuel pin after irradiation. This alloy has an ultimate tensile strength of 37,500 psi at 2000°F, and it requires a stress of 10,500 psi at 2000°F to produce a creep rate of 0.1%/hr. This indicates that there would not be much irradiation-induced swelling up to at least 2000°F. The niobium–20 wt.% uranium alloy has a thermal conductivity of 0.041 cal/(sec)(cm)(°C) at room temperature. This makes its conductivity about 60% that of niobium. However, at 1800°F the thermal conductivity decreases to where it is only about 25% that of niobium.

Tests in NaK and sodium at 1600°F show negligible corrosion of the alloy after 1000 hr. It must be remembered, however, that the presence of impurities such as oxygen in the liquid metal will markedly increase the corrosion rate of the alloy. The material exhibits a surprisingly low corrosion rate in 680°F water; however, it does oxidize quite rapidly when exposed at elevated temperatures to an oxidizing atmosphere. Although no high-temperature compatibility studies with potential cladding material have been performed, it is reasonable to believe that, at the operating temperatures dictated by irradiation effects, no serious problems would exist with refractory metals.

The niobium–20 wt.% uranium alloy has been irradiated to a burnup of 5.5% of the uranium atoms (2.49×10^{20} fissions/cm^3) at a surface temperature of 1900°F. The specimen exhibited a decrease in density of only 1.7%, and no effect of the irradiation could be noted visually.

It is believed that this alloy could well fill a particular fuel requirement (surface temperature about 2000°F); however, it will be limited to operation at a temperature only slightly above 2000°F. Ample engineering data have been accumulated, but there is a need for more irradiation testing in order to establish the temperature and burnup limitations.

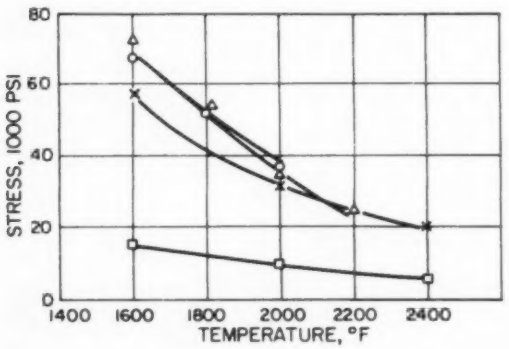

Fig. 5 Elevated-temperature strength of niobium-uranium alloys. △, 10 wt.% uranium and 3100 ppm oxygen; ×, 14.3 wt.% uranium; ○, 20 wt.% uranium; □, unalloyed niobium.

Future Work

If all technical reports and papers were collected which cover the fuel materials discussed in the preceding paragraphs, their combined weight would be a formidable payload

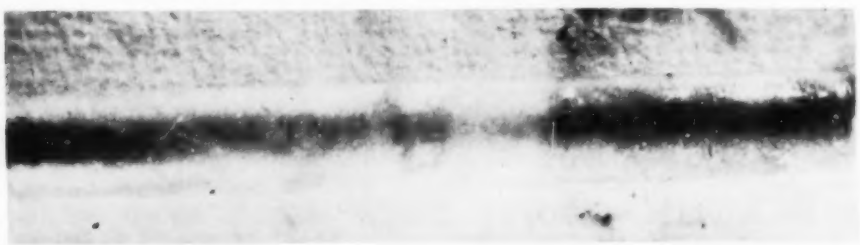

Fig. 6 Niobium–20 wt.% uranium fuel pin after ~0.6 at.% burnup at 1900°F.

for any of the existing rocket systems. These reports present a mass of data that is necessary if a fuel is to be thoroughly evaluated. However, even though these data may be considered as providing a 12-year jump on the development of space nuclear power systems, there is much materials-development work to be done before the goal of nuclear power for space is attained.

The AEC is cognizant of this and is attempting to plan integrated materials programs that will ultimately supply the answers. The rate of accomplishment of reactor fuels research and development will control the advance of space nuclear power technology. It will be less painful if the essential materials information is obtained as part of a general basic and applied fuel-development program instead of attempting to grind out empirical solutions to prevent slippage in reactor-fabrication schedules.

Acknowledgment

The author would like to acknowledge the assistance of R. F. Dickerson of Battelle Memorial Institute in the collection of data and in the preparation of this article.

References

1. J. Belle (Ed.), *Uranium Dioxide: Properties and Nuclear Applications*, U. S. Atomic Energy Commission, 1961 (available from the Superintendent of Documents, U. S. Government Printing Office, Washington 25, D. C., for $2.50, paperback).
2. W. D. Kingery, Thermal Conductivity: XIV, Conductivity of Multicomponent Systems, *J. Am. Ceram. Soc.*, 42: 617-627 (1959).
3. W. D. Kingery, J. Francl, R. L. Coble, and T. Vasilos, Thermal Conductivity: X, Data for Several Pure Oxide Materials Corrected to Zero Porosity, *J. Am. Ceram. Soc.*, 37:107-110(1954).
4. J. D. Eichenberg, P. W. Frank, T. J. Kisiel, B. Lustman, and K. H. Vogel, Effects of Irradiation on Bulk Uranium Dioxide, Fuel Elements Conference, Paris, November 18–23, 1957, TID-7546, pp. 616-716, March 1958.
5. J. A. L. Robertson, A. S. Bain, G. W. Allison, and W. H. Stevens, Irradiation Behavior of UO_2 Fuel Elements, in *Nuclear Metallurgy*, Vol. VI, pp. 45-70, American Institute of Mining, Metallurgical and Petroleum Engineers, New York, 1959.
6. A. S. Bain and J. A. L. Robertson, UO_2 Irradiations of Short Duration, Canadian Report CRFD-825, April 1959.
7. R. F. Dickerson, Battelle Memorial Institute, personal communications.
8. J. L. Bates, Thermal Conductivity of UO_2 Improves at High Temperature, *Nucleonics*, 19(9): 83-87 (June 1961).
9. F. A. Rough and W. Chubb, An Evaluation of Data on Nuclear Carbides, USAEC Report BMI-1441, Battelle Memorial Institute, May 31, 1960.
10. F. A. Rough and W. Chubb, Progress on the Development of Uranium Carbide-Type Fuels. Phase II on the AEC Fuel-Cycle Program, USAEC Report BMI-1488, Battelle Memorial Institute, Dec. 27, 1960.
11. F. A. Rough and W. Chubb, Progress on the Development of Uranium Carbide-Type Fuels. Final Report on the AEC Fuel-Cycle Program, USAEC Report BMI-1554, Battelle Memorial Institute, Nov. 17, 1961.
12. Atomics International, Annual Technical Progress Report, AEC Unclassified Programs, Fiscal Year 1960, USAEC Report NAA-SR-5350, Aug. 1, 1960.
13. L. Silverman, The High Temperature Chemical Reactivities of the Uranium Carbides, USAEC Report NAA-SR-Memo-4269, Atomics International, Aug. 19, 1959.
14. E. M. Murbach, The Oxidation of Uranium Carbides, USAEC Report NAA-SR-Memo-5494, Atomics International, July 14, 1960.
15. A. W. Hare and F. A. Rough, The Effect of High-Burnup Irradiation on Massive Uranium Carbide, USAEC Report BMI-1491, Battelle Memorial Institute, Jan. 6, 1961.
16. W. Sheridan, A. Strasser, J. Anderson, and K. Taylor, Carbide Fuel Development. Phase III Report, September 15, 1960–September 15, 1961, USAEC Report NDA-2162-5, Sept. 30, 1961.
17. D. I. Sinizer, B. A. Webb, and S. Berger, Irradiation Behavior of Uranium Carbide Fuels, USAEC Report NAA-SR-7248, Atomics International, Aug. 15, 1962.
18. B. W. Dunnington, Battelle Memorial Institute, personal communications.
19. D. L. Keller, Development of Uranium Mononitride. Quarterly Progress Report for October–December 1961, USAEC-Euratom Report BMI-X-186, Battelle Memorial Institute, Jan. 1, 1962.
20. D. L. Keller, Development of Uranium Mononitride. Quarterly Progress Report for January–March 1962, USAEC-Euratom Report BMI-X-197, Battelle Memorial Institute, Apr. 1, 1962.
21. S. J. Paprocki, D. L. Keller, G. W. Cunningham, and D. E. Kizer, Preparation and Properties of UO_2 Cermet Fuels, USAEC Report BMI-1487, Battelle Memorial Institute, Dec. 19, 1960.
22. D. L. Keller and D. Kizer, Battelle Memorial Institute, personal communications.
23. J. A. DeMastry, F. R. Shober, and R. F. Dickerson, Metallurgical Studies of Niobium-Uranium Alloys, USAEC Report BMI-1400, Battelle Memorial Institute, Dec. 7, 1959.

24. J. A. DeMastry, F. R. Shober, and R. F. Dickerson, Niobium–20 Wt.% Uranium, High-Temperature Metallic Fuel of the Future, *Nucl. Sci. Eng.*, 9(3): (March 1961).

25. J. A. DeMastry, D. P. Moak, S. G. Epstein, A. A. Bauer, and R. F. Dickerson, Development of Niobium-Uranium Alloys for Elevated-Temperature Fuel Applications, USAEC Report BMI-1536, Battelle Memorial Institute, Aug. 9, 1961.

26. J. A. DeMastry, A. A. Bauer, and R. F. Dickerson, Niobium-Uranium Alloys for Elevated Temperature Fuel Applications, *Trans. Am. Nucl. Soc.*, 5(1): (1962).

27. J. A. DeMastry, Battelle Memorial Institute, private communications.

Section

I

Reactor Materials

Fuel and Fertile Materials

Uranium Metal and Alloys

Unalloyed Uranium

The English[1] have developed a method for mathematically formulating sets of p-values into a single growth index that is descriptive of the amount of irradiation growth to be expected in uranium. For uranium rolled within controlled temperature ranges, the growth index decreases with increasing temperature of rolling for a given reduction in area.

Rolling at room temperature builds up a single (0 1 0) texture rapidly with increasing reduction. The compression texture is centered around the [1 1 4], [1 1 3], and [1 1 2] pole directions. After 40% reduction the [1 0 0] poles are aligned transverse to the rolling direction. The growth index in the rolling direction increases with increasing deformation.

Beta heat-treatment of rolled uranium, followed by water quenching, substantially reduces the growth index.

The texture of extruded uranium varies along the length of the rod. This variation can be correlated with microstructure. At the front of the rod, there is a duplex (0 1 0) (1 1 0) texture associated with warm extrusion. In the middle the texture is (1 3 0) to (1 3 1), which is more representative of a recrystallization texture. At high reductions and temperatures in extrusion, a predominantly (1 0 0) texture is developed. This leads to a negative growth index. A single beta-quenching operation reduces the texture in extruded uranium, particularly the [1 0 0] component. Subsequent beta quenching appears to regenerate the texture.

Small additions of molybdenum, chromium, and aluminum affect the hot-rolled textures of uranium by increasing the (0 1 0) tension texture and reducing the (1 1 0) texture. For the same temperature of hot rolling, the uranium alloys have a higher growth index than unalloyed uranium.

A summary report[2] that presents a critical discussion of the crystal structure of alpha uranium has been published by the English. Also presented is a compilation of crystallographic data and a tabulation of parameters descriptive of various features of the unit cell, together with values of functions required for the interpretation of crystallographic measurements.

A critical review[3] of investigations of the alpha-to-beta transformation in pure uranium also has been presented by the English.

The oxidation of uranium at an oxygen pressure of 10^{-3} torr has been investigated in the temperature range of 200 to 370°C.[4] During 12-hr oxidation tests, three different stages are observed. Transition points are marked by breaks in the kinetic curves. In all cases a UO_2 layer is formed initially on metallic uranium in the above-mentioned temperature range. At high temperatures a slight solubility of oxygen in uranium probably takes place (stage I). In the lower temperature range (197 to 232°C), UO_2 picks up oxygen during a linear oxidation stage (stage II). Finally a tetragonal oxide appears with the approximate composition $UO_{2.3}$ in another linear stage (stage III). In the medium temperature range (290 to 323°C), a mixed oxide consisting of UO_2 and a phase similar to U_3O_8 is found in stage III. After oxidation for several hours at 372°C, UO_2 is no longer detected. The curve representing the changes in resistance, which are due to oxidation for 12 hr, as a function of the oxidation temperature shows a sharp break at about 230°C that clearly reveals the change of the oxidation mechanism.

Evaluation of "sponge fuel" is continuing at United Nuclear Corp.[5] Sponge fuel consists of metallic uranium shot, tightly packed in a con-

tainer tube and infiltrated with sodium. Limited irradiation data are available; however, one fuel specimen examined after irradiation to 0.95 at.% burnup at 1200°F was found to be in excellent condition. It appears that in-pile sintering of uranium particles in sodium is slight at 1400°F and moderate at 1600°F.

At Nuclear Metals[6] the behavior of helium in uranium and in several uranium alloys was studied metallographically after room-temperature irradiation with alpha particles in a cyclotron. This was followed by various heat-treatments. The observed gas bubbles were classified in two classes differing in size, concentration, and mechanism of formation. These bubbles appear to resemble those resulting from fission-product gases in neutron-irradiated uranium. The findings of this study seem to be applicable to the understanding of the factors affecting bubble formation and thus the suppression of swelling in neutron-irradiated materials.

A recent review of uses for depleted uranium and nonenergy uses for natural uranium has been published by Battelle.[7] (M. S. Farkas)

Alpha-Phase Uranium Alloys

As part of the effort to develop a fuel material with improved irradiation behavior, Nuclear Metals[8] is involved in metallurgical studies on uranium–350 ppm iron–900 ppm aluminum alloys modified with various amounts of either silicon or chromium. Hot-hardness tests have shown that only 200 ppm of silicon is necessary to develop the maximum hardness in the beta-quenched alloy; no further benefit is obtained with additions of silicon to 1100 ppm. The hardening effect of silicon is markedly reduced by overaging at 600°C. In the aged material, silicon nevertheless has a hardening effect that increases as the silicon content increases to 1100 ppm. Additions of chromium increase the hot hardness of the beta-quenched uranium-iron-aluminum alloy to the level obtained with silicon additions. In contrast to the silicon additions, the chromium additions do not contribute to the hardness of the uranium-iron-aluminum alloy after overaging at 600°C.

Investigators at Argonne[9] studied the equilibrium microstructures and the kinetics of gamma decomposition of uranium-fissium alloys containing technetium. The technetium concentration in the fissium was 12.5 wt.%, and the uranium-fissium alloys that were examined contained from 3 to 10 wt.% fissium. The presence of technetium does not result in the presence of any new phases; it produces only minor changes in the phase relations and in the stability of the gamma-uranium solid solution. Studies of aging behavior and of the structure of slowly cooled alloys indicate that the gamma phase is slightly more sluggish in its transformation characteristics in the presence of technetium. On this basis it appears that the property measurements made earlier on uranium-fissium alloys that did not contain technetium can be reliably applied to true fissium alloys.

In another Argonne[10] study, the swelling of uranium and of a few selected uranium alloys on postirradiation annealing was investigated by utilizing density measurements in conjunction with the observation of pores in the microstructures of annealed specimens. Specimens were irradiated to about 0.3 at.% burnup in a constrained condition at approximately 275°C and were subsequently pulse annealed. The amount of swelling was found to be less than 1% for uranium specimens that were pulse annealed up to 75 hr at temperatures below 550°C; the amount of swelling, however, increased considerably on annealing at temperatures between 550 and 650°C. Specimens pulse annealed up to 75 hr at 618°C decreased in density by approximately 18%. The swelling was accompanied by the formation of bubbles on grain boundaries in recrystallized regions. The observations suggest that recrystallization is a necessary prerequisite for pronounced swelling in the alpha phase.

Uranium specimens pulse annealed up to 75 hr at temperatures between 650 and 750°C in the beta phase decreased in density by about 5%. Specimens annealed in the beta phase, in contrast with those annealed at 618°C in the alpha phase, were badly cracked and contained pores of a smaller diameter, which were uniformly distributed within the grains.

A specimen pulse annealed up to 16 hr at 822°C decreased in density by about 20%. This heat-treatment produced pores of large diameter located along grain boundaries, as well as pores of smaller diameter distributed uniformly within the grains.

Uranium alloys that contained between 1 and 9 wt.% titanium, zirconium, niobium, or molybdenum generally swelled more than pure uranium on pulse annealing up to 75 hr at 618 and 740°C. An exception was the behavior of a

uranium–4.0 wt.% niobium alloy that swelled less than uranium on annealing at 618°C. A carbon addition of 0.11 wt.% to uranium substantially decreased the swelling on pulse annealing up to 75 hr at 618°C, whereas the effect of 0.02 wt.% nitrogen was small; at 750°C, a nitrogen addition of 0.02 wt.% to uranium caused an appreciable increase in the swelling, but the effect of 0.11 wt.% carbon was slight.

A book[11] published recently contains papers dealing with irradiation effects on uranium and various metallic fuels. A monograph[12] has also recently appeared which contains papers concerned with grain size, phase-change measurements in uranium–0.5 wt.% chromium alloy, creep of alpha uranium, oxidation of uranium in CO and CO_2, and irradiation effects in alpha uranium. (M. S. Farkas)

Uranium-Steam Reaction

Argonne[13] has reported additional results of the reaction of solid uranium with steam by the volumetric method. Experiments have now been completed in which steam was reacted with pure uranium at temperatures up to 1500°C and uranium–1 wt.% aluminum alloy at temperatures up to 1400°C. Preliminary results indicate that aluminum has a negligible effect on the reaction. Results for pure uranium at 1400 and 1500°C do not appear to be consistent with results up to 1200°C. The parabolic rate constants are 50 to 100% higher than expected from previous results. For example, at 1400°C the parabolic rate constant was 1360 (ml STP/cm^2)^2/min; previous data would have suggested a value of about 700 (ml STP/cm^2)^2/min. Later analysis[14] indicated that the reaction at 1400 and 1500°C appeared to follow a rate law intermediate between a linear and a parabolic rate law, a ½-power law. Rates were independent of steam flow rate. However, visual observation of the reaction at these higher temperatures showed that the protective oxide developed cracks at random times. Cracking resulted in accelerated local reaction, local temperature excesses, and an overall higher reaction rate. (A. W. Lemmon, Jr.)

Plutonium

Plutonium Metal and Alloys

Investigators in the United Kingdom report[15] that the resistivity of plutonium increases as a result of self-induced radiation damage while being held at liquid-helium temperatures. A somewhat lower rate of radiation-damage accumulation at liquid-hydrogen temperature indicates that, even at this low temperature, a certain amount of annealing seems to occur.

Table I-1 LATENT HEAT OF TRANSFORMATIONS IN UNALLOYED PLUTONIUM[17]

Phase transformation	R. G. Loasby, Aldermaston		Mound Laboratory	
	Temp., °C	Latent heat, cal/gram-atom	Temp. on heating, °C	Latent heat, cal/gram-atom
$\alpha \rightarrow \beta$	119	803 ± 10	127	810 ± 5
$\beta \rightarrow \gamma$	204	152 ± 15	207	124 ± 12
$\gamma \rightarrow \delta$	311	125 ± 5	320	136 ± 7
$\delta \rightarrow \delta'$	458	30 ± 10	460	25 ± 8
$\delta \rightarrow \epsilon$	480	444 ± 10	481	441 ± 8
ϵ liquid	638	693 ± 10	640	655 ± 6

Unalloyed plutonium can be rolled at temperatures high in the beta phase (175 to 200°C), according to Hanford,[16] provided care is taken to prevent an inadvertent beta-to-alpha transformation. A 2- by 2- by 0.135-in. slab was rolled to a thickness of 0.018 in. in 13 passes in a 4-high rolling mill. Rather severe surface veining was observed in the stock after it was cooled to room temperature. A technique for rolling an aluminum–1.8 wt.% plutonium alloy to 0.030-in. foil is described.

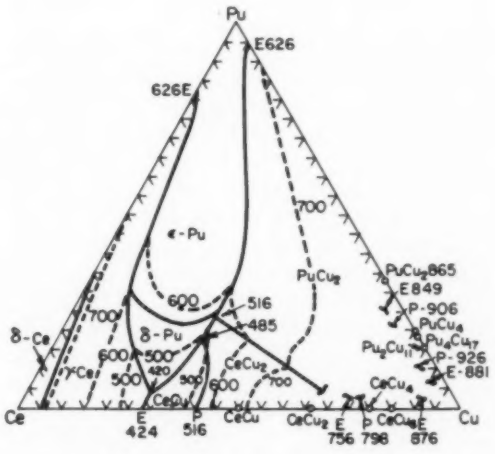

Fig. I-1 Tentative plutonium-cerium-copper phase diagram.[17]

The heats of transformation in unalloyed plutonium have been measured at Mound,[17,18] using a high-temperature calorimeter. As shown in Table I-1, the data compare favorably with those obtained by U. K. investigators.

Plutonium-cerium-copper alloys are being investigated as possible molten-plutonium reactor fuels. A partial tentative phase diagram for the alloy system is presented in Fig. I-1. The viscosity of a filtered plutonium–56.2 at.% cerium–24.2 at.% cobalt alloy was measured at temperatures from 444 to 931°C. The data, as plotted in Fig. I-2, agree with previous measurements made on an unfiltered sample (circled points).

The approximate densities of alloys in the plutonium-cerium-cobalt system have been measured at Los Alamos[19] and are shown in Fig. I-3.

Los Alamos[19–21] has also reported results of investigations of a number of binary plutonium-alloy systems. The solubility of carbon in liquid plutonium has been measured over the temperature range of 700 to 950°C. The solubility increases from 690 ppm (by weight) carbon at 700°C to 2350 ppm at 950°C. The data fit the empirical equation

$$\log N_c = 0.50 - 2.3 \times 10^3 \, T^{-1}$$

where N_c is the mole fraction of carbon and T is the temperature in degrees Kelvin.

Solubility of silicon in liquid plutonium was found to be 3.75 at.% at 614°C, 4.9 at.% at 719°C, and 8.1 at.% at 832°C. The maximum solubility of silicon in delta plutonium is estimated to be 1.2 ± 0.1 at.% at 495°C.

In studies of the plutonium-indium system, the congruent melting temperature of the $PuIn_3$ phase has been tentatively placed at 1225 ± 10°C. A eutectic reaction was found to occur between PuIn and Pu_3In at 1068 ± 10°C and 59 at.% indium. The eutectoid decomposition of the delta phase occurs slowly, and increasing the indium content increases the sluggishness of the reaction. The equilibrium temperature for the eutectoid reaction lies between 275 and 300°C.

Investigations of binary plutonium–rare earth systems indicate that no intermediate phases occur between plutonium and samarium, europium, gadolinium, terbium, dysprosium, holmium, erbium, thulium, ytterbium, and lutetium. Europium and ytterbium are both immiscible in liquid plutonium. Europium, ytterbium, and gadolinium appear to be the only rare earths that are not dissolved sufficiently in delta plutonium to permit retention of the delta phase to room temperature. Maximum terminal solid solubility of each of the rare earths in plutonium from praseodymium to lutetium (with the exception of europium and ytterbium) is from 2 to 3 at.%. The solubility limit of plutonium in the rare earths is about 20 at.%. An addition of 5 at.% praseodymium to plutonium lowers the

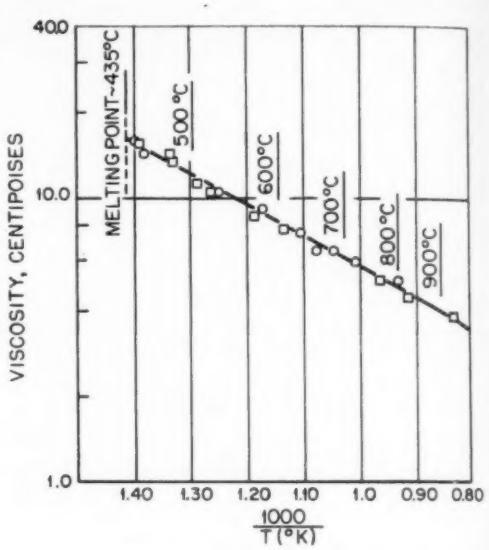

Fig. I-2 Viscosity of a plutonium-cerium-cobalt eutectic alloy.[18] ○, unfiltered alloy; □, filtered alloy.

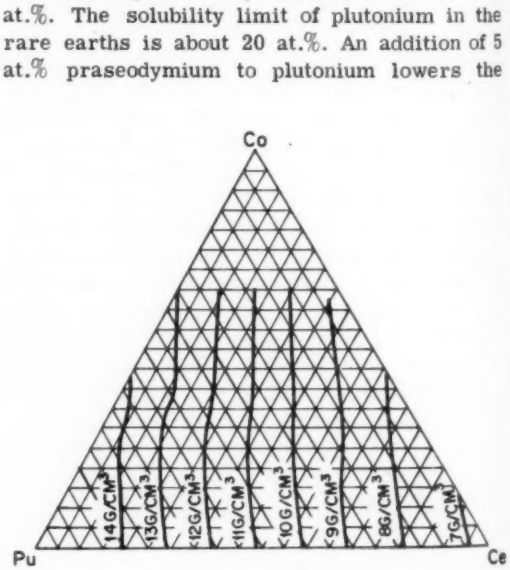

Fig. I-3 Isodensity lines for the plutonium-cerium-cobalt system at room temperature.[21]

melting point to a eutectic temperature of 627°C. The solidus temperatures then rise with increasing atomic number rare-earth alloying element (5 at.% additions) to a maximum of 645°C for holmium and erbium and decrease to 634°C for lutetium. The solidus changes from a eutectic to a peritectic horizontal at gadolinium.

Table I-2 THERMAL CONDUCTIVITY OF URANIUM–20 WT.% PLUTONIUM–5 WT.% FISSIUM (HIGH ZIRCONIUM) ALLOY[23]

Temperature, °C	Thermal conductivity, cal/(sec)(cm)(°C)
200	0.041
300	0.047
400	0.054
500	0.060
600	0.066
700	0.071*

*Extrapolated.

Studies of uranium-plutonium and uranium-plutonium-fissium alloys are continuing at Argonne.[22] Specimens of uranium–10 wt.% plutonium–10 wt.% fizzium (fizzium denotes fissium of higher than normal zirconium content) and uranium–15 wt.% plutonium–10 wt.% fizzium exhibited little dimensional changes when cycled 100 times between 450 and 700°C. A similarly cycled uranium–10 wt.% plutonium alloy, on the other hand, lengthened 30%, swelled to a 7% diameter increase, and decreased 35% in density. The tensile strength of the uranium–10 wt.% plutonium alloy was found to be 35,000 psi at room temperature and 19,000 psi at 502°C. Brittle failures occurred at both temperatures. Rockwell C hardness values of 30 to 40 were obtained for uranium–20 wt.% plutonium–10 wt.% fissium and uranium–20 wt.% plutonium–10 wt.% fizzium alloys. Impact tests showed that both alloys have very low shock resistance in the as-cast condition.

Results[23] of measurements of thermal conductivity of a uranium–20 wt.% plutonium–5 wt.% fissium alloy are shown in Table I-2.

In studies of the effects of plutonium additions to alpha uranium on the lattice constants, it was found[24] that a_0 and c_0 increased with increasing plutonium and that b_0 decreased with increasing plutonium. For uranium–15 wt.% plutonium, a_0 = 2.8625 A, b_0 = 5.8562 A, and c_0 = 4.9631 A.

The results of U. K. irradiations of uranium-molybdenum-plutonium alloys at surface temperatures of 600°C have been reported at a recent American Nuclear Society topical meeting at Hanford.[25] Data are shown in Table I-3.

In the issue before last, an error in the "Plutonium Metal and Alloys" subsection was carried over from the source reference. In the table entitled "Exposure of Test Container to Uranium–4.5 At.% Plutonium–20.4 At.% Manganese Fuel at 900°C for 2 Hr," the exposure time was 200 hr instead of 2 hr.

(V. W. Storhok)

Plutonium Compounds

More attention is being directed toward the best fast-breeder-fuel concept. A recent report[26] delves extensively into the relative advantages of a (Pu,U)C loading as opposed to a $(Pu,U)O_2$ fuel.

Argonne[14] has determined the electrical resistivity of PuC to be 250 μohm-cm at room temperature, compared with a value of 41 μohm-cm for UC. The same source reports a reaction between PuC and tantalum at 1535°C when sintering crushed material. Mulford et al.[19]

Table I-3 IRRADIATION OF URANIUM-MOLYBDENUM-PLUTONIUM ALLOYS[25]

Composition, at.%				Density, g/cm³		Increase in volume (ΔV), %	Burnup, Mwd/metric ton	$S = \frac{\Delta V}{\%\ \text{burnup}}$	Rating, watts/g
U^{238}	Mo	Pu	U^{235}	Before irradiation	After irradiation				
66.9	15.0	7.6	10.5	17.72	11.52	53.8	7,630	51	73
66.9	15.0	7.6	10.5	17.69	9.77	81.1	14,760	55	103
69.6	15.0	14.9	0.5	17.78	10.02	77.4	8,170	70	78
69.6	15.0	14.9	0.5	17.78	9.28	91.6	14,880	59	110
57.2	25.0	7.5	10.4	17.06	13.49	26.5	7,880	25	75
57.2	25.0	7.5	10.4	17.05	11.73	45.4	14,440	29	103
59.7	24.9	15.0	0.4	16.99	15.22	11.6	8,720	10	85
59.7	24.9	15.0	0.4	17.03	10.42	63.4	16,300	41	119

found that PuC and PuN are mutually soluble as solids and that significant solid solubility exists in the pseudobinary system PuC-PuN. Kruger[27,28] has recently expanded his work on PuC to extend further the original phase diagram prepared by Los Alamos. The French have prepared a publication[29] on the high volatility of both PuC and PuN from a general viewpoint. Argonne workers report[30] that (U,Pu)C is a stoichiometric compound as regards carbon content in the range 0 to 35 at.% plutonium. In this range, increased plutonium content increases the unit cell size of the solid solution. Above 35 at.% plutonium the structure shows larger metal-to-carbon ratios in the form of a defect structure wherein a_0 decreases with increased plutonium content.

The nitride of plutonium has been shown to melt congruently at a temperature greater than 2770°C, and the true decomposition pressure exceeds 370 psi.[19] D. F. Carroll has prepared a summary of work on PuN, including synthesis and properties.[31] Properties include a coefficient of linear thermal expansion of $13.8 \times 10^{-6}/°C$, measured by X-ray techniques from 0 to 800°C. A hardness value of 370 kg/mm^2 was reported, but this was determined on material containing free plutonium.

Nuclear Materials & Equipment Corp.[32,33] has shown that nearly 100% yield can be obtained by using an argon-nitrogen atmosphere to produce spheroidized $(U,Pu)O_2$. However, numerous voids existed within individual particles for a UO_2–20 wt.% PuO_2 feed.

The $(U,Pu)O_2$ elements that contain considerable PuO_2 segregation have been found satisfactory for in-reactor operation. Microscale homogenization occurred in the high-temperature regions of such elements irradiated in the Plutonium Recycle Test Reactor, but gross segregation was not decreased.[34] Some elements showed a 0.0005-in.-thick reaction zone with the Zircaloy cladding. These tubes were UO_2–2.57 mole % PuO_2 irradiated to an average exposure of 9100 Mwd/ton.[35] Radial plutonium migration was indicated since hot spots were not in the geometric center.

Two groups of investigators[36,37] have reported on the fabrication and compatibility of PuO_2–stainless-steel cermets. Los Alamos[41] found major reaction zones between PuO_2 and AISI type 302B stainless steel. This was attributed to the high silicon content. Hanford has prepared zirconium–21.4 vol.% PuO_2 by arc melting to produce a continuous zirconium matrix.[35]

Further investigation[38] of the plutonium-oxygen phase diagram indicates that between the oxygen-to-plutonium ratios of 1.0 and 1.5 there exists a two-phase field, PuO_2 plus β Pu_2O_3. A tentative melting point for PuO has been observed at approximately 1800°C. PuO_2 has been shown to be a *p* type semiconductor, and most resistivity and thermoelectric properties for the oxides $PuO_{1.77}$ to $PuO_{2.0}$ have been tabulated.[39]

Attempts to prepare PuP by hydriding plutonium, decomposing, and reacting with red phosphorus were unsuccessful,[40] although plutonium and phosphorus were combined by arc melting.

Mound[18] reports that 0.533% of the plutonium content in a silicate glass is leached out in water after 19 months. Increasing the sodium oxide content of the glass increases the solubility of the PuO_2.

Two excellent reports on the state of the art of plutonium-compound technology were recently issued.[25,41] (W. M. Pardue)

Dispersion Fuels

Sample fuel plates have been prepared by Phillips[42] with cores containing UAl_3 powders blended with X8001 or 6061 aluminum-alloy powders and clad with X8001 or 6061 aluminum, respectively. The cores contained 35 wt.% fully enriched uranium and 0.19 wt.% B_4C, and they have been irradiated to 25% burnup in the Materials Testing Reactor. Tensile tests of various compositions of these fuel elements have been performed at ambient temperatures, 200 and 400°F in the unirradiated condition. Also, cladding materials of approximately the same thickness as the fuel plates have been tested and are listed in Table I-4. Generally, the data indicate that strength and ductility decrease with increasing temperature for these sandwich-construction type fuel plates.

Hanford[25] has been interested in making dispersions of spherical PuO_2, UO_2, or PuC grains in a metallic matrix such as zirconium-niobium base alloys. These fuel elements are of potential interest for reactors having a high specific power output. The PuO_2 and UO_2 grains are spheroidized on a vibratory screen or in a vibratory cylinder and sintered to 95% of the

Table I-4 TENSILE PROPERTIES OF VARIOUS UNIRRADIATED SAMPLE FUEL PLATES AND CLADDING MATERIALS[42]

Item	Cladding	Core	Room temperature			200°F			400°F		
			Tensile strength, psi	Yield* strength, psi	Elongation,† %	Tensile strength, psi	Yield* strength, psi	Elongation,† %	Tensile strength, psi	Yield* strength, psi	Elongation,† %
1	15 mils Al	25 mils 54 wt.% UO_2 + Al	12,800	12,700	0.6	12,100	12,000	0.5	10,000	9,400	0.8
2	15 mils Al	25 mils 25 wt.% UAl alloy	16,300	9,300	18.4	13,700	8,800	15	10,200	5,700	
5	15 mils Al	15 mils 30 wt.% UO_2 + Al	14,600	12,600	1.8	11,200	9,700	1.6	8,800	8,400	1.1
14	15 mils Al	20 mils 22.7 wt.% UO_2 + 0.12 wt.% B + Al	16,100	14,700	4.1	15,300	14,300	2.5	11,300	9,600	2.4
19	15 mils Al	20 mils 18 wt.% UAl alloy	16,800	9,300	24.3	13,900	7,800	20.8	10,800	6,700	21.1
47	15 mils Al	20 mils 22 wt.% U_3O_8 + Al	18,500	17,000	1.4	15,400	13,900	1.8	12,100	9,700	2.3
53	15 mils 6061	20 mils 19 wt.% UAl alloy	39,800	27,000	12.2	36,200	30,400	9.9	30,700	28,000	9.2
55	20 mils 6061	10 mils 45 wt.% U + 3 wt.% Si + Al	43,100	38,000	7.9	37,500	36,700	2.2	33,000	30,000	2.0
60	8 mils X8001	16 mils 32 wt.% UAl alloy	15,700	13,300	5.6	13,300	9,600	3.2	10,000	8,500	2.9
84	15 mils 1100	20 mils 34 wt.% UAl_3 + Al	18,300	17,300	0.7						
113	15 mils X8001	20 mils 50 wt.% UAl_3 + 19 wt.% B_4C + 6061-T6	15,600			15,000	14,900	0.6			
114	15 mils 6061-T6	20 mils 50 wt.% UAl_3 + 19 wt.% B_4C + 6061-T6	32,000	31,000	1	30,000	28,700	0.9			
		50 mils 1100 Al HT at 600°F	13,300	5,800	37.9	10,800	5,900	37.9			
		50 mils 1100 Al HT at 1000°F	13,500	6,600	35.6	12,700	8,000	33			
		50 mils 6061-T6	49,700	44,200	13.1	45,500	41,200	11.1			
		50 mils APM 257	43,300	36,700	6.5	37,200	30,400	3.2			

*Values are for the 0.2% offset yield strength.

†Values are for the percent elongation in a 1-in. gauge length.

theoretical density. To eliminate the potential reaction between the PuO_2 and UO_2 fuel particles with the zirconium-matrix metal, steps have been taken to coat the PuO_2 and UO_2 with niobium, nickel-copper (double layer), molybdenum, and chromium. In connection with this work, effort is also being directed toward producing a niobium-zirconium-vanadium alloy that will have good mechanical properties and better nuclear characteristics than stainless steel. The best results to date have been obtained with zirconium–2 wt.% niobium–2 wt.% vanadium and zirconium–3 wt.% niobium–3 wt.% vanadium.

Battelle[43] has recently published results from high-temperature irradiation tests of UO_2 cermet fuels. Fuels investigated were niobium-clad niobium cermets and type 430 stainless-steel-clad molybdenum and chromium cermets. All cermets contained 80 vol.% of 20% enriched UO_2 and were prepared either by vapor-deposition techniques or from the powders. All were densified and clad by gas-pressure bonding. Because of a probable weld failure in both capsules, irradiation temperatures were higher than the intended 0.6 of the matrix melting point, and all the chromium cermets in one capsule and all the cermets in the other capsule were lost. The remaining specimens were given a postirradiation dimensional and metallographic examination. The niobium-clad niobium-UO_2 cermet exhibited excellent stability at an estimated center-line temperature above 2500°F. Figure I-4 shows the continuous niobium phase surrounding every UO_2 particle. No evidence of damage to the niobium network was observed following a calculated burnup of about 4 at.% with a measured density decrease of only 1.4%. On the basis of the two UO_2-molybdenum specimens metallographically examined, this cermet shows promise as a high-temperature fuel. Although the excessive heating caused the molybdenum-UO_2 cermet to melt partially, areas only a distance of two UO_2 particles away from the molten zone were completely intact, and they exhibited no evidence of damage from the adverse conditions of the irradiation. Figure I-5 represents the as-polished structure of the continuous molybdenum region away from the melted zone.

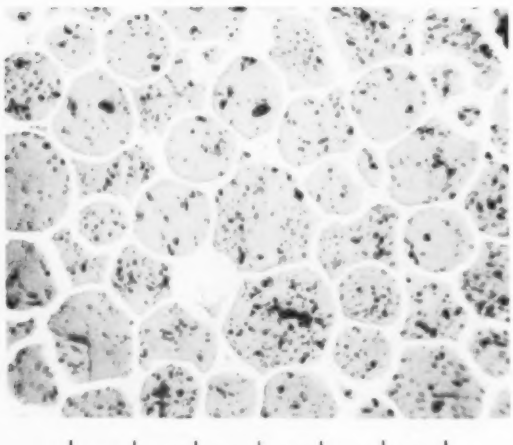

Fig. I-4 As-polished microstructure of 80 vol.% UO_2–niobium cermet clad with niobium after irradiation above 2500°F to 4 at.% burnup.[43]

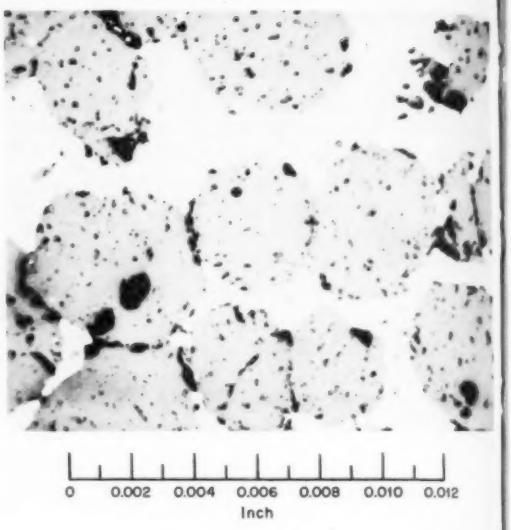

Fig. I-5 As-polished microstructure of 80 vol.% UO_2–molybdenum cermet clad with type 430 stainless steel after irradiation above 2500°F to 4 at.% burnup.[43]

A method based on judicious selection of a metal and an oxide that will react exothermally to produce desirable ceramic and metallic phases along with sufficient heat to sinter or fuse these phases is being investigated.[41] The system currently receiving the most attention for fuel elements is a cermet of U_3O_8 in aluminum. Compacts that contained 52 to 68 vol.% U_3O_8 in aluminum were cold pressed and sin-

tered. During the heating of the compacts, aluminum sweated out of the samples at temperatures near its melting point. When specimens were heated to 1600 to 1800°F, rapid and spontaneous reactions were observed. With identical pellets, these reactions occurred at approximately the same temperatures in air, in vacuum, or in inert atmosphere. Surface temperatures of 4000°F were reached for pellets without insulation. Some material loss generally occurred as a result of the violence of the reaction. X-ray analysis indicated that UO_2, UAl_2, UAl_3, and Al_2O_3 were produced from the reaction.[41] (D. L. Keller)

Coated-Particle Fuel Materials

Preparation and Fabrication

Oxide-Base Fuel. A summary[41] of the status of coated-oxide-fuel development was recently presented by the AEC's Division of Reactor Development. Coating studies on UO_2 and PuO_2 were reviewed. The results of several Euratom programs[44a–46] on coated oxide fuel also became available this quarter. In the CEN studies, metallic deposits of molybdenum, chromium, nickel, and iron from 2 to 15 μ in thickness were applied by vacuum evaporation to spherical UO_2 particles. The chromium-coated particles were dispersed in an iron matrix and subsequently swaged.[44a] In work by the Belgium Society of Studies of Research and Applications for Industry,[45,46] niobium coatings were applied to uraniferous ceramic particles by halide reduction. The U. S. Bureau of Mines at Albany, Oreg., revealed its studies on tungsten coating on gadolinium oxide particles for cermet applications,[47] and a recent patent[48] was awarded to the AEC which involved the coating of oxide particles while in suspension in a halide melt.

The major emphasis in the Battelle coating studies[49–51] during the past three months has been on the vapor deposition of BeO. Analysis of leaching data for various samples of BeO-coated UO_2 indicated a significant correlation between the calcia content of the coatings and their failure in acid leaching. The best coatings had calcium contents below 200 ppm, whereas all samples with higher values suffered more severe failure in the leach tests. Correlation of leach data with silica content was less significant, and there was no correlation with alumina content. On the basis of this information, a new coating reactor design was completed which uses only high-purity alumina as the construction material.

In petrographic studies, BeO coatings deposited at 1400°C revealed a tendency for orientation of the *c*-axis of the BeO crystals along the particle radius, i.e., the growth direction. In coating layers deposited at lower temperatures (1250 to 1300°C), this orientation was less apparent. In some cases crystals from one layer are continued into the next, and this verifies equiaxial growth. Some coating layers show a radial crystal structure, i.e., narrow crystals elongated in the direction of the radius, whereas other layers consist of more nearly equiaxial crystals. The data at present are too limited to permit correlation and prediction of crystal habit from processing conditions. It was also found that the BeO coatings are somewhat sensitive to thermal shock, and they tend to crack if heated too rapidly to elevated temperatures. Apparently, although a 50°C/min temperature rise is too rapid, a 10°C/min temperature rise was satisfactory for the particular sample studied.

The oxidation resistance of Al_2O_3 vapor-deposited coatings on UO_2 particles has been recently summarized.[52] The oxidation resistance of the high-temperature coatings (deposited at 1200 and 1400°C) is superior to that of coatings deposited at lower temperatures (1000°C). The oxygen permeability through 40-μ Al_2O_3 coatings on 100-μ spherical UO_2 particles was determined and correlated with the following equations:

For coatings at 1000°C,

$$P = 3.16 \times 10^{-5} \exp(-197{,}000/RT)$$

and for coatings at 1300 to 1400°C,

$$P = 6.3 \times 10^{-4} \exp(-42{,}000/RT)$$

where the permeability P is expressed in grams of oxygen per cubic centimeter per second. Extrapolation of the measured data indicates that particles coated at 1300 and 1400°C should have satisfactory oxidation resistance for several thousand hours at temperatures of 1100°C or lower in flowing oxygen at 1 atm of pressure.

A summary of a preliminary study that included the use of coated UO_2 particles in the

preparation of niobium-matrix fuel elements was also presented by Battelle.[44b] Values of the thermal conductivity and electrical resistivity were obtained, but the relative merit of using coated UO_2 was not clearly established. It was suggested that the advantages would be most pronounced at oxide loadings higher than those studied.

Although there appear to be no significant problems associated with the dispersion of oxide-coated fuel particles in graphite matrices, a completely satisfactory method for the preparation of oxide-matrix fuels containing coated particles has not yet been found. This is in part due to the fact that satisfactory-quality BeO-coated fuel has not generally been available for matrix studies. Battelle has reported[50,51] on the use of $Be(OH)_2$ burnout layers applied by pelletizing techniques to provide volume for oxidation of the UO_2 in case of localized failure. The original fuel particles, Lot 855C, consisted of 127-μ dense UO_2 coated with 60-μ vapor-deposited, 1400°C BeO films. These particles were subsequently coated by pelletizing with a 112-μ-thick $Be(OH)_2$ burnout layer and with a 190-μ thickness of UOX-grade BeO. The composite particles were compacted uniaxially at 40,000 psi to form cylinders 0.3 in. in diameter and 0.3 in. high. The compacts, together with the as-received Lot 855C particles, were heated for 2 hr in flowing hydrogen at temperatures of 1425, 1540, or 1650°C and were evaluated by leaching and neutron activation. The results shown in Table I-5 indicate that the vapor-deposited coatings were not damaged mechanically by their incorporation into BeO matrices. Although vapor-deposited coatings have been made which retain fission products at moderate temperature levels, they have been heavily contaminated with impurities which lead to coating failure at the high temperatures necessary for matrix sintering.

Another approach under study by Battelle[49-51] is to fabricate BeO matrix bodies using pressure-bonding techniques and thereby obtain matrix densification at lower temperatures. Burnout layers or void volumes also seem to be necessary, since one particle failure in a fully dense matrix seems to result in further matrix damage as a result of fuel oxidation and volume increases. Burnout layers of molybdenum and carbon have been applied to BeO-coated UO_2 particles before bonding, but oxidation of these materials at 650°C resulted in a high degree of fragmentation that apparently progressed from the specimen surface. The latest modification involves the use of a porous fuel substrate overcoated with a dense vapor-deposited film. The matrix material is then pelletized over the coated particles, and the pelletized material is bonded under conditions so that the matrix is densified but the fuel substrate retains its original porosity. The evaluation results for these materials are not yet available.

Carbide-Base Fuel. The loading of the first fuel charge in the Dragon reactor is envisaged during the first half of 1964. Because of this delay it appears that coated-particle fuels may be employed in the initial charge, and a number of subcontractors have been carrying out research in support of this goal, including the CEA at Saclay, RAE at Farnborough, Metallwerk Plansee at Reutte, SGAE at Seibersdorf, and the CEN at Mol. Data have been presented[53]

Table I-5 EFFECTS OF SINTERING TEMPERATURE ON LOT 855C BeO-COATED UO_2 PARTICLES AND FUELED COMPACTS[51]

Sample	Maximum sintering temperature,* °C	UO_2 removed during HNO_3 leaching,† wt.%		Xe^{133} release in 1 hr at 1100°C after neutron activation, ppm
		1 hr	8 hr	
As-received particles		0.002	0.037	485
	1425	0.014	0.257	707
	1540	0.082	0.584	157
	1650	0.010	0.010	15
Compacts	1425	0.008	0.040	470
	1540	0.129	0.132	53
	1650	0.257	0.343	847

*For 2 hr in flowing hydrogen.
†In 8*N* HNO_3 at 95°C.

on densities, interlayer spacings, and apparent crystallite sizes of pyrolytic carbon (PyC) coatings prepared at Farnborough. The dependence of the rate of deposition on the length of run was investigated by Metallwerk Plansee, and the rate was found to be essentially constant with time. Since the surface area of the particles changes appreciably during deposition, such a dependence is rather interesting. Investigation of the consolidation of coated particles into graphite matrices is being carried out at Farnborough and Winfrith. Impregnation of the bodies by gas cracking is included.

Coating studies at Battelle[49–51] on PyC coatings involved the preparation of porous carbon deposits, the codeposition of zirconium carbide in PyC deposits, an investigation of the effect of coating conditions on the stability of oxide undercoats, and the resistance of PyC coatings to thermal shock. A 37-μ porous coating was deposited on 200-μ UC_2 particles at a deposition rate of 450 μ/hr. This material was then overcoated with a 68-μ nonporous carbon coating by reducing the rate to about 10 μ/hr. The codeposition of zirconium carbide is being accomplished by feeding zirconium tetraiodide along with the acetylene feed. Both vapor- and solid-feed systems were investigated, the solid-feed system evidently being more satisfactory. The crushing strength of a carbon coating containing 11 wt.% zirconium was increased 30% by the addition of the zirconium. The previously reported inability to retain nonporous oxide coatings after overcoating with PyC was further confirmed. The mechanism of failure is unknown, but both Al_2O_3 and BeO coatings were found to be cracked after overcoating. The thermal-shock studies were initiated as a result of irradiation tests that indicated PyC coatings usually failed at the time of a power excursion. Although no evidence was found of unusual sensitivity to thermal shock in the as-deposited condition, after heat-treatment at 1250°C, the coatings appeared to be considerably more sensitive to subsequent thermal shock.

Oak Ridge has now initiated a program[54,55] to prepare experimental lots of carbon-coated particles as a supplement to their evaluation program. Angular 200- to 300-μ particles were coated at 1400°C, using undiluted methane at 200 mm Hg. Metallographic examination revealed the coating structure to be both laminar and columnar, with the apparent degree of columnar structure decreasing from the inner to the outer surface. Oak Ridge has also initiated studies to determine the feasibility of removing surface activity of coated particles by selective chlorination and is continuing its studies on fuel migration. There appear to be very significant differences in the migration characteristics of materials furnished by various vendors, but the factors leading to such differences are unknown. National Carbon has recently issued a summary report[56] on its fabrication program in support of the Oak Ridge irradiation studies.

General Atomic is continuing its program[57] related to graphite-matrix elements containing coated particles. Studies on improved binders, hot working of graphite, and the diffusion of uranium in pyrolytic graphite in PyC coatings are under way. The migration of uranium through PyC coatings on UC_2 particles is being studied as a function of time and temperature at high temperature to furnish quantitative data for the estimation of fuel lives at lower temperature. Samples of PyC-coated UC_2 particles were heated at four different temperatures (1850 to 2300°C) for four different times. By means of microradiography, the distance of migration of uranium into the PyC was determined. A tentative value for the activation energy for the migration process was reported to be 65,000 cal/gram-atom.

In the attempt to prepare pelletized matrix dispersions containing PyC-coated fuel particles, rather severe damage to the coated particles was unexpectedly experienced at Battelle under conditions that were previously found satisfactory for oxide-coated particles.[50,51] A rather comprehensive study was carried out to determine conditions suitable for PyC-coated fuel. In effect, it was found that uniaxial pressure could not be applied to the pelletized particles unless a temperature of about 250°C was maintained; but with isostatic techniques, pressures as high as 100,000 psi could be applied at room temperature. Satisfactory bodies were prepared using warm uniaxial pressure treatments, either with or without isostatic cold molding. (J. H. Oxley)

Irradiation and Evaluation of Coated-Particle Fuels

Oxide-Base Fuel. A topical report[58] on the in-pile behavior of Al_2O_3-coated UO_2 particles at temperatures ranging from 100 to 1070°C

Table I-6 SUMMARY OF RESULTS OF STATIC CAPSULE IRRADIATIONS OF ALUMINA-COATED UO_2 PARTICLES[60]

	Coating*		Tests of unsupported particles†						Tests of particles in a matrix‡					
			100°C			1070°C			100°C			1070°C		
Lot	Material	Thickness, μ	U^{235} burnup, at.%	Xe^{133} released, ppm	Uranium dissolved, %	U^{235} burnup, at.%	Xe^{133} released, ppm	Uranium dissolved, %	U^{235} burnup, at.%	Xe^{133} released, ppm	Uranium dissolved, %	U^{235} burnup, at.%	Xe^{133} released, ppm	Uranium dissolved, %
4E	d-Al_2O_3	8	2.9	8.1	28							3.9	0.29(G)	0.65
	p-Al_2O_3	6												
	d-Al_2O_3	28												
715A	d-Al_2O_3	42	3.0	100	52	1.7	0.09	0.9	3.5	1.9(G)	33	1.7	(G)	0.007
			3.3	100	54	3.2	0.02	0.2	5.0	0.70(G)	43, 38§	3.3	<3.2(G)	
			3.9	50	23									
			4.7	120	39									
715A-HT	d-Al_2O_3	42	3.9	0.01	95	4 (est.)	87		3.6	0.39(G)	93	4 (est.)	(G)	0.3
717B	d-Al_2O_3	43	3.9		(1.5)	4 (est.)	190							
721C	d-Al_2O_3	8	3.1	26	95	1.7	4.0	3	3.0	1.7(C)	33	1.6	(C)	0.5
	p-Al_2O_3	18	3.4	1.8	88	3.2	44	0.2	3.4	(G)	44	1.7	(G)	0.004
	d-Al_2O_3	28	4.6	15	3.1				4.8	1.8(G)	30	3.3	(C)	0.09
									4.9	32(C)	43	3.4	130(G)	
725D	d-Al_2O_3	56	3.9	17	(0.2)	3 (est.)	760¶					3 (est.)	34(G)¶,**	3
						5.7	8000††							
733B	d-Al_2O_3	47	3.9		(3)	4 (est.)	28							
734C	d-Al_2O_3	45										5.7	1400(G)††	

*In order of deposition. Code used is as follows: d-Al_2O_3, essentially fully dense Al_2O_3 layer; and p-Al_2O_3, relatively porous Al_2O_3 layer.

†The data in parentheses are uncertain. Only a small fraction (<15%) of the particles could be recovered from the cans, and in some cases foreign material was present in the recovered specimens.

‡The letter G indicates a relatively graphitized matrix, and C indicates a relatively ungraphitized matrix.

§This specimen consisted of two fueled-graphite pellets. A leach of one pellet as recovered from the capsules yielded a 43% uranium recovery. The second pellet was heated to 815°C, at which temperature 270 ppm of Kr^{85} was driven off. A subsequent leach of second pellet yielded a 38% uranium recovery.

¶These specimens were in capsule CFP-S-6 which did not remain at 1070°C throughout the irradiation. It operated at 1070°C for 4 days, at 440°C for 3 days, and at 750°C for the remaining 37 days.

**This specimen consisted of two fueled-graphite pellets. Analysis of gas samples from within the specimen can after irradiation indicated 34 ppm of Xe^{133} was released by both pellets. Subsequent heating of one pellet to 540°C drove off an additional 1.4 ppm of Xe^{133}.

††These specimens were in capsule CFP-S-10, which did not remain at 1070°C throughout the irradiation. It operated at 1070°C for 3½ days, at 800°C for 6 weeks, at 320 to 400°C for 18 hr, and at 600°C for the remaining week.

and to fuel burnups of about 5 at.% of the U^{235} was issued by Battelle. The particles had 40- to 50-μ coatings and a final diameter of about 200 μ. At 1070°C the particles exhibited excellent integrity and showed essentially complete fission-product retention to 3 to 4 at.% burnup of the fuel. Similar exemplary behavior was not found at 100°C where the samples investigated failed rapidly. Failure was essentially complete in just a few hours. Studies carried out at intermediate temperatures indicated that the low-temperature failure occurred only at temperatures below about 500°C. It was postulated that the failure was a result of radiation damage to the Al_2O_3 coatings which was caused by bombardment of the interior surface of the coatings with fission recoils and that no failure occurred above 500°C because sufficient annealing of the damage above this temperature took place. The in-pile studies were performed on both unsupported particles and particles supported in graphite or carbon matrices. Specimen performance was also evaluated by post-irradiation examinations, including fission-gas release measurements, determination of the fraction of exposed uranium, and visual and metallographic examinations. A summary of the static capsule irradiation data is presented in Table I-6.

More recent information on the irradiation performance of oxide-coated fuel particles has also been reported by Battelle.[49–51] At the higher temperature levels, a 42-μ coating on 127-μ UO_2 has exhibited R/B's of 10^{-8} to 10^{-9} at irradiation temperatures of 1100°C for a period of 1500 hr and after 5 at.% burnup. In addition, some oxide materials that resist low-temperature failure have also been reported. A 63-μ Al_2O_3 coating deposited at 1025°C on a porous UO_2 substrate appears very promising, as well as a 64-μ Al_2O_3 coating with a 4-μ inner layer of PyC on the same type of substrate. These materials showed R/B's of about 10^{-10} after irradiation to 1 or 2 at.% burnup at 100°C. It is not clear at present if the variation in substrate density or coating thickness or both is the controlling factor.

Another Battelle study this period[59] concerned the use of coated oxide particles as possible catalytic activators. The catalyst used was a $CaCl_2$–35 wt.% $MgSO_4$ mixture to which was added about 5 wt.% Al_2O_3- or PyC-coated oxide fuel. Conversion efficiency of this catalyst combination for cyclohexanol dehydration was compared before and after irradiation at three neutron dose levels. The experimental results indicated that little, if any, change occurred in the efficiency of the catalyst as a result of this novel beta-radiation treatment.

Carbide-Base Fuel. The results of both sweep and static tests on commercially supplied carbon-coated carbide particles have been summarized by Oak Ridge.[60] Minnesota Mining & Manufacturing Co., High Temperature Materials, Inc., and National Carbon Company

Table I-7 SELECTED RESULTS FROM IRRADIATION TESTING OF UNSUPPORTED COATED FUEL MATERIALS[60]

Lot	Coating type	Fractional fission-gas release of Kr^{88}, $(R/B) \times 10^{-5}$	Cracked coatings, %	Irradiation conditions: Approximate temp., °C	Irradiation conditions: Burnup, at.% of total U
		Static Capsules			
3M-SP-2	Laminar	*	2 to 4	1370	6
HTM-1	Columnar	*	1 to 2	1095	5
HTM-2	Columnar	*	50	1370	6
NCC-BE	Duplex	*	0.3	1095	6
		Sweep-Gas Capsules			
3M-101-U	Uncoated	530		815	4
3M-SP-2	Laminar	18	5	815	15
HTM-1	Columnar	2.7	2	815	8
HTM-2	Columnar	250†	50		6
NCC-AD	Duplex	0.4	*	815	15

*Not determined.
†Estimate based on 50% cracked coating.

(NCC) have cooperated in the initial phases of the Oak Ridge program. As can be seen from the data presented in Table I-7, the NCC duplex coating performed most satisfactorily over the range of conditions tested. As suggested by Oak Ridge, there are now some data to indicate that thickness of the coating may be the controlling factor with regard to retention of fission products.

coating to yield an overall coating thickness of about 97 μ, also had R/B values of 10^{-10} after 1 at.% burnup (all samples irradiated at temperatures of about 100°C). The NCC duplex material exhibited R/B values of 10^{-5} after 1 at.% burnup at this low temperature, although the R/B ratios were only 10^{-7} at the start of the experiment. Previously, coating thicknesses in the range of 60 μ had failed fairly rapidly at these low temperatures. Additional high-temperature tests are planned to evaluate further the thicker coatings. (J. H. Oxley)

Table I-8 CALCULATED PRESSURES AND STRESSES IN CARBON-COATED UC_2 PARTICLES[61]

Pressure Buildup in Coated UC_2 Particles at 1500°C for Burnup of 10% of Uranium Atoms

Voidage in particle, %	Pressure, atm: Volatile and nonvolatile fission products	Pressure, atm: Volatile fission products only
20	Infinite	1480
30	1960	855
40	850	550
50	475	360
60	290	240

Tensile Stress in Coating on UC_2 Particles at 1500°C After 10% Burnup of Uranium Atoms

Voidage, %	Tensile stress, psi: 500-μ-dia. particle, 100-μ coating	Tensile stress, psi: 300-μ-dia. particle, 100-μ coating	Tensile stress, psi: 100-μ-dia. particle, 100-μ coating
30	39,200	26,300	15,800
40	17,000	11,400	6,900
50	9,400	6,400	3,900
60	5,700	3,800	2,300

Harwell has presented some calculations to indicate that pressure buildup in the coated particles may eventually rupture the coating.[61] This possibility was also a concern of General Atomic in their early work. The results of the Harwell calculations are shown in Table I-8.

Further irradiation studies were also carried out by Battelle on carbon coatings in an attempt to define the variables affecting coating failure.[49–51] Of particular interest is the fact that the coating thickness was demonstrated to be a very important variable, at least with respect to failure at low temperatures. A sample consisting of a 113-μ columnar coating on 200-μ UC_2 particles had R/B values of about 10^{-10} after 3 at.% burnup. A similar material with a 118-μ laminar coating showed R/B values of 10^{-10} after approximately 1 at.% burnup; and a composite coating consisting of layers of dense and porous carbon, overcoated with a 47-μ columnar

Refractory Fuel and Fertile Materials

Properties and Behavior of Uranium Oxide Fuels

The results of comprehensive thermal-conductivity studies on UO_2, performed jointly by Battelle and Hanford,[62] are summarized in Fig. I-6. High-density, nonsintered compacts have a low thermal conductivity that is nearly independent of temperature. Sintered polycrystalline UO_2 exhibits a typical decreasing conductivity inversely proportional to temperature.

Single-crystal UO_2 is characterized by increasing heat-transfer rates above 700°C. This effect can be explained by the contribution of radiant-heat transfer which becomes significant at the higher temperatures. Sintered UO_2 irradiated below 100°C results in a decrease in thermal conductivity; however, this damage appears to anneal out at higher temperatures.

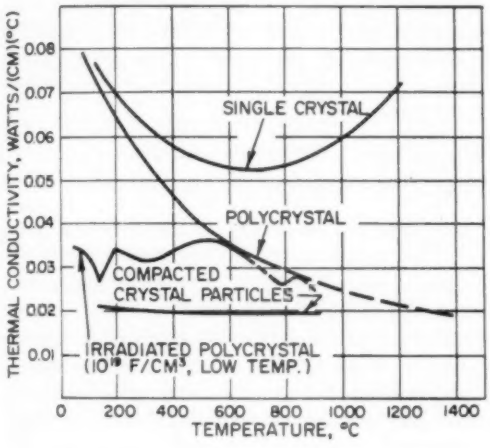

Fig. I-6 Thermal conductivity of UO_2.[62]

Above 1000°C, irradiation appears to have no significant effect on the thermal conductivity of polycrystalline UO_2. The thermal conductivity of unirradiated single-crystal UO_2 can be represented by the equation:[63]

$$k = 0.323 + 17.9\ T^{-1} + 4.1 \times 10^{-12}\ T^3 + 7.5 \exp(-9580/T) \quad \text{watts/(cm)(°K)}$$

The thermal conductivity of molten UO_2 was estimated to be about 0.05 watt/(cm)(°C).[64]

An investigation was made at Bettis[65] of the irradiation behavior of ZrO_2-UO_2 fuels at high temperatures and high burnups. Fuels containing 25 to 46 wt.% UO_2 exhibited swelling that increased linearly with exposure. Temperature appeared to influence swelling only slightly. The two-phase tetragonal structure homogenized to a single phase after a short exposure and then stabilized in the metastable cubic structure at higher exposures. Fission gases were observed to precipitate as bubbles, even at low exposures. In other studies, Johansen and Cleary[66] measured the high-temperature electrical conductivity for various compositions in the UO_2-ZrO_2 system.

At Argonne,[67] urania-neodymia compositions sintered in air and hydrogen were studied by chemical, X-ray, and differential thermal analysis. Solid solutions were found to form readily in air-sintered compositions in the range from 20 to 60 mole % Nd_2O_3. In hydrogen, solid solutions formed slowly and incompletely at temperatures up to 1650°C. (R. H. Barnes)

Fabrication of UO_2-Containing Ceramics

Investigators at Hanford[68] have heated sintered UO_2 from 1000°C to melting and back to 1000°C in less than 3 sec. This is termed "explosive melting" and is done by direct resistance heating. Specimens were 0.1- by 0.25- by 1.0-in. bars. Energy inputs were varied between 5 and 30 kw; heating rate was controlled by varying the voltage across the specimen. The character of melting observed in this process is similar to that observed in UO_2 fuel elements; i.e., a central column is fused, and the outer area is substantially unchanged.

Drops of molten UO_2 were photographed at up to 16,000 frames/sec, and the surface tension of the melt was calculated from drop profiles. A mean value for the surface tension at the melting point (2800°C) was 490 dynes/cm, which is roughly the same as that of mercury and molten lead.

Also measured was the specific volume of UO_2 between 1200 and 3100°C. High-temperature radiographs were made of single-crystal UO_2. From these it was determined that the increase in volume on melting was 9.65% and that the coefficient of thermal expansion of the liquid was 3.7×10^{-5}/°C (2800 to 3100°C).

Research is reported by Hanford[69] on a process for incorporating UO_2 particles into a metal matrix. It involved:

1. Coprecipitating uranium and iron compounds from HNO_3 solution
2. Roasting the compounds at 600°C to form oxides
3. Roasting in hydrogen at 1000°C to yield a mixture consisting of about 10 wt.% UO_2 and 90 wt.% iron powders
4. Encapsulating in steel, evacuating, preheating to 1000°C, and compacting, possibly by swaging

Electron- and optical-microscope examinations of the final compact revealed 0.2- to 0.5-μ

UO_2 particles uniformly distributed in a fine-grained iron matrix. Similar experiments are in progress on making molybdenum-matrix fueled cermets by this technique.

(A. K. Smalley)

Properties of Uranium Carbides, Nitrides, and Sulfides

Uranium-carbon-oxygen alloys based on uranium monocarbide have been studied by S. Namba et al.[70] An alloy having a lattice constant of $a = 4.944$ A was found, and it is indicated that this alloy has the formula $UC_{0.17}O_{0.83}$ and the theoretical density of 13.91 g/cm³.

The entropies of UC and UC_2 have been measured by Westrum[71] from 10 to 350°K. The results are shown in Table I-9.

Table I-9 HEAT CAPACITIES AND ENTROPIES OF URANIUM CARBIDES[71]

Temp., °K	UC		UC_2	
	C_p	$S°$	C_p	$S°$
10	0.079	0.03	0.085	0.03
50	2.735	1.32	2.933	1.57
100	6.035	4.28	6.37	4.74
200	10.08	9.84	11.76	10.93
300	12.15	14.36	14.71	16.27
350	12.76	16.28	15.63	18.59
298.15	12.10	14.29	14.65	16.18

P. A. Vozzella et al.[72] are in agreement with previous findings to the effect that the congruently vaporizing composition in the uranium-carbon system at 2175°C is $UC_{1.1}$ and that the vapors are elemental uranium and carbon. The partial pressure of uranium over uranium monocarbide varies from 1.3×10^{-7} atm at 2010°C to 26×10^{-7} atm at 2230°C. The partial pressure of carbon over uranium monocarbide varies from 0.3×10^{-7} atm at 2010°C to 6.4×10^{-7} atm at 2230°C.

Some preliminary observations of uranium-carbon alloys irradiated to estimated burnups of 14,000 to 15,000 Mwd per ton of uranium have been made by United Nuclear Corp.[73] Estimated surface temperatures ranged up to 870°C, and center-line temperatures, to 1100°C. Examination revealed that fuel had been extruded from the center of the unrestrained ends of mechanically bonded specimens containing 4.4 ± 0.1 wt.% carbon. This extrusion took place in both cast and sintered specimens and is attributed to melting of the uranium in these specimens near the center line. No evidence of this effect was noted in specimens containing 4.8 or 5.2 wt.% carbon or sodium-bonded specimens containing 4.4 ± 0.1 wt.% carbon.

Argonne[14] reports that US has a melting point of 2450°C and a thermal conductivity of 0.026 cal/(sec)(cm)(°C). Thorium monosulfide has a melting point of 2335°C. F. Groenvold et al.[74] have investigated the structures of the sulfides, selenides, and tellurides of uranium. Most of these compounds have structures of low symmetry.

(W. Chubb)

Fabrication of Refractory Fuels Other Than Uranium Oxides

At United Nuclear Corp.,[75] the uranium metal in substoichiometric UC powder (4.5 wt.%) compacts was evaporated during a 3-hr vacuum-sintering treatment at 1800°C. The sintered product contained 4.86 wt.% carbon. A density 90 to 93% of the theoretical UC density resulted.

Ball-milled US powder was not pyrophoric above an average particle size of 0.8 μ, according to Argonne workers.[40] There was excessive contamination of US powder ball milled in an argon-filled mill operated in air. Two methods were tried to eliminate an undesirable UOS phase from sintered US. US containing about 3 wt.% UOS after a previous sinter in argon to 91% of theoretical density was fired 6 hr at 1825°C in vacuum. There was no remaining sign of UOS or UO_2 phases. In the second method, carbon powder was added to the US before compacting and firing in argon for 3 hr at 1825°C. Additions of 1, 2, 3, 4, 5, 7, and 9 mole % carbon were made. There was a slight decrease in the UOS phase with up to 2 mole % carbon additions. With more carbon, there was a progressive increase in the amount of a darker gray phase. The lattice parameter of the US decreased only slightly, indicating that the carbon is probably in this secondary phase instead of in solid solution with the US.

By high-energy impaction (Dynapak), Hanford workers[35] compacted US powder to 10.81 g/cm³ (99.5% of theoretical density) at 1200°C, and UN powder to 14.25 g/cm³ (99.5% of theoretical density) at 1100°C.[68]

ThO_2 with 1.35 wt.% CaO added sinters more rapidly than does pure ThO_2, although the densities achieved were characteristic of the sintering temperature and independent of the heating rate.

The diffusion coefficient of thorium ions seemed to be unaffected by the CaO additions, but creep was greater in sintered ThO_2–1.35 wt.% CaO than in pure ThO_2. It is suggested that the calcium ions cause an increased initial sintering rate, but plastic flow, rather than diffusion, is the rate-controlling mechanism.[54]

(E. O. Speidel)

Basic Studies of Irradiation Effects on Fuel Materials

Metallic Fuels

Uhlmann[76,77] has brought his bibliography on radiation effects in uranium-based fuel materials up to date.

Leteurtre and Brebec[78] have found that dislocation loops and twins are formed in uranium foils when krypton is introduced by gas discharge. After annealing was done at 620°C, bubbles in the range of 50 to 400 A diameter were present. With the aid of electron-transmission microscopy, Belgian workers[79] have observed partial dislocations, twins, emissary dislocations, and defect clusters in irradiated alpha uranium.

A single parameter has been developed for the description of preferred orientation of uranium which correlates well with the observed growth during irradiation.[80] The parameter is derived from inverse pole figures. Controlled irradiation experiments can now be performed to investigate the effects of other variables on anisotropic growth, thus eliminating the effects of differences in preferred orientation.

Argonne[81] reports swelling of uranium irradiated to 0.30 at.% burnup as a function of time and temperature of postirradiation heating. Swelling was slight up to 600°C but was considerable at high temperatures in the alpha phase; in the beta phase, there was little swelling but pronounced cracking; in the gamma phase, swelling was greater than in the other phases. The swelling occurring at 600°C may have been due to recrystallization; however, the rate of swelling decreased with time at all temperatures.

Hanford[68] has developed an empirical equation describing swelling of clad uranium fuel elements as a function of environmental variables. The model contains many adjustable parameters for which statistical values have been obtained by computer analysis.

Pawelski and Strobe[82] have measured thermal expansion and resistivity or longitudinal specimens from core and rim positions in uranium fuel bars. The measurements are used to predict the irradiation growth rates at these positions as percentages of the growth rate of a single crystal; the assumptions necessary to make these predictions are explained and justified. During irradiation the cores of the uranium bars examined are expected to shrink, relative to the rims, at rates between 3.5 and 14.1% of the single-crystal growth rate.

Buckley[83] reviews the evidence of irradiation growth in uranium. Current results show that anisotropic growth rates are identical in single and polycrystals and are much greater at low temperatures. Anisotropic growth was also observed in zinc, zirconium, titanium, and cadmium irradiated by fission recoils, especially at −196°C. Growth rates decrease with decreasing atomic mass. This mass dependence indicates a displacement spike mechanism.

(F. R. Winslow and F. A. Rough)

Ceramic Fuels

The axial distribution of fission products in cylindrical UO_2 fuel elements has been analyzed at Hanford.[84] Pronounced migration occurs which results in maximum segregation at the center and the outside of the core. The large-grained columnar region of the UO_2 contained the least amount of fission products. The use of cesium as an indicator of burnup is shown to be unreliable, even if an entire cross section is analyzed, because of release from the surface.

Padden and Schnizler[85a] report that precipitates, presumably fission products, occur in the grain boundaries of UO_2 at low burnups and also in subgrain boundaries at higher burnups. Noggle and Stiegler[85a] describe experimental techniques in which it is possible to identify the class of fragment giving rise to a particular length of track in a thin film of UO_2, the direction of travel of the fragment in producing the track, and the depth of the fragment below the surface at points along the track. The results obtained by the use of these techniques are correlated with the structures observed. The proposed mechanisms of energy loss of fission fragments are discussed and related to the

studies of track structure. A new mechanism by which ionization energy may be converted into lattice damage is described.

British workers[85b] report the presence of fine-scale bubbles (400 A in diameter) within grains of UO_2 irradiated to 0.25 to 6% burnup. The defects occur at a concentration of 10^{15}/cm^3 and often occur in clusters or in linear groups.

Toner and Scott[86b] used the postirradiation-anneal technique to determine the release rate of Xe^{133} from 95% dense UO_2 pellets between 1000 and 2000°C. Release-rate measurements indicated that, below the sintering temperature, an initial rapid release of xenon was followed by a slower diffusion-controlled release. Below approximately 1600°C the rate of release can be explained in terms of the equivalent sphere model for fission-gas release. Above this temperature the rate of release is higher than would be predicted on the basis of diffusion. The release-rate data have been compared with the release rates obtained in-pile. Results showed that the release rate was independent of burnup up to 16,400 Mwd per metric ton of UO_2. (F. R. Winslow and F. A. Rough)

References

1. G. F. Slattery and D. E. Connolly, A Compendium of X-Ray Growth Indices for Mechanically Worked Uranium, British Report TRG-360(S), Sept. 21, 1962.
2. D. E. Connolly, The Crystal Structure of Alpha Uranium, and Tables of Crystallographic Functions, British Report TRG-359(S), Sept. 18, 1962.
3. J. Burke and P. Dixon, The Phase Transition in Pure Uranium, *J. Nucl. Mater.*, 7: 38-45 (September–October 1962).
4. E. Gebhardt, H. Seghezzi, and R. Rothenbacker, The Oxidation of Uranium at an Oxygen Partial Pressure of 10^{-3} Torr in the Temperature Range from 200 to 370 C (in German), *Z. Metallk.*, 53: 513-516 (August 1962).
5. J. M. McKee, Sponge Fuel Evaluation — Phase II Report, August 23, 1961 to January 31, 1963, USAEC Report UNC-5046, United Nuclear Corp., Jan. 31, 1963.
6. H. M. Green, A Metallographic Study of Gas Behavior in Uranium Irradiated with Alpha Particles, USAEC Report NMI-7009, Nuclear Metals, Inc., Sept. 28, 1962. (Classified)
7. Review of Uses for Depleted Uranium and Non-Energy Uses for Natural Uranium, Report DMIC Memorandum-165, Battelle Memorial Institute, Defense Metals Information Center, Feb. 1, 1963.
8. S. Isserow, R. W. Anderson, W. J. Richmond, D. M. Davies, and W. L. Larson, Power Reactor Program. Progress Report to Savannah River Operations Office, United States Atomic Energy Commission, for the Period October 1–October 31, 1962, USAEC Report NMI-7256, Nuclear Metals, Inc., Nov. 30, 1962.
9. R. W. Bohl and M. V. Nevitt, A Study of Uranium-Fissium Alloys Containing Technetium, USAEC Report ANL-6495, Argonne National Laboratory, October 1962.
10. B. A. Loomis and D. W. Pracht, Swelling of Uranium and Uranium Alloys on Postirradiation Annealing, USAEC Report ANL-6532, Argonne National Laboratory, September 1962.
11. *Properties of Reactor Materials and the Effects of Radiation Damage*, Butterworth & Co., Ltd., London, 1962.
12. *Uranium and Graphite*, Proceedings of a Symposium Held in London on 20 and 21 March, 1962, Monograph No. 27, Institute of Metals, London, 1962.
13. Argonne National Laboratory, Reactor Development Program Progress Report, September 1962, USAEC Report ANL-6619, Oct. 15, 1962.
14. Argonne National Laboratory, Reactor Development Program Progress Report, November 1962, USAEC Report ANL-6658, Dec. 15, 1962.
15. J. A. Lee, K. Mendelssohn, and D. A. Wigley, Accumulation of Radiation Damage in Plutonium, *Cryogenics*, 2: 183-184 (March 1962).
16. Hanford Atomic Products Operation, Plutonium Metallurgy Operation Quarterly Progress Report, January-March 1962, USAEC Report HW-73318, Apr. 16, 1962.
17. G. R. Grove, L. V. Jones, J. F. Eichelberger, and E. A. Rembold, Mound Laboratory, Jan. 11, 1963. (Unpublished)
    1142, Jan. 11, 1963. (Unpublished)
18. G. R. Grove, L. V. Jones, and J. F. Eichelberger, Mound Laboratory Progress Report, July 1962, USAEC Report MLM-1139, July 31, 1962.
19. Los Alamos Scientific Laboratory, Quarterly Status Report on LAMPRE Program for Period Ending November 20, 1962, USAEC Report LAMS-2815, Dec. 26, 1962.
20. D. F. Bowersox and J. A. Leary, The Solubility of Selected Elements in Liquid Plutonium. I. Carbon, USAEC Report LAMS-2832, Los Alamos Scientific Laboratory, Dec. 18, 1962.
21. Los Alamos Scientific Laboratory, Quarterly Status Report on LAMPRE Program for Period Ending August 20, 1962, USAEC Report LAMS-2753, September 1962.
22. Argonne National Laboratory, Reactor Development Program Progress Report, January 1963, USAEC Report ANL-6683, Feb. 15, 1963.
23. Argonne National Laboratory, Reactor Development Program Progress Report, August 1962, USAEC Report ANL-6610, Sept. 15, 1962.

24. A. F. Berndt, Room-Temperature Lattice Constants of Alpha Uranium-Plutonium Alloys, USAEC Report ANL-6460, Argonne National Laboratory, October 1962.
25. F. G. Dawson (Comp.), Plutonium as a Power Reactor Fuel, Proceedings of American Nuclear Society Topical Meeting, Richland, Washington, September 13 and 14, 1962, USAEC Report HW-75007, Hanford Atomic Products Operation, December 1962.
26. K. M. Horst and B. A. Hutchins, Comparative Study of PuC-UC and PuO_2-UO_2 as Fast Reactor Fuel. Part I. Technical Considerations, USAEC Report GEAP-3880, General Electric Company, Atomic Power Equipment Department, Jan. 19, 1962.
27. O. L. Kruger, Phase Studies on Arc-Melted Plutonium-Carbon Alloys Near the Monocarbide Composition, USAEC Report ANL-FGF-343, Argonne National Laboratory, Apr. 23, 1962.
28. O. L. Kruger, Preparation and Some Properties of Arc-Cast Plutonium Monocarbide, USAEC Report ANL-FGF-321, Argonne National Laboratory, Feb. 5, 1962.
29. F. Anselin and R. Pascard, The Volatility of the Carbide and Nitride of Plutonium, *Compt. Rend.*, 255: 698-700 (July 1962).
30. E. Rosen and M. V. Nevitt, The Uranium Monocarbide-Plutonium Monocarbide System, USAEC Report ANL-FGF-345, Argonne National Laboratory, May 2, 1962.
31. D. F. Carroll, Synthesis and Properties of Plutonium Mononitride, USAEC Report HW-SA-2755, Hanford Atomic Products Operation, Aug. 17, 1962.
32. Nuclear Materials & Equipment Corp., Mar. 5, 1963. (Unpublished)
33. Nuclear Materials & Equipment Corp., Feb. 5, 1963. (Unpublished)
34. M. D. Freshley, Irradiation Testing of Prototypic UO_2-PuO_2 PRTR Fuel Elements, USAEC Report HW-SA-2668, Hanford Atomic Products Operation, Nov. 8, 1962.
35. Hanford Atomic Products Operation, Reactor and Fuels Laboratory Monthly Report, December 1962, USAEC Report HW-75925A, Jan. 15, 1963. (Classified)
36. M. J. F. Notley et al., Powder Metallurgy Studies Involving Plutonium, in *Powder Metallurgy in the Nuclear Age*, pp. 44-45, edited by F. Benesovsky, Metallwerk Plansee AG., Ruette/Tirol, Austria, 1962.
37. W. C. Pritchard, K. A. Johnson, and J. A. Leary, Compatibility of the Major Elemental Components of Type 302B Stainless Steel with PuO_2 and UO_2, USAEC Report LA-2828, Los Alamos Scientific Laboratory, Oct. 25, 1962.
38. Hanford Atomic Products Operation, Reactor and Fuels Laboratory Monthly Report, January 1963, USAEC Report HW-76315A, Feb. 15, 1963. (Classified)
39. C. E. McNeilly, Electrical Properties of Plutonium Oxides, USAEC Report HW-75120, Hanford Atomic Products Operation, September 1962.
40. Argonne National Laboratory, Reactor Development Program Progress Report, February 1963, USAEC Report ANL-6698, Mar. 15, 1963.
41. Nuclear Fuels and Materials Development, USAEC Report TID-11295(2nd ed.), September 1962.
42. Phillips Petroleum Co., Materials Testing Reactor-Engineering Test Reactor Technical Branches Quarterly Report July 1-September 30, 1962, USAEC Report IDO-16827, Jan. 15, 1963.
43. D. L. Keller, G. W. Cunningham, W. E. Murr, E. O. Fromm, and D. E. Lozier, High-Temperature Irradiation Test of UO_2 Cermet Fuels, USAEC Report BMI-1608, Battelle Memorial Institute, Jan. 7, 1963.
44. F. Benesovsky (Ed.), *Powder Metallurgy in the Nuclear Age*, Metallwerk Plansee AG., Reutte/Tirol, Austria, 1962.
    a. C. Sari and E. Jonckheere, Coating of Particles by Vacuum Metallizing, Chap. 28.
    b. G. W. Cunningham, D. E. Kizer, and S. J. Paprocki, Cermet Fuel Elements, Chap. 22.
45. Société d'Études de Recherches et d'Applications pour l'Industrie, Coating of Uraniferous Ceramic Particles with Niobium Metal. Quarterly Report No. 4. April-June 30, 1962, USAEC-Euratom Report EURAEC-409, July 1962.
46. Société d'Études de Recherches et d'Applications pour l'Industrie, Coating of Uraniferous Ceramic Particles with Niobium Metal, Final Report No. 1, USAEC-Euratom Report EURAEC-487, July 1962.
47. Bureau of Mines, Metallurgical Quarterly Progress Report No. 17 for the Period of October 1-December 31, 1962, USAEC Report USBM-U-1001, Dec. 31, 1962.
48. W. R. Grimes, J. H. Shaffer, and G. M. Watson, Preparation of Refractory Oxide Crystals, U. S. Patent 3,063,794 (to USAEC), Nov. 13, 1962.
49. R. W. Dayton and R. F. Dickerson, Progress Relating to Civilian Applications During December, 1962, USAEC Report BMI-1607, Battelle Memorial Institute, Jan. 1, 1963. (Classified)
50. R. W. Dayton and R. F. Dickerson, Progress Relating to Civilian Applications During January, 1963, USAEC Report BMI-1614, Battelle Memorial Institute, Feb. 1, 1963. (Classified)
51. R. W. Dayton and R. F. Dickerson, Progress Relating to Civilian Applications During February, 1963, USAEC Report BMI-1619, Battelle Memorial Institute, Mar. 1, 1963. (Classified)
52. G. W. Cunningham and S. J. Paprocki, Oxidation Resistance of Al_2O_3 Coated Fuel Particles, *Trans. Am. Nucl. Soc.*, 5(2): 454 (November 1962).
53. P. Marien (Ed.), Research and Development Division, Third Semi-Annual Report for July 1 to

December 1, 1961, British Report DP-Report 92, May 1962.

54. Oak Ridge National Laboratory Status and Progress Report, January 1963, USAEC Report ORNL-3410, Feb. 11, 1963. (Classified)
55. Oak Ridge National Laboratory, Coated Particle Fuel Element Development Activity Letter for September 15 to November 15, 1962, Jan. 25, 1963.
56. National Carbon Co., Graphite-Matrix Nuclear Fuel Elements, Summary Report, Phase III, USAEC Report TID-17593, Dec. 21, 1962.
57. W. V. Goeddel and L. R. Zumwalt, General Atomic Div., General Dynamics Corp., Jan. 11, 1963. (Unpublished)
58. N. E. Miller, R. L. Ritzman, R. J. Burian, and C. W. Townley, Initial Irradiation Evaluation of Experimental Al_2O_3-Coated UO_2 Fuel Particles, USAEC Report BMI-1613, Battelle Memorial Institute, Jan. 30, 1963.
59. J. L. McFarling and J. F. Kircher, Experiments on Enhanced Catalytic Activity from Internal Irradiation of Catalysts, USAEC Report BMI-1620, Battelle Memorial Institute, Feb. 28, 1963.
60. Oak Ridge National Laboratory, Gas Cooled Reactor Program. Semiannual Progress Report for Period Ending September 30, 1962, USAEC Report ORNL-3372, Feb. 1, 1963.
61. F. Benesovsky (Ed.), *Powder Metallurgy in the Nuclear Age* (discussion section in Chap. 28, P. Murray), Metallwerk Plansee AG., Reutte/Tirol, Austria, 1962.
62. J. L. Daniel, J. Matolich, Jr., and H. W. Deem, Thermal Conductivity of UO_2, USAEC Report HW-69945, Hanford Atomic Products Operation and Battelle Memorial Institute, September 1962.
63. Hanford Atomic Products Operation, Research and Development Programs Executed for the Division of Reactor Development, Quarterly Progress Report, July–September, 1962, USAEC Report HW-75914, December 1962.
64. Hanford Atomic Products Operation, Reactor and Fuels Laboratory Monthly Report, February 1963, USAEC Report HW-76596, Mar. 15, 1963. (Classified)
65. Westinghouse Electric Corp., Bettis Atomic Power Laboratory, Bettis Technical Review. Reactor Technology, USAEC Report WAPD-BT-27, December 1962.
66. H. A. Johansen and J. G. Cleary, High-Temperature Electrical Conductivity in the System UO_2-ZrO_2, *J. Electrochem. Soc.*, 109: 1076-1079 (November 1962).
67. D. Kolar, J. H. Handwerk, and R. J. Beals, Investigations in the System Urania-Neodymia, USAEC Report ANL-6631, Argonne National Laboratory, December 1962.
68. Hanford Atomic Products Operation, Fuels Development Operation Quarterly Progress Report, July–September, 1962, USAEC Report HW-74378, Oct. 15, 1962. (Classified)
69. Hanford Atomic Products Operation, Reactor and Fuels Laboratory Monthly Report, December 1962, USAEC Report HW-75925A, Jan. 15, 1963. (Classified)
70. S. Namba, S. Imoto, and T. Sano, The Formation of $UC_{1-x}O_x$, Report NP-tr-901 [translated from *J. At. Energy Soc. of Japan*, 3: 457-461 (1961)].
71. E. F. Westrum, Jr., Thermodynamic Properties of Actinide Carbides with Special Reference to the Entropies of Uranium Mono- and Dicarbide, USAEC Report TID-16987, Dec. 4, 1962.
72. P. A. Vozzella, A. D. Miller, and M. A. De Crescente, The Thermal Decomposition of Uranium Monocarbide, USAEC Report PWAC-378, Pratt & Whitney Aircraft Division, Jan. 15, 1962.
73. United Nuclear Corp., Mar. 17, 1963. (Unpublished)
74. F. Groenvold, H. Haraldsen, T. Thurman-Moe, and T. Tufte, On the Composition, Structure, and Magnetic Properties of Some Uranium Chalcogenides, Norwegian Report ARL-62-427 (Part II), Mar. 31, 1962.
75. J. Crane, H. S. Kalish, and F. B. Litton, The Development of Uranium Carbide as a Nuclear Fuel. Third Annual Report, September 1, 1961 to October 31, 1962, USAEC Report UNC-5048, United Nuclear Corp., Jan. 15, 1963.
76. W. Uhlmann, Radiation Effects on Solid, Uranium Based Nuclear Fuel Materials, Vol. 2, No. 2. A Bibliography, Swedish Report VDIT-16(2.2), September 1962.
77. W. Uhlmann, Radiation Effects on Solid, Uranium Based Nuclear Fuel Materials, Vol. 2, No. 3. A Bibliography, Swedish Report VDIT-16(2.3), October 1962.
78. J. Leteurtre and G. Brebec, Electron Microscope Study of Uranium Containing Krypton, *J. Nucl. Mater.*, 6: 342-345 (August 1962).
79. Centre d'Étude de l'Energie Nucléaire, Swelling of Uranium, Quarterly Report No. 8, July 1-September 30, 1962, USAEC-Euratom Report EURAEC-464.
80. E. F. Sturcken and W. R. McDonell, An X-Ray Method for Predicting Anisotropic Irradiation Growth in Uranium, *J. Nucl. Mater.*, 7: 85-91 (September–October 1962).
81. B. A. Loomis, Swelling of Uranium, USAEC Report TID-15774, Argonne National Laboratory, March 1962.
82. B. Pawelski and J. J. Strobe, The Prediction of Irradiation Growth Rates in Uranium by Resistivity and Expansion Measurements, *J. Nucl. Energy: Pts. A & B*, 16: 477-481 (October 1962).
83. S. N. Buckley, Irradiation Growth, in *Properties of Reactor Materials and the Effects of Radiation Damage*, pp. 413-439, Butterworth & Co., Ltd., London, 1952.
84. J. L. Bates, J. A. Christensen, and W. E. Roake,

Fission Fragment and Plutonium Migration in Uranium Dioxide Fuel, USAEC Report HW-SA-2778, Hanford Atomic Products Operation, Oct. 15, 1962.

85. *Electron Microscopy*, Vol. 1, Academic Press, New York, 1962.
   a. T. R. Padden and P. S. Schnizler, Microstructural Changes Associated with Irradiation Burnup of Uranium Dioxide, Paper G-14.
   b. B. T. Bradbury, C. J. England, and J. W. Myles, Electron Microscope Study of Microstructural Changes Produced in Uranium Oxides During Neutron Irradiation at High Heat Ratings, Paper G-12.
86. *Symposium on Radiation Effects in Refractory Fuel Compounds*, American Society for Testing Materials, 1962.
   a. T. S. Noggle and J. C. Stiegler, Fission Fragment Tracks in Thin Films of UO_2, pp.47-63.
   b. D. F. Toner and J. L. Scott, Study of the Factors Controlling Release of Xe-133 from Bulk UO_2, pp. 86-96.

Section

II

Reactor Materials

Moderator Materials

Graphite

Graphites and semigraphites were exposed to liquid sodium between 500 and 900°F to establish design allowances for the volume increase in case of a sodium leak into the primary shield tank of the Enrico Fermi Atomic Power Plant.[1] The rate of sodium absorption and swelling of three graphites tested was rapid during the initial stages of immersion. In one instance approximately 90% of the sodium absorption and swelling occurred during the first 2 hr of exposure, and the rate dropped off to practically zero after 24 hr. The total amounts of sodium absorption and of swelling in a 24-hr exposure increased with increase in temperature and were greater for the semigraphites than for the graphites; the volume of sodium absorbed was equal approximately to the sum of the volume of swelling and the initial void volume. For the graphites tested, volume increases ranged from 2.5% for grades TSX and AGSX to 10% for prototype CGC. In restrained absorption tests, equivalent hydrostatic pressures on the order of 1000 psi were developed.

Additional data have been reported by Hanford on the effect of "nongraphitizable" components in graphite on radiation stability.[2] Samples prepared from 0 to 50 wt.% thermax carbon black, an artificial graphite filler, and varying amounts of pitch binder were formed by extrusion and graphitized together to 3000°C. Samples were irradiated at 600 to 650°C to approximately 6.2×10^{20} nvt ($E > 0.18$ Mev). In general, radiation-induced contraction in both the transverse and parallel directions increased with increasing carbon-black content. Also, there was an apparent reduction in the anisotropy of concentration with increasing amounts of carbon black. Higher exposures are planned for these samples.

Three types of low-permeability graphites, irradiated at approximately 650°C to 6740 Mwd/adjacent ton, showed[3] the following contractions:

Graphite type	Average contraction, %	
	Transverse	Parallel
HX-10	0.154	0.176
HX-12	0.266	0.281
EYX-60	0.541	0.472

Note that all samples contracted at a much higher rate than conventional nuclear graphites. For example, CSF graphite would have undergone about 0.08% transverse contraction after a comparable exposure. An expected increase in contraction which resulted from the use of furfuryl alcohol binder (nongraphitizing) is evident in comparing HX-12 results with those of HX-10 which employed a normal pitch binder. The EYX-60 is a proprietary product of Morganite Incorporated.

High-exposure data have been reported[2] for siliconized silicon carbide-coated graphites irradiated at approximately 650°C to 1.15×10^{21} nvt ($E > 0.18$ Mev). Some of the samples were first cycled in air between 250 and 1200°C, and weight changes were measured to determine whether the coatings contained cracks. The samples with intact coatings were then irradiated, and the thermal-cycling treatment was repeated. Weight changes of all of the latter specimens were very small, indicating that the coatings were not cracked by the irradiation and thermal cycling.

To study the effect of apparent density, filler particle size, and orientation ratio on radiation-induced contraction rate in graphite,[3] Hanford workers exposed specimens at

650°C to 6×10^{20} nvt ($E > 0.18$ Mev). The controlled-density series utilized hot-worked samples with densities ranging from 1.87 to 2.10 g/cm^3. Although the exposures were short, the tentative conclusion is that, except when the crystal density of 2.26 g/cm^3 is approached, density has little effect on the contraction of graphite under irradiation. The most dense material had the greatest transverse expansion, +0.62%, and the greatest parallel contraction, 0.31%. In the particle-size series, samples were prepared from Continental Coke filler of three different particle sizes, 0.015, 0.03, and 0.06 in., and pitch binder. The only distinctive behavior noted was the parallel-dimension change in samples that had the smallest particle size. The 0.034% contraction of these samples was significantly greater than the contraction in the other samples. In the transverse direction all samples contracted about 0.010%. In the orientation series the samples with the highest orientation displayed the least contraction, 0.003%.

A recent book[4] brings together 17 papers of a review nature on graphite technology. These cover the manufacture, properties, radiation effects, and uses of graphite. (M. C. Brockway)

Beryllium Metal and Alloys

Fabrication of Beryllium

A news release[5] appearing late in March 1963 stated that the United States will soon have a third beryllium-metal producer. Beryllium Metals and Chemicals Corporation is scaling up its pilot plant in Bessemer City, N. C., and beryllium scrap will be electrorefined into powder and ingots of up to 99.5% purity. The initial plant capacity is expected to be 25,000 to 35,000 lb/year.

The Beryllium Corporation has summarized[6] its findings after an extensive program directed toward the fabrication of beryllium bars, rods, channels, angles, zees, and tees. Target properties of 55,000-psi yield strength, 75,000-psi ultimate tensile strength, and elongations notably higher than those obtainable in hot-pressed block were obtained in all these forms. Except for the T-shapes, the preferred method of forming these structural shapes was by extrusion followed by mill rolling. Properties such as 90,000-psi yield, 120,000-psi ultimate, and 5% elongation appeared feasible.

Brush Beryllium[7] succeeded in producing finned beryllium tubing by means of warm extrusion through special dies. After a 45-min anneal at 1500°F, the product showed the following tensile properties:

Ultimate tensile strength, 1000 psi	Yield strength, 1000 psi	Young's modulus, 10^6 psi	Elongation, %
62.2 to 70.3	47.0 to 60.9	40.3 to 45.6	0.51 to 0.58

The as-drawn burst strength was in the range of 40,000 to 50,000 psi, with only a slight reduction resulting from the annealing treatment. As a result of this work, Brush suggested the following tolerances as practical for finned tube, warm drawn from extruded metal:

Outside diameter of fin (for $\frac{7}{8}$ to $1\frac{1}{4}$-in.-OD tubes only)	±10%
Inside diameter of tube	±0.002"
Tube wall	±10%
Eccentricity	10%

Vacuum hot pressing of beryllium powder produces sintered products with rather poor ductility unless they subsequently plastically deform, although the density may be close to the theoretical density of the metal. A combination of pressure application at convenient temperatures with plastic deformation at higher temperatures will yield semifinished products that, with a minimum of effort, can be processed to finished mill products (ingots, tubes, disks, and plates). Two successful processes[8] are sintering-forging and sintering-extrusion. The working temperatures are relatively low, and safety control is facilitated by sheathing.

Cupping tests on five beryllium sheets produced by the methods indicated below gave the following results:[9]

1. Extrusion of Brush QMV beryllium powder followed by cross rolling to 0.065-in.-thick sheet. Full cups could not be formed up to 600°C.

2. Hot cross rolling of hot-pressed blocks to 0.065-in. sheet. Full cups were produced at 600°C.

3. Rolling of cast vacuum-induction-melted Pechiney flake to 95% reduction. The material was rotated 90° between passes, finishing at 0.100-in. thickness. Full cups were formed at 300 to 500°C.

4. Rolling cast slabs of vacuum-induction-melted Pechiney flake to a 4-to-1 reduction with 90° rotation between passes, followed by unidirectional rolling to a reduction of 18 to 1 to produce a sheet 0.048 in. thick. Full cups were formed at 300 to 500°C.

5. Forging a cast slab of vacuum-induction-melted Peciney flake, followed by rolling as in sheet 3. The forging reduction was 50% and the total reduction 95%, finishing at 0.100 in. Full cups were formed at 200 to 600°C.

Texture in sheet 5 was essentially lacking; it was low in sheets 3 and 4 and was high in sheets 1 and 2. Sheets 1 and 2 showed a high elongation at 200°C (390°F), which fell off rather rapidly at higher temperatures. The other three sheets exhibited a normal brittle-to-ductile transition at about 200°C, and the elongations were relatively constant above this temperature. Sheets 1 and 2 were notably stronger than the rest at all temperatures.

An extensive series of brazing tests on beryllium with pure silver, silver-manganese, silver-aluminum-manganese, silver-vanadium, B-Ag3 (AWS designation), and silver-copper-lithium as filler metals showed that the brazes made with silver-copper-lithium filler by induction heating in a vacuum furnace exhibited the best elevated-temperature strengths and the minimum range of scatter.[10] The alloy demonstrated excellent wetting properties. The silver-aluminum-manganese alloy also produced excellent brazes much superior to those with pure silver. These brazes approached the strength values of the silver-copper-lithium brazement when brazing beryllium to titanium. Ultimate tensile strengths at 1060°F of brazed joints of beryllium to titanium–6 wt.% aluminum–4 wt.% vanadium made in a purified argon atmosphere with silver-copper-lithium were 13,000 to 15,200 psi. The brazing temperature was 1645°F. Beryllium-to-beryllium joints made at 1735°F with the silver-copper-lithium filler showed a room-temperature strength of 23,500 psi. Unfortunately a silver-lithium braze alloy was not tested in this work. In a separate program, workers at Aeronca[11] demonstrated the superiority of a fine silver-lithium braze alloy over silver-copper-lithium for brazing beryllium-faced honeycomb panels. They achieved a marked increase in tensile properties by aging the brazed panels for 16 hr at 1325°F.

Excellent diffusion bonds between beryllium end plugs and beryllium tubes were developed by Atomics International. The technique involves holding the parts for 1 hr at 1000 and 1100°C (1830 and 2010°F) in vacuum. A molybdenum restraining die is used to develop the necessary pressure for diffusion. Inert-gas-shielded welding proved unreliable in single-pass welds, and the welds invariably leaked when multiple-pass welds were attempted. Metallographic examination of the diffusion-bonded joints yielded almost indistinguishable bond lines with grain growth across the joints.[12,13] (W. Hodge)

Physical Metallurgy of Beryllium

In their paper "On the Behavior of Dislocations in Beryllium by Means of Transmission Electron Microscopy," presented at the Institute of Metals (London) Conference on the Metallurgy of Beryllium, Wilhelm and Wilsdorf reported numerous fine dark dots with diameters between 50 and 500 A as having been discovered in beryllium crystals of commercial purity. These dots were tentatively identified as precipitates. They now believe[14] that the dots are artifacts introduced by the etch used. However, the particles of 2-μ diameter and smaller which were reported by P. Vachet et al. (NMI-9520, June 20, 1962), and which apparently are intimately related to the ductility of beryllium, on the fracture surfaces of beryllium single crystals are real inclusions.

Transmission electron microscopy was used[14] to examine a beryllium–0.2 wt.% aluminum alloy in the cast and extruded state. It was found that the aluminum in the alloy begins to melt at considerably below the melting point of pure aluminum. This indicates that it has dissolved one or more impurities. When heating was continued at about 500°C (930°F), fusion of the aluminum was complete and the liquid penetrated deep into the grain boundaries. The progress of this penetration could be watched on the hot stage of the microscope.

Amonenko et al.[15] studied the parameters of whiskers formed during vapor crystallization of 99.99% pure beryllium. The whiskers were crystals several dozen microns in diameter

by several millimeters long. X-ray studies showed that the whiskers were not oriented in the maximum-particle-packing direction.

Several specially prepared beryllium-iron alloys and one containing aluminum in addition to iron have been investigated by Rooksby[16] by X-ray analysis. The results are used to explain structural changes that take place in commercial beryllium under different conditions of heat-treatment. In the aluminum-bearing alloy, a cubic phase, isostructural with Be_5Fe but of larger lattice parameter, was produced. This phase, denoted as $Be_5(Fe, Al)$, accounts for the cubic phase that several investigators have observed in commercial beryllium after aging. Cubic $Be_5(Fe, Al)$ goes into solution on heating commercial beryllium above about 850°C, but it may be reprecipitated on aging in the temperature range 600 to 800°C, provided solution treatment has not been too prolonged or at too high a temperature. Following a severe solution treatment, aging results in precipitation of Teitel and Cohen's hexagonal $Be_{11}Fe$ phase. Both intermetallic precipitates appear to maintain an ordered relation and coherence with the beryllium matrix. The orientation relations between the hexagonal matrix, cubic $Be_5(Fe, Al)$, and hexagonal $Be_{11}Fe$ have been identified.

Alloying of beryllium and aluminum by conventional means has never been very successful. Parikh[17] is studying alloys made by extruding aluminum with either fine beryllium fibers or beryllium powder to achieve the interesting results shown in Table II-1.

Studies at Nuclear Metals, as has been reported previously, have substantiated the reports of the formation of a beta phase in beryllium alloys that cannot be retained on cooling to room temperature. In one experiment[13] a beryllium–8 at.% nickel alloy at 1070°C (1958°F) showed a tensile strength of 5000 psi and a 19% reduction of area with beta present. The same alloy, cooled 10°C and without beta, showed a tensile strength of 4000 psi and no ductility.

Damiano[18] reported an experiment in which beryllium was deformed to 10% strain by compression at room temperature. The comparison surfaces were electrolytically polished, and etch pits were produced by sudden and brief increases in the current density. In this way foils were prepared that showed both dislocations and etch pits. The density of etch pits was an order of magnitude lower than the density of dislocations observed, since junctions of dislocations rather than single dislocations appeared to be preferred etching sites.

Table II-1 ROOM-TEMPERATURE STRENGTH AND MODULUS OF ALUMINUM-BERYLLIUM COMPOSITES IN THE AS-EXTRUDED CONDITION[17]

Beryllium, wt.% (balance Al)	Tensile strength, 1000 psi	Young's modulus, 10^6 psi
20 (powder)	32.0	15
30 (powder)	53.5	18
15 (fibers)	31.0	
25 (fibers)	40.1	14.7

Scott[19] observed replicas of rolled or extruded cast ingots of Pechiney flake beryllium which contained 0.15 wt.% iron, as well as thin foils prepared by a diamond-knife ultramicrotome or by chemical and electrochemical thinning. From these he produced an excellent series of electron photomicrographs. It was shown that marked changes in the dissemination of precipitates at the grain boundaries are produced by thermal treatments, but no evidence was obtained to support the current precipitation-aging hypothesis.

(W. Hodge)

Mechanical Properties of Beryllium

A monumental report[20] on beryllium properties and design data has been prepared by Lockheed.

A new class of beryllium, known as I-400, was developed by Brush for guidance-instrument applications.[21] This material has a minimum BeO content of 4.25%. Its principal advantage over hot-pressed QMV beryllium is that its proportional limit is very much higher. Upsetting of I-400 is difficult. However, when fabricated successfully, I-400 has mechanical properties that are superior to those of any other existing material on a strength/density basis from room temperature to at least 1000°F. Figure II-1 shows the comparative strengths of I-400, other forms of beryllium, a high-strength titanium alloy, and PH15-7Mo steel. Table II-2 compares[22] the properties of forged I-400 with those of forged S-200, the standard structural class of beryllium.

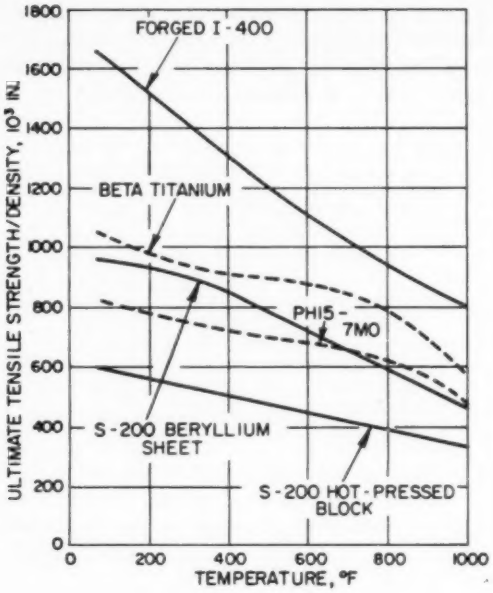

Fig. II-1 Strength-to-density ratios for several alloys.[21]

Chemical analysis of four beryllium extrusions by Nuclear Metals[23] shows the degree of purification that recent research effort has attained in polycrystalline samples. Analyses and tensile data are shown in Tables II-3 and II-4. The high strengths reported for the QMV and SR extrusions are attributed to the extremely fine grain size that was achieved in these materials, whereas the low strength of the double-distilled beryllium extrusion is probably due both to its larger grain size and higher purity. The double-distilled beryllium could be bent cold 50 to 70°, farther than any beryllium specimens of comparable width-to-thickness ratios reported in the literature. However, no large differences in elongation were found among any of the specimens.

(W. Hodge)

Corrosion and Nuclear Properties of Beryllium

British studies[24] of the oxidation rate of beryllium and its alloys in steam and water showed that the severity of attack increased in the following order: steam at 500°C (930°F), water at 325°C (615°F), and saturated steam at 325°C. In the saturated steam, complete oxidation occurred in two to three days. Alloys that contained 0.5 to 5 wt.% nickel, fabricated by arc melting, forging, and rolling, resisted saturated steam at 325°C for 14 days, and uniform oxidation took place with weight gains but little above those of the best unalloyed material in water at 325°C for 14 days.

Nuclear Metals reported[25] that the corrosion of beryllium in hot water is somewhat unpredictable. Accelerated corrosion of Brush QMV samples did not occur in water at 343°C (649°F) in 145 days. Preoxidation of the powders did not appear to improve corrosion resistance. Higher purity grades of beryllium were found to have very poor corrosion resistance in hot water. Corrosion of beryllium in steam, on the other hand, was very slow.

Tensile specimens of extruded beryllium were irradiated[26] at temperatures below 350°C to a maximum fission dose of 2×10^{20} nvt.

Table II-2 TENSILE DATA ON FORGED BERYLLIUM[22]

Material	Test temp., °F	Test direction	Ultimate tensile strength, psi	Yield strength (0.2% offset), psi	Elongation in 1 in., %
I-400	Room	Radial	110,000	75,000	10
S-200	Room	Radial	77,600	47,000	10.7
		Tangential	84,200	50,200	10.6
I-400	500	Radial	81,100	67,200	18.7
S-200	500	Radial	54,600	43,100	52.0
	500	Tangential	55,500	38,500	46.0
I-400	900	Radial	56,600	54,800	10.9
S-200	900	Radial	34,300	32,200	43.0
	900	Tangential	33,000	27,100	62.0
I-400	1100	Radial	45,400	44,800	12.0
S-200	1100	Radial	28,700	28,600	28.5
	1100	Tangential	23,400	21,900	33.0

Table II-3 CHEMICAL ANALYSES OF BERYLLIUM-POWDER EXTRUSIONS[22]

Material	Impurity, ppm			
	Fe	Ni	Al	Si
Brush QMV	1115	171	540	238
Vacuum-melted Pechiney CR	225	90	41	32
Pechiney SR	66	4	110	50
Double distilled	16	1	18	20

Effects of this irradiation on the mechanical properties at room temperature only became noticeable at doses greater than 3×10^{18} nvt. At temperatures above 350°C (660°F), no effect of irradiation was observed up to 2×10^{20} nvt. The low-temperature effects were partly associated with the formation of dislocation loops 200 to 500 A in diameter. Some recovery of properties was obtained by annealing at temperatures above 500°C. When the loops had annealed, small helium bubbles 100 A in diameter were formed which grew at progressively higher annealing temperatures.

(W. Hodge)

Table II-4 TENSILE DATA ON POWDER EXTRUSIONS[23]

Material	Yield strength (0.2% offset), psi	Tensile strength, psi	Elongation, %
Brush QMV	71,400	111,000	7.3
Vacuum-melted Pechiney CR	24,000	72,400	9.7
Pechiney SR	61,400	95,600	5.4
Double distilled	22,500	63,700	7.6

Beryllium Oxide

Continued studies by Austerman and associates at Atomics International[27] on the high-temperature crystal inversion in BeO have revealed a thermal arrest associated with the inversion. This arrest occurs at about 2144°C on heating and at about 2062°C on cooling. The transformation is endothermic, with a latent heat of about 50 ± 10 cal/g. It is quite rapid, proceeding as rapidly as heat can be supplied to the system. This suggests a diffusionless mechanism and probably a simpler relation between the high- and low-temperature forms than previously supposed.

Livermore investigators have reported a small anisotropy in the beryllium-oxygen interatomic spacings in single-crystal BeO. X-ray diffraction has revealed a spacing of 1.659 ± 0.003 A between beryllium and oxygen atoms parallel to the c_0 axis and a spacing of 1.645 ± 0.003 A parallel to the a_0 axis. The writers consider this difference real, and they report that the longer bond has 8 to 10% more ionic character than the shorter bond.

Also reported was polar behavior in single-crystal BeO, as evidenced by piezoelectric and pyroelectric effects, differential etching, and asymmetric hardness. This is in substantial agreement with observations made earlier at Atomics International.

The effects of porosity and temperature on the elastic properties of sintered BeO bodies have been studied by General Electric.[28] The following relations are best estimates for bodies in which the crystals are randomly oriented.

$$E = 56.00\,(1 - 1.87\,P) \times 10^6 \text{ psi} \quad RT$$

$$G = 21.29\,(1 - 1.90\,P) \times 10^6 \text{ psi} \quad RT$$

Percentage of decrease from $E_{20°C}$

$$= -0.137 + (7.56 \times 10^{-3}\,T) + (2.57 \times 10^{-6}\,T^2) \quad 20 \text{ to } 1400°C$$

Percentage of decrease from $G_{20°C}$

$$= 6.71 \times 10^{-2} + (6.81 \times 10^{-3}\,T) + (3.45 \times 10^{-6}\,T^2) \quad 20 \text{ to } 1400°C$$

where E = Young's modulus
G = shear modulus
P = fractional porosity
T = temperature, °C

Preliminary data have indicated that preferred orientation in a polycrystalline body causes increased Young's modulus. Experiments are in progress in this area and also in the area of effect of grain size on Young's and shear moduli.

General Electric workers have established a procedure, based on data for polycrystalline BeO bodies, for calculating the Young's modulus of single-crystal BeO they report.

$$E_{c_0} = 66.2 \times 10^6 \text{ psi}$$

$$E_{a_0} = 56.1 \times 10^6 \text{ psi}$$

The following relates E to the angle of measurement from the c_0 axis.

$$\frac{1}{E_0} = 0.0178 \sin^4 \theta + 0.0151 \cos^4 \theta + 0.0410 \sin^2 \theta \cos^2 \theta \quad \text{in } 10^6 \text{ psi}$$

Clarke of Harwell[29] has offered a model to explain radiation-induced powdering in BeO. He attributes it to the anisotropic crystal expansion that BeO experiences during irradiation. This anisotropic expansion generates strain energy at an interface where the crystallographic axes of two crystals are unaligned. This energy is stored and becomes available to propagate existing cracks. The magnitude of the energy will depend on the size of the areas of constraint and on the magnitude of the strain. According to Clarke the grain size of the BeO affects radiation cracking in at least two ways: (1) it determines the intergranular areas of restraint, and (2) it influences the size of preexisting cracks. The magnitude of intergranular strain was found to vary as (grain size)$^{-\frac{1}{2}}$. (A. K. Smalley)

Beryllium Compounds

Brush Beryllium[30] is continuing its studies of additives to $ZrBe_{13}$ in an effort to improve the oxidation resistance of this compound at temperatures from 1100 to 1800°F. Aluminum, NiAl, and silicon additions have improved the resistance to oxidation, but nickel, tin, and platinum additions were ineffective. Aluminum additions have also proven effective in increasing the oxidation resistance of Zr_2Be_{17}, but larger additions of this metal are required (possibly because aluminum is more soluble in Zr_2Be_{17} than in $ZrBe_{13}$). The mechanism of this improvement is believed to be related to the amount of aluminum in the grain boundaries. Preliminary work suggests that a similar improvement in oxidation resistance results when aluminum is added to $NbBe_{12}$. Studies are being made to determine the influence of the aluminum additions on the elevated-temperature mechanical properties of these beryllides.

In an irradiation experiment[31] the Australian AEC exposed samples of (U, Th)Be_{13} dispersed in a beryllium matrix to a neutron dosage of 4 to 11 × 10^{19} fissions/cm^3 at 530°C. All samples increased in volume during irradiation, the amount of increase depending on the volume fraction of fuel phase and on the number of fissions/cm^3. Release of fission gas was as high as 2%, which is greater than would be expected from recoil in specimens having no open porosity. No significant change in microstructure was observed after irradiation.

(R. W. Getz)

Solid Hydrides

The translation of a USSR monograph on the transition-metal hydrides has been published by the AEC.[32] This work contains 678 references through the year 1959, of which a large number cite European journals. It is somewhat lacking in criticality in that it includes without comment the studies which were made in the early 1900's and for which the purity of the metals used was doubtful.

Zirconium Hydride

The production of large hydride bodies without cracking has been announced by General Electric.[33] The addition of zirconium carbide, in amounts to give 0.3 to 0.5 wt.% carbon, has resulted in fine-grained zirconium hydride up to 5 in. in diameter and several feet in length. The fine-grained structure has permitted fabrication of crack-free material with an N_H of 6.0 to 6.6 which will retain more than 90% of its hydrogen after 1000 hr at 750°C in Mach 0.2 air.

The heat capacity of ZrH_2 and ZrD_2 has been measured over the range 5 to 350°F at Argonne.[34] From the heat capacity, the entropy, enthalpy increment, and Gibbs free-energy function at 298°K have been determined:

	C_p, cal/(deg)(mole)	$S°$, cal/(deg)(mole)	$H°-H_0°$, cal/mole	$G°-H_0°/T$ cal/(deg)(mole)
ZrH_2	7.396 ± 0.015	8.374 ± 0.02	1284 ± 2	−4.067 ± 0.01,
ZrD_2	9.631 ± 0.019	9.168 ± 0.02	1474 ± 3	−4.233 ± 0.01

Yttrium Hydride

Studies of yttrium hydride based on the 95 wt.% yttrium–5 wt.% chromium alloy have been reported by General Electric.[35] The alloy was hydrided to N_H = 5.0 to 5.3 and subjected to a total thermal-neutron flux of 5.6 × 10^{19} nvt in dynamic air at 700°C for 1950 hr.

Visual inspection, weight, and dimensional measurements indicated no change in any of the samples, and there was no measurable hydrogen loss.

The thermodynamic properties of YH_2 and YD_2 were also determined at Argonne:[34]

	C_p, cal/(deg)(mole)	S°, cal/(deg)(mole)	$H^\circ - H_{298}^\circ$, cal/mole	$G^\circ - H_{298}^\circ/T$, cal/(deg)(mole)
YH_2	8.243 ± 0.016	9.175 ± 0.018	1402 ± 3	−4.470 ± 0.009
YD_2	10.773 ± 0.022	10.294 ± 0.021	1659 ± 3	−4.729 ± 0.010

Titanium Hydride

Techniques for controlling microstructure and thereby improving resistance to microcrack formation have been applied to high-N_H titanium hydride at General Electric.[33] Titanium hydride of $N_H = 8.7$ was found to retain 97% of the hydrogen after 970 hr at 540°C.

Lithium Hydride

The properties of lithium hydride, as published in both the classified and unclassified literature through February 1962, have been compiled at NASA Lewis Research Center.[36] The text covers chemical, physical, nuclear engineering, and thermodynamic properties in addition to manufacturing, handling, and fabrication techniques. It contains 267 references.

Zirconium-Uranium Alloy Hydrides

The possible effect of transient reactor heating on zirconium-uranium alloy hydrides has been examined.[37] Pulse heating by passing a large current directly through zirconium-uranium alloy hydride samples gave initial heating rates of about 7500°C/sec, but, as hydrogen evolved, the sample temperature approached an equilibrium value of 1200°C. It was found possible to drive all hydrogen out of $\frac{1}{8}$-in.-diameter samples within 400 msec without catastrophic sample fracture. Up to power input rates of 6000 watts per gram of hydride, the rate of hydrogen evolution was controlled by power input rate and not by diffusion.

(H. H. Krause)

References

1. L. R. Kovac, Report on Sodium Compatibility of Graphites and Semi-Graphites, Report NP-12487, Atomic Power Development Associates, Inc., July 27, 1962.
2. M. M. Hendrickson and J. E. Brown (Eds.), Research and Development Programs Executed for the Division of Reactor Development, Quarterly Progress Report, July-September, 1962, USAEC Report HW-75914, Hanford Atomic Products Operation, December 1962.
3. Hanford Atomic Products Operation, Reactor and Fuels Laboratory Monthly Report, December 1962, USAEC Report HW-75925A, Jan. 15, 1963. (Classified)
4. R. E. Nightingale, *Nuclear Graphite*, Academic Press, New York, 1962.
5. Third in Beryllium, *Chem. Week* (Mar. 23, 1963).
6. E. E. Weismantel and K. C. Taber, Development of Techniques for Producing Beryllium Structural Shapes, Report ASD-TR-62-7-828, Beryllium Corp., May 1962.
7. E. A. Murphy and J. G. Klein, Helical Finned Tube Development, USAEC Report TID-17340, June 30, 1962.
8. R. Syre and J. M. Logerot, Application of Certain Techniques of Power Metallurgy to the Transformation of Beryllium (in French), in *Powder Metallurgy in the Nuclear Age*, pp.677-691, Plansee Proceedings 1961, Metallwerk Plansee AG., Reutte/Tirol. Austria, 1962.
9. R. E. Evans, M. J. C. Hill, and R. J. Wakelin, Forming and Anisotropy of Some Non-Cubic Metals, *Sheet Metal Ind.*, 39(427): 785-801 (November 1962).
10. C. L. Cline and R. A. O'Neill, Brazing Beryllium for Aerospace Applications, *Welding J. (N. Y.)*, 41(12): 1098-1106 (December 1962).
11. J. N. Krusos and W. B. Hunter et al., Sheet Beryllium Composite Structures, Report ASD-TR-7-845(IV), Aeronca Manufacturing Co., October 1962.
12. E. L. Reed, Yttrium and Beryllium End Plug Bonding, USAEC Report NAA-SR-Memo-7283, Atomics International, Apr. 5, 1962.
13. Nuclear Fuels and Materials Development, USAEC Report TID-11295 (2nd ed.), September 1962.
14. Nuclear Metals, Inc., Beryllium Research and Development Program. Quarterly Progress Report to Aeronautical Systems Division, April 1, 1962–June 30, 1962, Report NMI-9522, Nov. 5, 1962.
15. V. M. Amonenko, I. I. Papirov, G. F. Tikhinskii, and V. A. Finkel, Studies of Beryllium Crystals. I. Preparation and Orientation of Whisker Crystals (in Russian), *Fiz. Metal. i Metalloved.*, 13: 928-930 (1962).
16. H. P. Rooksby, Intermetallic Phases in Commercial Beryllium, *J. Nucl. Mater.*, 7(2): 205-211 (November 1962).
17. Illinois Institute of Technology, Armour Research Foundation, Fiber-Reinforced Metals and Alloys, Report ARF-B241-4, Jan. 4, 1963.

18. V. V. Damiano, Direct Observations of Etch Pits at Dislocations in Beryllium (in English), in *Electron Microscopy*, Vol. 1, p. B-6, Academic Press, New York, 1962.
19. V. D. Scott, Electron Microscope Studies of Beryllium, British Report AWRE-O-59/62, October 1962.
20. R. F. Crawford and A. B. Burns, Strength, Efficiency, and Design Data for Beryllium Structures, Report ASD-TR-61-692, Lockheed Missiles & Space Co., February 1962.
21. D. B. King, Beryllium for Aerospace, paper presented at the Fall Meeting of the Metallurgical Society of American Institute of Mining, Metallurgical, and Petroleum Engineers, Institute of Metals Division, Nov. 1, 1962.
22. M. B. Hornak and R. G. O'Rourke, Developing Technology To Forge Unclad Beryllium, TR 280-237, Phase I—Final Report on Contract AF 33(657)-8507, Brush Beryllium Co., Sept. 10, 1962.
23. Nuclear Metals, Inc., Beryllium Research and Development Program, Quarterly Progress Report to Aeronautical Systems Division, July 1, 1962 through September 30, 1962, Report NMI-9525, Jan. 28, 1963.
24. Atomic Energy Research Establishment, Harwell, August 1962. (Unpublished)
25. J. P. Pemsler and D. S. Kneppel, Beryllium Corrosion, USAEC-Euratom Report NMI-1905, Nuclear Metals, Inc., Oct. 30, 1962.
26. J. B. Rich and G. P. Walters, Some Effects of Irradiation on Beryllium (in English), in *Powder Metallurgy in the Nuclear Age*, pp. 668-676, Plansee Proceedings 1961, Metallwerk Plansee AG., Reutte/Tirol, Austria, 1962.
27. S. B. Austerman, High Temperature Phase Transformation in Beryllium Oxide: Thermal Arrest Measurements, USAEC Report NAA-SR-7654, Atomics International, Feb. 15, 1963.
28. General Electric Company, Flight Propulsion Laboratory Department, High-Temperature Materials Program Progress Report No. 18, Part A, USAEC Report GEMP-18A, Dec. 14, 1962.
29. F. J. P. Clarke, A Model for the Strength of Irradiated Beryllium Oxide, British Report AERE-R-4275, February 1963.
30. R. M. Paine, A. J. Stonehouse, and W. W. Beaver, Development of Intermetallic Compounds for Very High Temperature Applications, USAEC Report BBC-114, Brush Beryllium Co., Aug. 31, 1962.
31. G. L. Hanna, B. S. Hickman, and R. J. Hilditch, The Irradiation Behavior of Beryllium Based Dispersion Fuels—A Preliminary Irradiation Experiment, Australian Report AAEC/E-96, September 1962.
32. V. I. Mikheeva, Hydrides of the Transition Metals, USAEC Translation AEC-tr-5224, October 1962.
33. R. Van Houten and W. G. Baxter, Development and Evaluation of High N_H Metallic Hydrides of Zirconium and Titanium, *Trans. Am. Nucl. Soc.*, 5(2): 488 (November 1962).
34. H. E. Flotow and D. W. Osborne, Thermodynamic Properties of ZrH_2, ZrD_2, YH_2, and YD_2, USAEC Report TID-15795, March 1962.
35. J. C. Marshall, R. Van Houten, and W. G. Baxter, Yttrium Hydride Moderator Evaluation: In-Pile Thermal Stability, *Trans. Am. Nucl. Soc.*, 5(2): 489 (November 1962).
36. R. L. Smith and J. W. Miser, Compilation of the Properties of Lithium Hydride, Report NASA-TM-X-483, NASA Lewis Research Center, January 1963. (Classified)
37. R. E. Taylor, H. G. Weidberg, and R. T. Albee, Pulse Heating of Zirconium-Uranium Hydrides, USAEC Report NAA-SR-7398, Atomics International, Dec. 30, 1962.

Section

III

Reactor Materials

Nuclear Poisons

Metallic Poisons

Hafnium was tensile tested at elevated temperatures.[1] The results are given in Fig. III-1. Westinghouse[2] has completed a thorough study on different hafnium microstructures that result from various fabrication techniques.

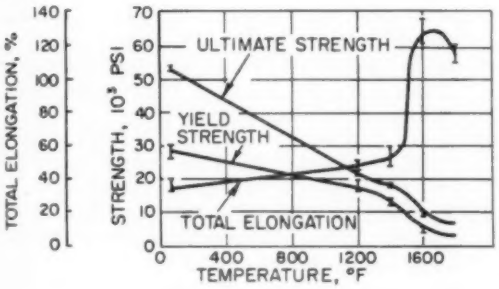

Fig. III-1 Short-time tensile properties of hafnium as a function of temperature.[1]

The neutron-absorption (high cross section) materials used for shutting down reactors are discussed with respect to selection and properties in a recent report.[3] The selection is based on abundance, properties, fabrication technology, and economic aspects. Materials that are discussed are boron, cadmium, lanthanons, Li^6, B^{10}, cadmium-indium-silver alloys, hafnium, and europium oxide dispersions.

A recent examination was completed on a control rod from a Calder reactor.[4] The control rod was made of 4 wt.% boron steel. The B^{10} burnup varied from 2 to 11%. Sections from this rod were annealed in vacuum at 800 to 1100°C for 2 hr to 10 days. Distribution and size of the helium bubbles were found to vary with burnup, annealing time, and annealing temperature.

Aluminum-lithium alloys that contain approximately 12.5 wt.% lithium are employed as part of target assemblies in reactors used for the production of tritium.[5] The lithium solubility in aluminum is 12 at.% at 550°C and 5.5 at.% at 120°C. No evidence was obtained of a previously suspected phase transformation in high-aluminum alloys near 540°C.

The thermodynamic activity of cadmium in cadmium-indium alloys was determined at 543 to 583°K, and the thermodynamic functions were calculated.[6] Also, the solubility of rare-earth metals (except promethium) in liquid cadmium was measured in the temperature range of 325 to 550°C.[7]

Constitutional diagrams for hafnium-rhenium[8] and cobalt-gadolinium[9] have been developed. Also, the following alloy systems were examined: lanthanum-yttrium, lanthanum-gadolinium, and gadolinium-yttrium.[10] The gadolinium-yttrium system exhibits complete solid solubility in both the α and β regions. The lanthanum-yttrium and lanthanum-gadolinium systems show complete solid solubility in the higher temperature body-centered-cubic region, with limited solubility in room-temperature phases. (M. Kangilaski)

Dispersion Poison Materials

Precht and Barr of the Martin Co. have issued a report[11] that covers their investigation of stabilized and hydration-resistant europium oxide. It was found that additions of SnO_2 and Fe_2O_3 resulted in limited stability, but the best results were obtained by additions of TiO_2. The $Eu_2O_3 \cdot 2TiO_2$ (31.1 wt.% TiO_2) showed no weight change after 160 hr in distilled water or after 150 hr in boiling water and a 0.04 wt.% loss after 140 hr in 570°F water at 1200 psi. Pure Eu_2O_3 disinte-

grated after $1\frac{1}{2}$ hr of water refluxing compared with a 0.06 wt.% loss after 67 hr of water refluxing for the $Eu_2O_3 \cdot 2TiO_2$ oxide. The major disadvantage of this material is the high volume percent loading required in the control rods. However, control blades fabricated with 50 vol.% ceramic by hot-rolling procedures showed no swelling, deformation, or appreciable weight change after being defected and subjected to 640°F, 2000-psi water for 284 hr.

Argonne[12] is investigating ceramic fuel materials containing rare-earth oxides as burnable poisons. They prepared UO_2 containing 3 wt.% Gd_2O_3, Dy_2O_3, Sm_2O_3, or Eu_2O_3 by sintering pellets at 1700°C for 4 hr in hydrogen. Evaluation of the stability of these materials showed that there was no significant change in weight, dimensions, or appearance of the pellets after exposure to 650°C oxygenated steam at 600 psi for one week.

Phillips[13] has evaluated a boron–stainless-steel control-rod material for use in the Experimental Organic-Cooled Reactor. The composition was not given, but the material was a B^{10}–stainless-steel powder core clad with stainless steel. After irradiation to 1.07×10^{20} nvt (thermal) in the Materials Testing Reactor, the core was embrittled whereas the cladding remained ductile. Before irradiation, fracture was initiated at a bend angle of 70°, but after irradiation the angle was 5° or less.

(G. W. Cunningham)

References

1. University of California, Lawrence Radiation Laboratory, Oct. 4, 1962. (Unpublished).
2. J. G. Goodwin, Some Information on the Metallographic Appearance of Hafnium, USAEC Report WAPD-TM-325, Westinghouse Electric Corp., Bettis Atomic Power Laboratory, September 1962.
3. W. K. Anderson, Applications of Absorber Materials in Nuclear Reactor Technology, USAEC Report TID-16597, Knolls Atomic Power Laboratory, Sept. 4, 1962.
4. E. Roberts, Some Observations of Gas Bubble Formation in Irradiated Boron Steels, in *Properties of Reactor Materials and Effects of Radiation Damage*, pp. 478-482, Butterworth & Co. (Publishers), Ltd., London, 1962.
5. E. D. Levine and E. J. Rapperport, The Aluminum-Lithium Phase Diagram, USAEC Report NMI-7010, Nuclear Metals, Inc., Feb. 6, 1962.
6. G. V. Pozharskaya and A. M. Evsen, Investigation of the Thermodynamic Properties of Cd–In Alloys (in Russian), *Zh. Fiz. Khim.*, 36: 1053-1054 (May 1962).
7. I. Johnson, Solubility of Rare-Earth Metals in Liquid Cadmium, in *Proceedings of the Second Conference on Rare Earth Research, September 24 to 27, 1961*, pp. 125-131, Gordon and Breach, Science Publishers, New York, 1962.
8. E. M. Savitskii et al., Constitution Diagram of Hf-Re Alloy (in Russian), *Zh. Neorgan. Khim.*, 7: 1608-1610 (July 1962).
9. E. M. Savitskii et al., The Phase Diagram of Cobalt-Gadolinium System (in Russian), *Zh. Neorgan. Khim.*, 7: 2572 (November 1962).
10. F. H. Spedding et al., Some Rare-Earth Alloy Systems, *Trans. Am. Soc. Metals*, 55: 483-491 (September 1962).
11. W. Precht and H. Barr, Investigation of Stabilized and Hydration Resistant Europium Oxide, USAEC Report MND-M-2346, Martin Co., June 1960.
12. Argonne National Laboratory, Reactor Development Program Progress Report, January 1963, USAEC Report ANL-6683, Feb. 15, 1963.
13. Phillips Petroleum Co., Materials Testing Reactor–Engineering Test Reactor Technical Branches Quarterly Report, July 1–September 30, 1962, USAEC Report IDO-16827.

Section IV

Reactor Materials

Cladding and Structural Materials

Corrosion

Zirconium Corrosion

Fundamental studies at Knolls[1] on zirconium single crystals have shown that black oxide films were single crystals whereas white oxide films were polycrystalline and more strain-free, suggesting that recrystallization of the oxide was associated with the black-to-white transition in aqueous corrosion of zirconium alloys. Nuclear Metals[2] has developed anodizing techniques to measure oxygen gradients in corroding zirconium alloys. Experimental results agreed well with calculated values. Hanford[3] has measured electrical resistances ranging from 10^6 to 10^1 ohms in ZrO_2 corrosion films and has suggested that a lower electrical resistance in the oxide film may lead to lower hydrogen adsorption during aqueous corrosion of zirconium. Harwell[4] has found that corrosion rates increase with increased pressure in 1- to 1000-atm steam at 500°C. This pressure dependence decreased as the corrosion resistance of the zirconium alloys increased. This was attributed to a pressure drop that accompanied the flow of steam through cracks or pores in the oxide film.

After more than 3000 hr of exposure, Armour[5] has found that the following alloys are comparable with or superior to Zircaloy-2 with respect to corrosion behavior and hydrogen uptake: 680°F water–zirconium–1 wt.% antimony, zirconium–1 wt.% chromium, zirconium–0.5 wt.% niobium, and zirconium–0.5 wt.% tin with small additions of tellurium, germanium, chromium, or iron; 750°F steam–zirconium–3 wt.% chromium–1 wt.% iron, zirconium–3 wt.% chromium–0.25 wt.% iron, and zirconium–1 wt.% vanadium–1 wt.% iron.

Knolls[1] found that corrosion rates of Zircaloy-2 in concentrated NH_4OH (11.3*M*) were comparable with those obtained in neutral high-purity water at 680°F. On the other hand, Bettis[6] noted increased corrosion rates for Zircaloys in LiOH- or KOH-treated water at 680°F and above *p*H 11.7, with LiOH being the more aggressive.

Bettis[7] reported no dimensional changes, oxidation of the fuel, waterlogging of the fuel, or hydriding failure of the Zircaloy cladding in a defective fuel rod removed from PWR core 1.

Chalk River[8] found that chlorides in organics at 375°C markedly increase hydrogen uptake in Zircaloy-2. It is more severe on abraded or pickled material than on preoxidized specimens. (W. E. Berry)

Aluminum Corrosion

Oak Ridge[9] has concluded that there must be an effect of heat transfer per se on the aqueous corrosion of aluminum. This was based on results where the metal surface temperature was maintained at 400°F and oxide thickness was found to be 1.3 to 1.4 mils at 1.0, 1.5, and 2.0×10^6 Btu/(hr)(sq ft), but only 0.8 mil thick at 0.5×10^6 Btu/(hr)(sq ft). Failure of X8001 aluminum in high-temperature water at Hanford[10] at a heat flux of 228,000 Btu/(hr)(sq ft) was correlated with increased surface temperature. Argonne[11] observed no unusual or accelerated corrosion on Alloy A-288 with a heat flux of 134,000 Btu/(hr)(sq ft) in 485°F water.

A new aluminum alloy, KY (aluminum–1.8 wt.% iron–1.2 wt.% nickel) developed at Hanford,[12] was found to have aqueous corrosion resistance comparable with or superior to that of X8001 in the temperature range 315 to 360°C.

A comprehensive state-of-the-art report[13] was issued by Argonne on the water chemistry and corrosion of aluminum, stainless steel,

zirconium, and other alloys in boiling-water reactors. (W. E. Berry)

Stainless-Steel Corrosion

Argonne[14] found that electropolished specimens of stainless steel and nickel-base alloys exhibit much greater metal loss after seven days in 650°C, 600-psi steam than do wet-ground specimens. An effect of surface preparation on the corrosion behavior of stainless steels was also reported[15] for exposure to 1200°F, 5000-psi steam.

Allis Chalmers[16] found little or no corrosion-erosion of austenitic stainless steels in flowing superheated steam (700°F, 670 psi) or in saturated steam (489°F, 600 psi with 30 ppm oxygen and 0, 0.1, or 0.5 wt.% moisture).

Alco[17] has reported corrosion-product-film growth and release rates for up to 10,469 hr of exposure to the all type 304 stainless-steel SM-1 reactor. For the coolant temperature, chemistry, flow rates, and neutron fluxes of this reactor, the deposition and release rates were high initially but became constant after about 1500 hr, running 4.2×10^{-3} mg/(dm^2)(hr) for deposition and 8.7×10^{-3} mg/(dm^2)(hr) for release. (W. E. Berry)

Corrosion of Uncoated Refractory Metals

The aqueous corrosion behavior of vanadium metal was studied at the Bureau of Mines.[18] At 60°C, vanadium resisted substantial attack by HCl, H_2SO_4, and H_3PO_4; however, at 100°C, all attacked vanadium rapidly. Dilute nitric acid attacked the metal rapidly at 35°C. Vanadium was nearly inert in 10% solutions of formic, acetic, lactic, tartaric, and citric acids, but was attacked slowly by 9% oxalic acid at 60°C and rapidly at 100°C. Tap water, simulated sea water, 3% NaCl, and 10% NaOH had little corrosive effect, but vanadium was attacked by 20% $FeCl_3$, 20% $CuCl_2$, and 5% $HgCl_2$ solutions. The galvanic behavior of vanadium coupled with several other metals was also investigated.

Theoretical calculations were conducted by Oak Ridge personnel[19] to define the contamination behavior of refractory metals subjected to vacuum at high temperatures. In the range from 500 to 1500°C, vacuum requirements depend on the level of contamination that can be allowed. In general, for exposures on the order of 1000 hr or greater, vacua of 10^{-6} to 10^{-9} torr are required to circumvent serious contamination effects.

Niobium alloys that contained titanium and/or vanadium additions appeared particularly promising for service in 1000°F, 1500-psi steam in recent studies at Battelle.[20] Typical corrosion rates for the more promising alloys in the initial screening were 400 to 700 mg/dm^2 in 56 days. Alloy optimization studies are in progress.

Norwegian studies[21] showed the addition of 10% tungsten to tantalum to exhibit little effect on the oxidation performance. The characteristic β-Ta_2O_5 oxide was formed, and contamination proceeded at about the same rate as in unalloyed tantalum.

Research at Westinghouse[22] included studies of the thermodynamics and kinetics of the process of oxidation of tungsten. Above 1250°C, volatilization of WO_3 was severe. At pressures from 5 to 100 torr, and within the 1150 to 1615°C temperature range, kinetics were about linearly dependent on pressure and exponentially dependent on temperature, as defined by

$$\frac{dW}{dt} = 1.87 \times 10^{-3}\ P^{1.122}\ e^{-14,300/RT}$$

where dW/dt is the initial rate of reaction, in grams per square centimeter per second, and P is the pressure, in torr. The 50 wt.% tungsten–50 wt.% tantalum alloy oxidized nearly parabolically at temperatures from 1068 to 1468°C in 0.1 to 0.2 atm of oxygen. The protective scale formed was $Ta_{10}W_8O_{49}$, analogous to the $W_{18}O_{49}$ form (which is protective to tungsten for limited times at lower temperatures). This alloy exhibited only about 4% of the weight gain of tantalum in 1 hr at 1400°C, for example. (E. S. Bartlett)

Corrosion of Coated Refractory Metals

Recent issues by the Defense Metals Information Center (DMIC)[23–25] have reviewed the majority of current data concerning protective coatings for refractory metals. This section will be limited to pertinent information not covered by DMIC.

Concurrent deposition of titanium and silicon on niobium resulted in $NbSi_2$ coatings that contained titanium in solution, according to a recent Russian report.[26] This coating was reported to oxidize at only two-thirds the rate of the unmodified $NbSi_2$ coating at 1200°C.

Workers at Armour[27] have observed excellent oxidation behavior with siliconized vanadium–1 wt.% titanium–60 wt.% niobium alloy, as shown below:

Exposure temp., °F	Time without failure, hr
2000	1000
2200	290
2500	50
2800	4

This system is also extremely tolerant of defects.

The oxidation behavior of silicides of molybdenum (which comprise most protective coating systems for molybdenum) was investigated at A. D. Little.[28] All silicides ($MoSi_2$, Mo_5Si_3, Mo_3Si) were found to approximate logarithmic kinetics upon oxidation. Although only $MoSi_2$ oxidized at low enough rates to be considered protective in a practical sense, the scale formed upon oxidation of the Mo_5Si_3 compound was "protective" when of sufficient thickness.

(E. S. Bartlett)

Corrosion of Miscellaneous Metals and Alloys

Aqueous Corrosion. Work at Cebelcor, Brussels,[29] on stainless steels (AISI types 410, 304, and 316) in bicarbonate solutions that contain sodium chloride shows that there is a critical chloride level below which no attack takes place. This level varies with composition, heat-treatment, etc. Above the critical level in the presence of an oxidizing agent, localized attack is apt to take place. Breakthrough potentials can be used to study methods of improving the surface state.

Knolls[30] studied chloride stress-corrosion cracking of high-nickel alloys and weld overlays as U-bend specimens in two environments: (1) 200 hr at 500°F, in aerated boiler water with 500 ppm chloride at *p*H 10 (NaOH), and (2) 672 hr at 550°F, in aerated natural sea water at *p*H 6.9 to 7.2. The alloys ranged from 46 to 76 wt.% nickel, 7 to 24 wt.% chromium, 0.1 to 16 wt.% molybdenum, plus iron. Cracking was intergranular for wrought material and interdedritic for weld overlays. The susceptibility of high-nickel alloys was a function of the molybdenum-plus-iron content. Chloride stress-corrosion cracking of >45 wt.% nickel alloys did not occur if the critical mean atomic diameter was less than 2.530 A. Combinations of 4 to 16 wt.% iron with 18 to 0 wt.% molybdenum in >45 wt.% nickel alloys were susceptible to cracking. Combinations with less than the above ranges for iron and molybdenum did not crack. High-nickel wrought alloys that showed stress-corrosion failure in hot sea water included AOS W_x (61 wt.% nickel, 13 wt.% iron, 10 wt.% molybdenum), Hastelloy C, and Hastelloy X-280 (47 wt.% nickel, 17 wt.% iron, 10 wt.% molybdenum). Hastelloy X failed in boiler water plus chloride and was not tested in sea water. Inconel was free from cracking in both waters.

Inconel corrosion, as affected by composition and heat-treatment, was studied in experiments at Knolls.[30] Lithiated water was used at 550°F, at 15 to 30 ft/sec flow velocity, and with 20 cm^3 of hydrogen per kilogram of water present. A hydrotest of the experimental system before exposure to loop water resulted in accelerated corrosion, extending the time to reach a linear corrosion rate from 2000 to 3000 hr. Cold work increased the rate of attack; however, the lowest corrosion rate was observed for reannealed material after cold work. Intergranular attack may have developed as a result of stress-relief treatment. No stress-corrosion cracking was observed for Inconel with a variety of welds, overlays, welded joints to type 304 stainless steel, etc. Contacts with metals such as Zircaloy and type 347 stainless steel did not accelerate attack. Surface treatment affected the rate of attack. Inconel annealed after machining showed a rate of 2.9 ± 0.7 mg/(dm^2)(month) up to 3500 hr. Other treatments (e.g., grit blasting) resulted in higher rates of attack.

Hanford[31] evaluated construction materials for water-cooled reactor systems. Steel and low-alloy steels are not favored because there is (1) considerable colloidal corrosion product, crud, etc., in the coolant, and (2) fouling of heat-transfer surfaces by deposits that at some locations may be radioactive. There is evidence that water chemistry could control this corrosion in a full-size plant, but a good demonstration is needed. The complete removal of oxygen, for example, will prevent corrosion at crevices.

Oxidation. So-called TD nickel contains 2 vol.% ThO_2 dispersed to provide elevated-temperature strength and hardness. At 1000°C,

Haynes Alloy 25 showed[32] one-fifth of the weight gain of TD nickel in oxygen at 25 mm pressure for 1000 min. TD nickel[33] was superior to INCO 270 (99.97Ni + 0.02C) in the same environment. X-ray studies proved that surface blisters on TD nickel after oxidation show no relation to local segregation of thoria.[34]

Helium. Superalloys[33] were exposed to grade A helium at 1900°F for 10 days at a velocity of 2 in./sec. After 10 days all samples showed oxidation, some of which sloughed off and the rest was easily scraped off.

An Inconel[32] tube sample, taken from the DR-1 gas loop 3 ft from a break, showed a maximum oxide penetration of 2 mils on both the inner and outer surfaces. At the break it was 5 mils, but intergranular penetration (probably due to sulfide) was several times the oxide penetration.

Carbon Dioxide. Hastelloy N and Inconel 625 showed superior oxidation resistance in dry CO_2 at 1800°F for 280 hr.[35]

Steam. Iron-base and nickel-base alloys were evaluated in 550°C, 3000-psi steam, with 3 to 4 ppm oxygen for 100 days.[35] Of those tested, the most corrosion resistant were AISI 446, Hastelloy X, Incoloy, Inconel X, and PDR L-102 (composition was not given in the reference). (F. W. Fink)

Corrosion by Liquid Metals, Fused Salts, and Organics

Several papers at the International Conference on the Corrosion of Reactor Materials, Salzburg, Austria, June 4 to 8, 1962, dealt with corrosion by liquid metals, fused salts, or organics.[36] The following very brief résumés are given to provide an idea of the material presented; in many cases the subject matter has been covered in somewhat greater detail in past Reviews:

1. Liquid-metal corrosion mechanisms are discussed by scientists from Brookhaven National Laboratory.[36a] Subtopics include the thermodynamics and kinetics of key reactions, corrosion inhibition, the state of structural model theory, electrochemical processes, and boiling liquid-metal corrosion.

2. Data from the investigation of refractory-metal–lithium systems at Oak Ridge National Laboratory[36b] are described, with emphasis on the sensitivity of the corrosion process to the refractory-metal oxygen level.

3. The experience of Oak Ridge in the area of fluoride-salt corrosion is described.[36c] Various pumping-loop data are given, and the development of INOR-8 as a successful containment material is treated.

4. Molten-plutonium-alloy corrosion studies conducted at Los Alamos are reviewed.[36d] A high oxygen level in tantalum was found to affect adversely its compatibility with 650°C plutonium-iron (eutectic) alloy. Improvement was obtained by resorting to high-purity tantalum prepared by special fabrication procedures; carbon additions to the fuel were also beneficial. The first core of the Los Alamos Molten-Plutonium Reactor Experiment (LAMPRE) exhibited virtually no corrosion effects after 10 months at 475 to 525°C and 115 Mw-hr of operation.

5. The investigation of organic-coolant corrosion at Atomics International is reported.[36e] In general, it was demonstrated that wide varieties of materials are inert to virgin organic coolants but, with certain impurities present, notably water and hydrogen, these same organics can produce catastrophic corrosion damage.

6. Russian contributions include a discussion of many facets of the mechanism of carbon transfer in liquid sodium (up to 650°C)[36f] and a report on 600 to 700°C sodium corrosion on certain steels.[36g] A point made in the latter paper is that, under isothermal conditions, the addition of 0.2 wt.% calcium to sodium significantly lowers its attack on austenitic steels.

7. Japanese contributions include a treatment of corrosion and cavitation erosion of ferritic steels by liquid bismuth in the 600 to 950°C range[36h] and a description of work to provide organic-coolant corrosion data.[36i]

Flowing sodium experiments at 850°F (oxygen <10 ppm) were conducted at Atomics International[37] to establish the 500- and 1000-hr behavior of several potentially useful cladding materials. Beryllium, zirconium, and Zircaloy-2 exhibited slight weight gains, whereas niobium and niobium–1 wt.% zirconium alloy exhibited slight weight losses. The 3Z1 alloy (zirconium base containing 1.23 wt.% aluminum, 1 wt.% tin, and 1 wt.% molybdenum) exhibited a severe weight loss between the 500- and 1000-hr periods. The general behavior of 3Z1 was unexpected in view of prior data from longer time, somewhat higher temperature exposures.

Type 304 stainless-steel samples were carburized in sodium to levels of 0.06 (as received),

0.27, 1.0, 1.37, and 1.66 wt.%, and then checked for mechanical-property behavior.[37] At the 0.27 wt.% level, room-temperature ductility had decreased significantly, but at elevated temperatures this effect was less pronounced. At the 1.0 wt.% level, elongations at both room and elevated temperatures were markedly decreased. Data for high- and low-carbon samples are summarized in Table IV-1.

Table IV-1 TENSILE PROPERTIES OF TYPE 304 STAINLESS STEEL CONTAINING TWO DIFFERENT CARBON LEVELS[37]

Test temp., °F	Tensile strength, psi	Yield strength (0.2% offset), psi	Elongation in 1 in., %	Reduction of area, %
		0.06 wt.% Carbon		
Room	84,250	38,900	52.0	52.0
500	63,700	27,300	37.5	46.9
800	62,000	24,200	35.5	38.8
1050	55,350	21,300	34.8	40.1
1200	48,350	20,400	32.5	42.4
		1.66 wt.% Carbon		
Room	135,800	49,500	4.9	4.8
500	107,000	56,800	5.5	8.4
800	99,300	46,500	10.0	11.2
1050	82,100	41,200	13.5	21.0
1200	69,500	37,600	16.3	31.3

Experiments in a large recirculating polyphenyl loop were conducted to obtain detailed information about the effects of temperature, flow rate, and impurity level on the corrosion of containment materials of interest.[37] Findings from the first experiment, an 1117-hr run with 650°F Santowax OMP, indicated good corrosion resistance for the test materials that included AMP-XAP-001 (composition not given), niobium, and several steels. Weight changes ranged from −0.01 mg/(cm^2)(month) for type 304 stainless steel and XAP-001 to +0.29 mg/(cm^2)(month) for niobium and +0.32 mg/(cm^2)(month) for carbon steel. The carbon steel and the niobium demonstrated some tendency for increased weight gains with decreased flow velocity. For the second experiment, the temperature was increased to 750°F and 500 ppm water was added to the Santowax OMP. Corrosion rates of the niobium were somewhat higher than in the first experiment, but the results for the steel were not appreciably different.

Ames Laboratory[38] performed a thermal-convection loop experiment to evaluate the compatibility of 2.25 wt.% chromium−1 wt.% molybdenum alloy steel with the lead-bismuth eutectic (with 50 ppm zirconium added as a corrosion inhibitor) circulating between 300 and 700°C. During a 7280-hr operating period, no corrosion products were formed in the fluid as determined from spectrographic analyses of frequent samples.

From an investigation of the effects of exposure to potassium liquid and vapor on the mechanical properties of selected structural materials, Battelle workers[39] made the following observations:

1. Exposure of molybdenum−0.5 wt.% titanium (stress relieved at 1800°F) to potassium vapor at temperatures up to 2000°F has no noticeable effect on its stress-rupture behavior.

2. The stress-rupture properties of SAE 4340 stainless steel (normalized) are not influenced by potassium-vapor environments at temperatures up to 1000°F.

3. The endurance limit in reversed bending of niobium−1 wt.% zirconium sheet (parallel to the rolling direction) in liquid potassium at 800°F is approximately 27,000 psi.

Items of particular interest in the area of liquid metals, which were reported by the USA Fast Reactor Team that visited the United Kingdom and France during the spring of 1962,[40] are as follows:

1. The Dounreay Fast Reactor is based on a sodium coolant and niobium-jacketed fuel elements. To protect the niobium from hydrogen embrittlement, the hydrogen content of the sodium must be kept below 50 ppm; similarly, to protect from oxygen contamination, the oxygen level of the sodium must be kept below 5 ppm, the target being in the neighborhood of 2 ppm. These stringent contamination-level specifications require extremely careful trapping techniques, and experimentation toward the development of suitable trapping schemes has been extensive.

2. The Risley Engineering Test Laboratories are gaining in prominence as a liquid-metals testing center. Facilities planned for this site will be capable of large-scale testing, with some emphasis on fuel-element subassembly testing in liquid-metal loops to evaluate flow characteristics, temperature gradients, the effect of hydraulic forces, thermal shock, and cycling. Also, comparative testing in large systems, similar except for contamination levels, is planned.

3. In France, major liquid-metal loop test facilities are associated with the development of Rapsodie I, a 20-Mw(t) fast-neutron experimental reactor. Many of these facilities are concentrated at the Cadarache site, where in particular a 10-Mw test loop, which simulates a full-size Rapsodie loop, is in operation.

The following equilibrium solubility data in rubidium were obtained at Aerojet-General.[41]

Material	Equilibrium concentration, ppm	Temp., °F
Nb (in Nb–1 wt.% Zr)	<14	Below 1400
	14 to 30	1400 to 1700
Zr (in Nb–1 wt.% Zr)	1 to 10	1000 to 1400
	10 to 100	1400 to 2000
Mo (in Mo–0.5 wt.% Ti)	1 to 10	1400 to 2000
Ti (in Mo–0.5 wt.% Ti)	1 to 4	1400 to 2000
V	<1	1000 to 1400
Be (QMV)	<1	1000 to 1400
T (in Haynes Alloy 25)	Slightly below detection limit of 14 ppm	1400 to 1700
Fe (in Haynes Alloy 25)	10 to 125	1000 to 1700
Others*		

This investigation also determined the corrosion resistance of containment materials to rubidium (liquid and vapor) in 1000-hr boiling refluxing capsule experiments. A résumé of the corrosion data obtained is presented below.

Material	Observations
Nb–1 wt.% Zr	No corrosion from 1400 to 2000°F; possible evidence of Zr leaching at 2000°F
Mo–0.5 wt.% Ti	No corrosion from 1400 to 2000°F; possible evidence of Ti leaching at 2000°F
V	No corrosion at 1000 or 1400°F
Be	No corrosion at 1000 or 1400°F; some BeO scale at 1400°F
Haynes Alloy 25	No corrosion at 1400 or 1700°F; some surface roughening and anomalous hardness and property changes at 1700°F

Initial data from a study[42] to determine the effect of 1100 and 1200°F sodium exposure on the mechanical properties of type 316 stainless steel and 2¼ wt.% chromium–1 wt.% molybdenum steel indicate the following trends:

1. Type 316 stainless steel exhibits similar stress-to-rupture life in sodium and in air; the rupture life of the 2.25 chromium–1 molybdenum steel is somewhat shortened by sodium exposure.

2. Each material exhibits creep rates in sodium higher than those in air; in some cases the factor is over 3.

3. Each material exhibits comparable fatigue characteristics in sodium and in helium; air exposure tends to shorten fatigue life.

Irradiation experiments to investigate "sodium logging" within a clad UO_2 fuel pin were conducted[43] in conjunction with the development of Fast Ceramic Reactor fuels. This is the effect which would be produced if sodium would enter the fuel zone through a minute cladding defect during reactor shutdown and, during the subsequent startup, would generate a very high pressure through a combination of rapid heating and a limited capability for backflow through the defect. Sodium-immersed pins with small defects in the 6-mil type 304 stainless-steel cladding were subjected to a series of rapid in-pile thermal cycles; the cladding temperature was approximately 1000°F, and the fission heating rate was high enough to produce a central void in an undefected control sample. Postirradiation examination of the defected pins revealed:

1. No cladding deformation greater than that exhibited by the undefected control

2. Absence of a central void, indicating that the sodium promoted heat transfer and thereby reduced the specimen temperature

3. No particular damage to a special pin that had an axial hole along the fuel-center line filled with sodium before the irradiation exposure

Attention is called to a recent bibliography[44] on corrosion by liquid metals prepared at Los Alamos Scientific Laboratory. Emphasis is

*Equilibrium concentrations of cobalt, nickel, manganese, and chromium (in Haynes Alloy 25) fluctuated within the 1- to 100-ppm range at temperatures between 1400 and 1700°F. The equilibrium solubility of tantalum (in Haynes Alloy 25) appeared to be three or four orders of magnitude higher than anticipated. Experimental error is not held responsible for this; rather, the possibility is advanced that a compound of the form $Rb_xTa_yO_z$ is formed and subsequently reduced to liberate free tantalum.

placed on listing references on corrosion of or by alloys of cesium, cobalt, iron, plutonium, tantalum, and tungsten. (J. H. Stang)

Metal-Water Reactions

Studies of the aluminum-water reaction by the levitation melting method are continuing at Argonne.[45] The experiment consists of suspending a ball of aluminum in an atmosphere of steam by means of a radio-frequency field. The aluminum is then rapidly heated to the test temperature at which the sample is maintained for a period of time. The amount of reaction is obtained by a gravimetric determination of the aluminum oxide (Al_2O_3) produced. Preliminary studies at 1400, 1500, and 1600°C have shown that the reaction is linear. Typical values for 10-min reaction times are 1.28 ± 0.33, 3.19 ± 0.59, and 7.7 ± 0.2 mg of aluminum per square centimeter, obtained at 1400, 1500, and 1600°C, respectively. Later information[46] indicates an activation energy of about 50 kcal/mole and a preexponential factor of about 4.2×10^5 mg of aluminum per square centimeter per minute. Experiments at 1200 and 1300°C follow more closely a cubic rate law. Reaction rates, however, were approximately one-half of those obtained in the range 800 to 1200°C by the pressure-pulse method. No reason has yet been found for this discrepancy.

Study of the reaction of type 316 stainless steel with water by the condenser-discharge method was continued.[47] The percentage of metal that reacted with water varied with the initial temperature of the metal in six runs as follows:

Calculated initial temp. of metal, °C	% reaction
2200	10.1
2300	16.5
2600	17.8
2800	21.8
2900	31.6
3500	34.2

The extent of reaction obtained in this series of runs made in water at 315°C (1500 psia) was nearly identical to the extent of reaction observed in previous experiments carried out in water at 100°C (15 psia) and 200°C (225 psia). These and other findings suggest that the kinetics of the oxidation process for both stainless steel and zirconium are independent of pressure over a wide range. Other experiments[48] with type 302 stainless steel are in good agreement with the type 316 results.

Experiments[46,48] with 2S aluminum-clad and unclad aluminum-uranium (fully enriched) fuel elements show total reactions of the aluminum as high as 10.4 and 14.2% respectively, for energy bursts of 672 and 530 cal/g. No explosive pressure rises were recorded, but each plate was transformed into a single globule of metal. (A. W. Lemmon, Jr.)

Radiation Effects in Nonfuel Materials

Defects: Structure and Properties

Metals. Relocation of the fuel in the vicinity of the helium cryostats in the Oak Ridge Graphite Reactor has allowed measurements of the damage effects produced in metals by thermal and fast neutrons separately.[49] There is a significant amount of damage resulting from the thermal neutrons (see Table IV-2) through the recoils of atoms from the (n,γ) reactions. The damage that resulted from the thermal neutrons in all the metals reported anneals to a greater extent at low temperatures, with more annealing peak structure, than the damage produced by the faster neutrons. The mean recoil energy for the (n,γ) reaction calculated for many elements ranges from about 50 ev for the heavier elements to several hundred ev for the lighter elements. The effects of recoils from decay or beta-atom collisions are small compared with those from the (n,γ). Fission neutron damage in copper is also shown, and the recovery is suppressed even more than that observed for fast reactor neutrons.

Sosin,[50] in studying the pinning and thermal depinning of dislocations in electron-irradiated copper, concludes that point defects are tightly bound by dislocations, but the defects do not lose their identity. The thermal depinning results cannot be explained in terms of a single type of dislocation pinned by point defects. Thompson's[51] studies of internal friction in neutron-irradiated-copper single crystals suggests that some conversion of the primary

Table IV-2 OBSERVED NEUTRON DAMAGE RATES AT 4.5°K[49]

(Values Are Change of Electrical Resistivity in Units of 10^{-11} ohm-cm/hr)

Element	Thermal flux	Fast flux
Aluminum	0.001	8.70
Copper	0.567	2.37
Silver	2.958	1.92
Gold	2.71	1.69
Platinum	3.31	5.52
Cadmium	126.0	15.54
Nickel	2.313	

dislocation pinning defect occurs in the neighborhoods of the dislocations between 270 and 400°K. It is felt that this is divacancy controlled. The activation energy of 0.56 ev is interpreted as the motion of divacancies near the dislocations. Another paper[52] reports the delayed pinning produced in copper around room temperature after short neutron irradiations. This process is governed by a single activation energy of 1.1 ev. Although this energy is reasonable for the diffusion of vacancies to dislocations, the shape of the delay-time distribution does not agree with theory, and the apparent number of jumps at the end of the process is anomalously low. Observations by Lomer and Niblett[53] of the variations in internal friction of pure copper due to electron irradiation at 100 and 300°K have been explained in terms of pinning of dislocation lines by point defects. The variations in room-temperature-irradiated samples are consistent with a displacement energy of 20 to 25 ev. Annealing is observed in two stages at 200 and 270°K and is compared with resistance-annealing data. Zakharov's[54] studies of neutron-irradiated copper have shown an increase in elastic modulus, reduction in damping capacity, and a shift in the threshold of the amplitude dependence of damping capacity to larger amplitudes. Annealing in the recrystallization region removes all irradiation effects. Gelli et al.[55] have used internal friction and dynamic-modulus measurements to study neutron-produced damage effects in aluminum which are due to dislocation pinning at point defects. Dislocation pinning was also observed in body-centered cubic iron[56] after an exposure of 5×10^{17} neutrons/cm^2 (>1 Mev).

An unexpected enhancement of neutron-irradiation damage in deformed aluminum suggests that long-range transfer of energy processes is important.[57] This energy transfer cannot be attributed to focusing collisions, but it might be explained by tunnel focusing where knock-on atoms are focused between close-packed rows of atoms for large distances. This type of focusing is not limited by knock-on energy and might be very important in aluminum. This process has been labeled "channeling" and is mentioned again in a later section of this review. In a continuation of their studies of focused recoil trajectories, Nelson et al.[58] have shown that, in copper bombarded with 25-, 50-, and 75-kev Ar^+ ions, there is focusing (or channeling) between the {1 1 1} atomic planes. This is inferred from ejection of atoms in directions contained in {1 1 1} planes. Data also have been published for tungsten and molybdenum[59] where the channeling occurs between {1 1 0} planes.

The energy spectrum of atoms ejected from gold bombarded with heavy ions shows a low-energy peak at 0.15 ev that accounts for 12% of all atoms sputtered by 43-kev Xe^+ ions and 4% by 42.5-kev Ar^+ ions.[60] This phenomenon cannot be associated with focused collision sequences and is explained in terms of evaporation from heated spike regions. A deduction that the focusing range is much greater than the range of the recoil atom leads to a model of constant-radius spikes. Calculations are reported that correctly predict the shape of the spectrum, its magnitude, and its dependence on the bombarding ion. An effective radius of 110 A with a maximum temperature of 1750°K is deduced for spikes caused by recoils with 43-kev Xe^+ ions. This thermal mechanism of sputtering accounts for a small amount of the total observed and will be important only for the highest recoil energies in solids where the focusing range exceeds the recoil range.

X-ray diffraction techniques have been used to study the damage produced by fast neutrons in single-crystal aluminum with varying degrees of perfection.[61] A disordered layer is observed only on the surfaces of irradiated crystals that have a high degree of crystal perfection. It is suggested that this layer is formed by radiation-produced point defects that have migrated toward the surface. The interiors of the crystals are still highly perfect after the irradiation, which implies that stable defect configurations are not present. Etch-pit studies of dislocations in copper crystals were reported

by Young.[62] In neutron-irradiated samples Young observed a cube-root dependence of the yield stress on neutron dose, and in gamma irradiation he observed no hardening after 10^{18}/cm^2 cobalt gamma rays. This latter observation is interpreted as evidence that point defects in low concentrations do not cause hardening.

In a pair of papers[63,64] deJong and Koehler report on their studies of vacancy diffusion (and annealing) in quenched gold. Of specific interest are the observed binding energy of a divacancy, 0.10 ± 0.03 ev, and its energy of migration, 0.66 ± 0.06 ev. It also was observed that a divacancy has a resistivity $4.6 \pm 3\%$ less than that of two well-separated single vacancies. Other electrical measurements in 99.999% gold[65] at pressures up to 11,000 atm, resistance heated to 680°C, resulted in determinations of the activation volume for vacancy formation (0.53 ± 0.04 atomic volumes) and the electrical resistivity of vacancies ($1.8 \pm 0.4 \times 10^{-6}$ ohm-cm/at.%).

A recent note reports on observations of the decay of trapped flux in superconductors resulting from alpha irradiation.[66] Polonium alphas were used as the source and produced no permanent damage affecting ultimate levels of trapped flux. Similar results were obtained a number of times in the same sample. Silver wires and foils exposed to neutrons and gamma rays oxidized at temperatures where only a monomolecular layer of oxide is formed in the absence of radiation.[67] The oxidation is explained in terms of the O^- and O_2^- ions that are formed by the gamma irradiation.

Defects in Metal Alloys. Crystallographic changes in several irradiated metal boride systems, studied with X-ray diffraction, show that the damage produced can be related to the strength of the structural bonds independent of the crystal system.[68] In particular, the metal diborides (TiB_2, ZrB_2, HfB_2) with their tightly bonded hexagonal structures are most resistant to radiation damage. The hexaborides (YB_6, EuB_6) with their loosely bonded cubic structures are extensively damaged by radiation. The intermediate tetraborides (YB_4, B_4C) also are intermediate in structure damage.

The Canadians are conducting a number of interesting experiments. N. L. Swanson[69] is studying the neutron irradiations of high-purity (HP) gold and has shown that its damage rate is very sensitive to small amounts of impurity and to plastic deformation. L. M. Howe[69] observed foils of ordered CuAu that had been irradiated with between 8.2×10^{17} and 7.4×10^{19} neutrons/cm^2 (>500 ev). All the irradiated foils exhibited dark spots that ranged in size from ~30 to ~300 A and increased in number with neutron irradiation. Similar spots were also produced by fission fragments, in ordered foils of CuAu containing U^{235}, after irradiations of 3.7×10^{15} and 1.4×10^{16} thermal neutrons/cm^2. Antiphase boundaries were observed in unirradiated ordered CuAu foils and in ordered material irradiated with 8.2×10^{17} neutrons/cm^2 (>500 ev). However, no antiphase boundaries were observed in the remainder of the foils irradiated with either fast neutrons or fission fragments. Foils of ordered Cu_3Au have been irradiated with 6.1×10^{19} neutrons/cm^2 (> 500 ev), and foils containing U^{235}, with 1.9×10^{15} and 1.4×10^{16} thermal neutrons/cm^2. Dark spots were observed in all the irradiated material, and these spots had features identical to those observed in the irradiated CuAu foils. Antiphase boundaries were present in the unirradiated material and in the foils irradiated with fission fragments but not in the foils irradiated with 6.1×10^{19} neutrons/cm^2 (>500 ev). M. Sumizawa[69] studied fission-fragment damage in ordered Fe_3Al by evaporating U^{235} on both sides of an electropolished foil. The foils were irradiated with 5×10^{15}, 1.5×10^{16}, and 4×10^{16} thermal neutrons/cm^2. Examination by electron microscopy showed some black and white mottled images that covered the sample. These mottled images are thought to be aggregates of small B2 type ordered domains.

Fujita and Damask[70] have prepared two reports on their studies of radiation-induced carbon precipitation in iron. This system was chosen for study since carbon diffuses interstitially in iron; hence its rate is not accelerated by the vacancies and interstitials produced by the irradiation. Observations were made of the rate of decay of the Snock internal-friction peak and of the microstructure with the use of electron microscopy. The results show that samples irradiated at 57°C contain upwards of 10% more nucleation sites for carbon precipitation than unirradiated samples. Irradiations at −100°C produced entirely different results. The carbon disappears from solid solution over a thousand times faster than in unirradiated material, with second-order kinetics and an activation energy of 19.8 kcal/

mole. This value is the activation energy for carbon diffusion in iron. Complete carbon removal is obtained after only four days in the Brookhaven reactor. This disappearance is explained in terms of carbon trapped at point defects, presumably vacancies, thus effectively delaying the carbon precipitation until higher temperatures (~250°C) than that observed in the unirradiated samples (~150°C). Changes in these temperatures are also observed with resistivity measurements.

An additional investigation of the effects produced by the damage resulting from different neutron spectra has been reported by Claiborne.[71] Crude estimates of relative damage are made by assuming that the damage in steel is at least proportional to the number of lattice defects occurring. Correlations are made with fission neutron damage, where corrections to the estimates are found by changing the distance between the steel and the fission source. Rossin[72] has presented data showing the effects of neutron spectra on SA-212B carbon steel.

Defects in Other Materials. The microstructural effects produced in graphite by neutron irradiation are being studied at Culcheth.[73] Annealing experiments have been carried out on graphite flakes irradiated at 200°C to neutron doses of 0.8×10^{20} and 4.14×10^{20} nvt. The lower dose samples, during annealing at 1600 and 1740°C, showed a large initial decrease in cluster density accompanied by an increase in cluster diameter from approximately 40 to 100 A. Two annealing processes were observed that corresponded to activation energies of less than 5.7 ev and 6.3 ± 0.3 ev in the temperature range used. Baker and Kelly[74] reported vacancy loop annealing in quenched graphite with an activation energy of 6.0 to 6.3 ev. This suggests that the defects observed are vacancy clusters. Irradiation at 650°C to a dose of 6×10^{20} neutrons/cm^2 revealed different damage. The defect clusters were much larger (up to 400 A diameter) with a reduced cluster density (6×10^{15}/cm^3). Annealing experiments are now in progress on these samples.

The activation energy for the process of annealing single interstitials in neutron-irradiated graphite and the absolute rate of formation of displaced atoms have been determined experimentally[75] from both the dimensional and *c*-axis expansions of graphite irradiated at temperatures between 77 and 490°K. The activation energy obtained is 0.068 to 0.074 ev and lies between the value of 0.1 ev estimated by Dienes and the value of 0.016 ev calculated by Iwata, Fujita, and Suzuki for the migration energy of a single interstitial. The absolute rate of formation of displaced atoms corresponds to the rate of displacement when no annealing occurs during the irradiation process. The value obtained (5×10^{-3}% displaced atoms per megawatt day) is 2.5 times the rate of displacement at 30°C and is in excellent agreement with theoretical estimates. The dimensional changes occurring during the first irradiation of graphite are the result of three processes. Reaction 1 is the displacement of a single interstitial by collision of a fast neutron and the graphite lattice. This reaction is temperature independent. Reaction 2 is the collision of two interstitials to form a stable C_2 complex. The dimensional growth occurring in graphite is due to the constant (zero-order) rate of formation of C_2. Some of the single interstitials anneal (without causing dimensional changes) by being trapped at pores, edge atoms, etc. Reaction 3 describes this process. The rate-determining step for both reaction 2 and reaction 3 is the rate of migration of the single interstitial.

Lattice defects in quartz induced by fast-neutron irradiation were studied by combined methods of X-ray diffraction and transmission electron microscopy.[76,77] The developed defect structure is characterized by clusters of interstitials enriched in ruptured silicon atoms. The size and density of the defect clusters increase with increasing dose until mutual interaction occurs. The result is the formation of a stable, hexagonal-like structure resistant to prolonged annealing at 500°C. In thin crystals the size and volume fraction of the defect clusters are dependent on crystal orientation, since they are related to the ease of diffusion of the interstitials in directions relative to the open screw channels of the quartz structure. A relation was established between the total volume fraction of defect clusters and fractional decrease in density induced by neutron irradiation. This accounts satisfactorily for the hydrostatic density measurements reported elsewhere in the literature.

Price and Walker[78–80] have continued work on the observation of heavy particle tracks in materials with layer structures. Fission-frag-

ment-track widths showed little correlation with the decomposition temperatures as observed by others. From this evidence, the authors conclude that the track formation cannot be described by a simple thermal-spike model. Electron-diffraction data indicate that the track regions consist of disordered volume and not of a definite crystalline phase. Annealing experiments did show that the tracks serve as nucleation centers for the initiation of transformations to high-temperature phases. In general, tracks have been observed from bombarding particles only if this mass has exceeded about 30. Kelsch and Kammerer[81] have reported on observations of alpha tracks from the $Li^6(n,\alpha)H^3$ reactions. Childs and Slifkin[82,83] have reported on the use of AgCl crystals as particle detectors. Here they are observing 1.55-Bev proton-induced nuclear disintegration. Additional information regarding fission-fragment-induced vaporization of materials has been reported.[84,85]

As LiF crystals harden owing to gamma irradiation at 300°K, it is observed that a good correlation exists between flow stress and the concentration of F centers.[86] The magnitude of the hardening suggests that it was caused by interstitials, and comparison with the hardening produced in additively colored crystals indicates that the hardening defects are interstitial fluorines. Levy[87] has measured the number of defects formed in NaCl by fast reactor neutrons. Unstrained crystals were first irradiated with gamma rays that saturated existing vacancies and formed color centers. After such treatment the defects formed by the reactor neutrons produced new vacancies that could then be colored with the gamma rays. The measured increases in vacancy concentration were propotional to total fast-neutron flux and were in good agreement with the theories proposed by Kinchin and Pease and by Seitz and Koehler. The coagulation of vacancies in KCl crystal during electron irradiation has been observed with the electron microscope and electron diffraction.[88] The results of the experiments reported suggest that similar changes may also occur in other ionic crystals or even in thin metallic crystals prepared by vacuum evaporation. The effects of thermal-neutron irradiation of LiF crystals at −195°C were deduced from small-angle X-ray scattering.[89] It was concluded that the defects formed were not point defects and that their size, which increased on annealing, was remarkably uniform for a given time and temperature of annealing.

Correlation has been reported between the enhancement of the number of gas atoms (oxygen or hydrogen) chemisorbed on the surface of a fast-neutron-irradiated magnesium oxide and the number of displacements produced in the surface region of the oxide lattice.[90]

(T. G. Knorr)

Theories of Radiation Effects

Recent analysis of atomic displacements in cascades[91] has led to the suggestion that the energetic atoms can be channeled in certain directions in crystal-like lattices. This channeling is accomplished by a number of low-angle collisions that transfer little energy and allow the energetic atom to move for relatively large distances. The resulting proposal can be used to explain the fact that experimental observations on damage have always been below theoretical predictions. In fact, many irradiation effects that have been interpreted in terms of focusing collisions may probably be reinterpreted in terms of channeling. Besco and Beeler[92] have also expanded their computer studies of collision cascades in binary materials. The present report considers krypton and iodine bombardment of BeO.

Aspects of predicting the amounts of radiation damage sustained by metals in reactor neutron fluxes have been discussed.[93] It is noted that a first-order anisotropic correction factor for the energy exchange in elastic collisions may be obtained from measured or calculated differential scattering cross sections. The discussion is limited to elastic collisions of fast neutrons with energies between 0.5 and 5.0 Mev. The amount of energy transferred to a displaced lattice ion as a result of an elastic collision by a fast neutron is related to the angle through which the neutron is deflected in the scattering event. The average fraction of available energy transferred per neutron collision ($f/2$) may be calculated from measured differential scattering cross sections. For the materials investigated, it is found that f may be represented as a decreasing linear function of the neutron energy in the range 0.5 to 5.0 Mev. At a constant neutron energy, the periodic variation in f with atomic mass agrees qualitatively with results based on the optical interaction model of Feshbach, Porter, and Weisskopf. In radiation-damage calculations the

assumption of isotropic scattering of fast neutrons leads to an overestimate of the number of induced defects in the material. The average errors for eight of nine materials investigated ranged from 23% for a monochromatic 0.5-Mev spectrum to 71% for a $1/E$ spectrum between 0.5 and 5.0 Mev. In another discussion[94] the number of defects formed by an energetic recoil has been estimated in terms of the effective temperature in the thermal spike and energy of formation of the defect. The volume of the thermal spike is estimated; however, no specific model of defect formation is discussed. Defect formation by the proton bombardment of silicon[95] and gamma irradiation of solids[96] have also been discussed.

Another calculation[97] for the energy of various interstitial configurations has appeared. Here, Morse potential functions for copper are used for the interaction between atoms. The energies of formation for the body-centered configuration are 4.55 ev, and those for the split configuration are 4.54 ev. The mathematical study of Corciovei et al.[98] of the distribution function of displacements arising from a primary atom has continued. Considerations are restricted to elastic collisions. It is now concluded that the distribution is Gaussian about all three axes.

A solution has been found for the problem of predicting the annihilation of heterogeneous pairs during radiation annealing processes.[99] This solution gives a good description of the process for long (>50 min at 350°C) annealing times and results in a value of the capture radius that is approximately equal to the lattice constant. Solutions for homogeneous pair annihilation are also discussed. Dienes and Damask[100] have presented an analysis of the kinetics of vacancy-interstitial annihilation with specific concern for the situation where interstitials migrate to sinks. Both analytical and computer techniques have been used. Defect concentrations during irradiation have also been studied at temperatures where interstitials are mobile. The vacancy concentration goes through a maximum when plotted as a function of irradiation time. Beyond this maximum a steady-state approximation is valid, and subsequent growth of vacancy concentration can be described by a simple relation. The vacancy growth is independent of temperature and is only a function of the integrated exposure. Other considerations of annealing effects in solids have also been reported.[99–101]

A theory has been suggested that quantitatively describes the hardening produced during neutron irradiation of copper in terms of solution hardening by tetragonal distortions.[102] The assumption used for this specific example was that hardening is caused by interstitials or interstitial disks, whichever are present. Similar quantitative agreement with experiments is found for the predicted gamma hardening of LiF due to interstitial fluorine observed by Nadeau and the solution hardening of iron by carbon observed by West. These experiments are noted in the previous sections of this report. Cottrell[103] discusses the engineering aspects of brittle fracture in reactor steel pressure vessels. With the use of the concepts of clustered lattice defects, produced by the knock-on collisions from the fast neutrons, it is shown that the steel is hardened by a process analogous to precipitation hardening. Estimates of the increase in the ductile-brittle transition temperature can be made which allow choices of minimum operating temperatures to maintain the pressure vessel above the crack-propagating temperature. (T. G. Knorr)

Surveys on Radiation-Induced Defects

Abstracts of 735 papers concerned with the effects of neutron irradiation in nonfissionable metals and alloys were collected[104] in a bibliography covering the literature from 1956 to 1962. Topics covered include the effects of radiation on the principal properties of these materials, radiation-damage experiments, radiation-damage-measurement techniques, and general aspects of the problems. Another survey[105] that contains 500 references has been prepared and covers the radiation effects of neutrons and other elementary particles on various metals and high-melting materials. Structural changes, phase transformations, and changes in electrical, magnetic, and optical properties are discussed.

Goland[106] has prepared an extensive review of the status of the theories concerned with atomic displacements in solids produced by nuclear radiation. Where possible the experiments performed to test these theories are discussed in detail. The literature survey was concluded in February 1962. Goland[107] also has presented a brief but interesting survey concerned with the capability of the electron microscope in terms of investigating radiation

damage and the defects formed by such damage. Seitz[108,109] has presented an informative review of the effects of irradiation on metals. Various theories are noted, and the experimental discussions cover defects produced by thermal means and by various bombarding agents, including electrons, deuterons, and neutrons. A short outline of the effects of high-energy radiation on solids has been presented.[110] Attention is given to range, formation of Frenkel defects, replacements, disordering, and cascades. The correlation between radiation damage in several classes of materials and fast-neutron doses is summarized.

Nightingale[111] has presented a detailed summary of irradiation effects observed in reactor graphite. The radiation effects on metallic corrosion were reviewed by Stobbs.[112] Effects produced in the metal itself, in the protective layer, and in the corrodent are discussed. A state-of-the-art bibliography[113] on radiation effects has appeared. Topics covered include electronic devices, polymeric materials, fuels, structural materials, alloys, ceramics, space environment, and dosimetry. (T. G. Knorr)

Effects of Radiation on Mechanical Properties

The results from several investigations of property changes in structural metals and alloys resulting from fast-neutron irradiation have been published.[114a,114b] Reports covering a number of materials have been issued. Workers at Oak Ridge[115] have studied the effect of fast-neutron doses of 1.3×10^{17} and 2.6×10^{18} neutrons/cm^2 on the properties of some zirconium alloys, titanium alloys, a variety of austenitic stainless steels, and Incoloy.

A Swedish report[116] discusses changes in properties of several Swedish steels designated as 2103/R3, SIS 142103, NO345, and weld metal OD54P. The effect of dose rate and reactor-spectrum effects are discounted. The British[117] have shown that there is an insignificant effect of dose rate on radiation hardening in mild steels irradiated at temperatures in the 100 to 350°C temperature range. A method to determine the number of displaced atoms produced by (thermal n,γ) reaction was described and used to calculate their effect. Damage rates for iron irradiated in several computed reactor neutron spectra were calculated with the use of the Kinchin and Pease model. The importance of energy loss by electronic excitation was determined from the increases produced in the tensile lower yield stress of mild steel irradiated in different spectra at 150°C. The resulting damage function was used with the results of accelerated irradiation tests to predict the embrittlement of a Calder Hall pressure-vessel steel. This embrittlement is overestimated when both thermal- (n,γ) and fast-neutron displacements are considered. The hardening of mild steel irradiated at temperatures in the range of 100 to 350°C is not significantly dependent on the neutron dose rate. British[118] research workers have studied the tensile and impact properties of parent and weld metal of a 1 wt.% chromium–0.5 wt.% molybdenum pressure-vessel steel after irradiation at 250°C to doses of 1.0×10^{18} and 2.5×10^{19} neutrons/cm^2. Brittle-to-ductile transition temperatures and the room-temperature tensile properties were determined. Empirical relations are given for properties and total fast-neutron flux. A good review article, "Neutrons Embrittle Reactor Vessels of Carbon Steel,"[119] discusses the results of several irradiation programs. It also discusses the effect of neutron dose rate, elevated-temperature irradiation, and postirradiation annealing.

Austenitic stainless steels are utilized in reactor construction when corrosion is expected to be a problem. In some instances, stainless steel has been used to minimize difficulties associated with the increased transition temperature resulting from irradiation. Battelle workers have summarized[120,121] the effects of fast-neutron irradiation on type 347 stainless steel after doses of 5.7×10^{21} and 1.1×10^{22} neutrons/cm^2 at about 120°F in the Engineering Test Reactor. The effect of 1800°F postirradiation annealing on the tensile properties is discussed. The tensile properties are reported also for type 347 stainless-steel specimens that were cut from a pressure tube irradiated under pressure at about 750°F. The effects of postirradiation annealing at 1100 and 1800°F are described also. Nearly complete recovery was achieved by the anneal at 1800°F, whereas only partial recovery was noted for the 1100°F annealing temperature. A technique has been developed at Vallecitos[122] for studying the slow-cycle strain-fatigue properties of thin-walled tubing under reactor operating conditions. Data on type 304 stainless steel have been obtained under radiation and in the absence of radiation.

The presence of an instantaneous flux of 1.5×10^{14} neutrons/(cm^2)(sec) (>1 Mev) has been found to decrease the fatigue life about threefold at 1200 to 1300°F.

Investigations related to zirconium and zirconium alloys are continuing at many sites. The removal and subsequent examination of several Plutonium Recycle Test Reactor fuel elements by Hanford[123] revealed that exposures of about 1×10^{20} neutrons/cm^2 (>1 Mev) increased the burst strength of Zircaloy-2 from 77,000 to 110,000 psi and decreased the ductility. Some fretting corrosion, accompanied by a local hydriding, was noted in 3 of the 12 areas examined. The reactor is heavy-water cooled and moderated, with an inlet water temperature to the tube of 4780°F and an outlet water temperature of 530°F. Operating pressure is approximately 1100 psig. (F. R. Shober)

Selected Mechanical Properties of Cladding and Structural Materials

Ductility of Chromium

A detailed study of the ductility of chromium and chromium-base alloys is in progress at Ames.[38] Data obtained to date indicate that working enhances the room-temperature ductility, but that annealing of the worked metal has a detrimental effect upon the tensile properties of the metal, particularly the ductility parameter. This is illustrated in Table IV-3.

A number of binary chromium-base alloys containing from 0.1 to 3.0 wt.% alloying addition were prepared by Ames[38] to study the effect of alloying on the transition temperature. Their results are presented in Table IV-4. Note that selected additions of the precious metals and refractory metals provide the lowest transition temperatures.

Table IV-3 TENSILE PROPERTIES OF ANNEALED CHROMIUM AT ROOM TEMPERATURE[38]

Prior treatment	Yield strength, psi	Elongation, %		Reduction in area, %
		Uniform	Total	
As swaged at 750°C	75,400	4	17.6	75.9
300°C anneal	73,700	11.2	26.4	33.2
350°C anneal	72,600	2.2	2.2	2.9
400°C anneal	74,100	0	1.4	0
500°C anneal	72,800	0	0.4	0
800°C anneal	58,000	0	0	0

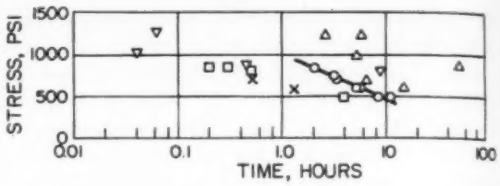

Fig. IV-1 Results of molybdenum stress-rupture tests in hydrogen and argon at 2200°C.[125] ○, Mo-A in hydrogen. □, Mo-B in hydrogen. ×, Mo-C in hydrogen. △, Mo-A in argon. ▽, Mo-B in argon.

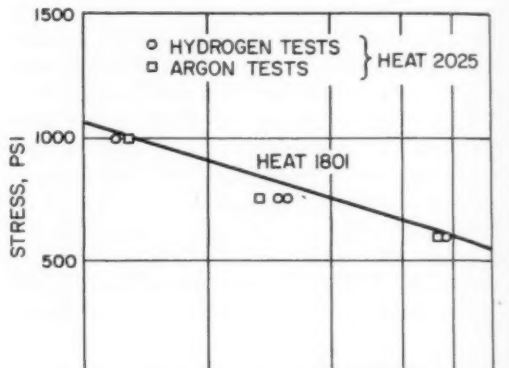

Fig. IV-2 Results of tantalum–10 wt.% tungsten sheet stress-rupture tests in hydrogen and argon at 2600°C.[125]

Properties of Refractory Metals

An article in *Materials in Design Engineering*[124] covers recent developments, properties, and new alloys of the six refractory metals, molybdenum, tantalum, niobium, tungsten, chromium, and vanadium. A table for refractory-alloy-sheet selection is presented.

General Electric[125] reports on tests being performed on a variety of high-temperature materials. Figure IV-1 shows the results of stress-rupture tests on three different types of molybdenum in hydrogen and argon. The strength of type Mo-A in argon is significantly higher than that in hydrogen. Figure IV-2

Table IV-4 BRITTLE-DUCTILE TRANSITION TEMPERATURES (BDTT) OF BINARY CHROMIUM-BASE ALLOYS[38]

Alloy, wt.%	BDTT, °C	Alloy, wt.%	BDTT, °C	Alloy, wt.%	BDTT, °C	Alloy, wt.%	BDTT, °C
3.0 Cu	>200	1.5 Pr	35	0.5 Al	−35	0.1 Re	−105
1.5 Cu	>82	3.0 Pr	20	0.5 Pd	15	3.0 Ag	−55
0.5 Cu	−20	3.0 Th	>25	0.1 Pd	−60	1.5 Ag	−70
1.5 Sn	>95	1.5 Th	>25	0.5 Ta	−55	0.5 Ag	−70
3.0 Sn	>25	0.5 Th	>25	0.5 Rh	−60	0.1 Ag	−55
0.5 Sn	>25	0.1 Hf	>25	0.1 Rh	−75	0.5 Ru	−75
0.1 Sn	−25	3.0 Y	5	0.1 Ir	>−40	1.5 Ru	−85
0.5 Gd	70	1.5 Y	5	1.5 Ir	−50	3.0 Ru	>−60
3.0 Gd	55	0.5 Y	5	0.5 Ir	−87	0.1 Ru	−85
1.5 Gd	50	3.0 V	25	0.1 Os	−85	3.0 Au	>25
0.5 Dy	60	1.5 V	15	0.5 Mo	−65	1.5 Au	>25
1.5 Dy	50	0.5 V	−15	3.0 Mn	−22	0.5 Au	>25
3.0 Dy	40	2.0 V	−20	3.0 Re	−35	0.1 Au	−82
3.0 Nd	35	1.0 V	−25	1.5 Re	−67	0.5 Pt	>−30
1.5 Nd	25	3.0 Al	>25	0.5 Re	−67	0.05 Pt	−75
0.5 Nd	10	1.5 Al	>−20			0.01 Pt	−125

shows the results of stress-rupture tests on tantalum−10 wt.% tungsten sheet in hydrogen and argon at 2600°C.

The effect of interstitial oxygen and hydrogen on the tensile and notch-tensile properties of tantalum, niobium, tantalum−10 wt.% tungsten, and F-48 alloy was studied by Battelle.[126] Oxygen and hydrogen additions were shown to increase notch sensitivity at higher temperatures, and the transition temperatures were increased by the interstitial additions. The F-48 alloy shows notch-sensitive behavior at higher temperatures and has a higher transition temperature than niobium. The tantalum−10 wt.% tungsten alloy was not notch sensitive and retained excellent ductility at −420°F.

Properties of Zirconium Alloys

The mechanical properties of a zirconium-base alloy 3Z1 (zirconium−1.23 wt.% aluminum−1 wt.% tin−1 wt.% molybdenum) are compared in Fig. IV-3 and Table IV-5 with those of Zircaloy-2 and other alloys. The 3Z1 alloy is far superior to Zircaloy-2. This work is being conducted by Atomics International.[37]

Long-term (~10,000 hr) creep tests under constant load and temperature and load cyclic conditions were conducted by Hanford[127] on Zircaloy-2 in the annealed and 15% cold-worked condition. For material in the annealed condition, creep behavior is substantially influenced by strain-age-hardening phenomena. Material in the 15% cold-worked condition creeps in a very regular and predictable fashion, and this condition is favored for general design applications. (J. A. DeMastry)

Selected Metallurgical Aspects of Cladding and Structural Materials

Miscellaneous Metals

The Russian workers, Svechnikov and Spektor,[128] in their report on the iron-zirconium phase diagram show a new temperature for triphase equilibrium, γ-iron-δ, or the second melting point, at 1345°C. The eutectic melting

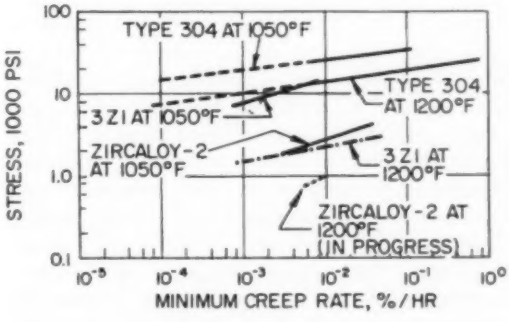

Fig. IV-3 Minimum creep rates of 3Z1, Zircaloy-2, and type 304 stainless steel.[37]

Table IV-5 TENSILE PROPERTIES OF TWO ZIRCONIUM-BASE ALLOYS[37]

Test temp., °F	Yield strength (0.2% offset), 1000 psi		Ultimate tensile strength, 1000 psi		Elongation, %	
					In 1 in.	In 2 in.
	Zr + 2 Sn + 2 Nb	3Z1	Zr + 2 Sn + 2 Nb	3Z1	Zr + 2 Sn + 2 Nb	3Z1
72	65.0	84.8	83.7	112.0	20	13
600	30.7	60.0	45.7	85.0	29	14
1000	23.2	43.0	35.4	63.0	36	36
1200	16.2	23.0	23.2	39.0	53	47

point was found at 1320°C, and this indicates a 25°C interval between the eutectic and second melting point. The solubility of zirconium in γ-phase iron at the eutectic melting point was approximately 1%.

The mechanism by which second-phase particles strengthen alloys was investigated by Aeronautical Research Laboratories.[129] Hardening in age-hardened nickel-aluminum and copper-cobalt alloys was found to be due to the precipitation of coherent-ordered Ni_3Al or cobalt particles, respectively. Both showed coherency strain fields that were particularly clear in the copper-cobalt alloys. The main contrast effects expected from coherent spherical particles were calculated and found to be consistent with those observed at cobalt particles. The shape and size of the cobalt particles agreed with earlier predictions based on bulk magnetic measurements. Overaging in copper-cobalt alloys was found to be caused partly by loss of full coherency that is helped by deformation. The presence of particles slightly decreased the spacing of fine slip lines in stretched samples. Dislocations apparently passed through the particles in nickel-aluminum, and commonly bowed out between particles, indicating local pinning. Particles substantially increased the dislocation density produced by stretching. After 5% strain, when the particle size was about 300 A, dislocations formed a network with particles at the nodes. In nickel-aluminum, dislocation tangles formed around each particle. In nickel-aluminum, particles substantially reduced or even eliminated the temperature dependence of the flow stress. This was first attributed to the elimination of thermally activated cross slip, but electron microscopic examinations did not show cross slip to be common in the solid solution. Preliminary observations indicated that the effect of particles on recovery is complex.

Internal friction peaks that appear in 10 metals after cold working were investigated at Tokyo University.[130] The ten metals are copper, silver, aluminum, nickel, titanium, zirconium, magnesium, cobalt, iron, and uranium. Two or three peaks, which disappear upon annealing at room temperature, were present in all metals. A peak that does not disappear after room-temperature annealing was found in some of the 10 metals. This peak was sometimes accompanied by a satellite. In the case of aluminum, this persistent peak is presumably different from the Bordoni peak. Activation energies and frequency factors were obtained from peak shifts which concerned all the peaks observed. Possible mechanisms for the processes responsible for these peaks are briefly discussed.

Ames[38] has examined the aluminum-tantalum alloy system. Two compounds believed to be peritectic in nature are reported. They are $TaAl_3$ (tetragonal) and Ta_2Al (tetragonal). X-ray data show that both compounds exhibit solid solubility. Incipient meltings of the stoichiometric compounds were observed for $TaAl_3$ at 1500 ± 50°C and for Ta_2Al at 2100 ± 50°C.

The solid solubility of lithium in aluminum has been determined by investigators at Du Pont.[131] Electrical resistivity and microhardness measurements indicate the solubility limits at 200, 300, 400, 500, and 600°C to be 6.0, 7.1, 8.5, 10.8, and 13.7 at.%, respectively. X-ray diffraction studies of the intermetallic compound LiAl indicate that its composition is nearly independent of temperature when it is in equilibrium with the terminal solid solution of aluminum.

Refractory Metals

Transmission-electron-microscopy techniques were used to study the process of

yielding and plastic flow in polycrystalline niobium by observing the dislocation substructure resulting from tensile deformation. This work was conducted at the University of California.[132] The tensile properties were found to vary markedly with the amount and distribution of impurity solute atoms, which, in turn, varied with the annealing conditions. Annealing at 1000°C resulted in the formation of networks of precipitate plates in addition to solute atom clusters. Annealing at higher temperatures, 1700 to 2100°C, resulted in a distribution of solute atom clusters 50 to 150 A in diameter.

Pratt & Whitney[133] has reviewed the work-hardening literature on refractory metals and published an analysis of these findings in the light of current dislocation theories. The results of niobium-crystal work-hardening studies at −196 to 100°C are also reviewed. The results of these investigations are applied in the interpretation of dislocation mechanisms and elevated-temperature creep mechanisms.

Zirconium Alloys

Atomics International[37] reports on the physical properties of 3Z1 (zirconium−1.23 wt.% aluminum−1 wt.% molybdenum). The data are shown in Table IV-6.

Table IV-6 ELECTRICAL RESISTIVITY AND THERMAL CONDUCTIVITY FOR 3Z1[37]

Temp., °F	Electrical resistivity, μohm-cm	Thermal conductivity, Btu/(hr)(ft)(°F)
200	128.2	4.84
400	134.0	5.80
600	137.8	6.79
800	140.3	7.80
1000	141.8	8.86
1200	141.8	9.97
1400	139.8	11.33
1600	133.0	13.04

Chalk River[134] investigators ran thermal cycling experiments on zirconium, Zircaloy-2, zirconium−2.9 wt.% niobium, and zirconium−0.07 wt.% niobium alloys. The variables examined included preferred orientation, grain size, alloy content, and time at temperature. Zirconium and zirconium−2.9 wt.% niobium alloys were found to be dimensionally unstable, whereas the zirconium−0.07 wt.% niobium alloy was stable. Zircaloy-2 showed variable but small amounts of growth or contraction on thermal cycling. (J. A. DeMastry)

Diffusion Studies

A useful bibliography of 165 selected references on diffusion in ceramic systems has been compiled at Ames.[135] Included are references to books, reports, and U. S. and foreign journals published from 1904 to 1961 on diffusion in oxides, silicates and glasses, borides, carbides, and graphites. The compilation gives data on the frequency factor, D_0, and the activation energy, Q_1, for various elements and ceramics.

An interesting theoretical analysis and discussion of enhanced diffusion in metals during plastic deformation has been prepared by Balluffi and Ruoff.[136] In their study they analyzed 14 sets of measurements on this effect. One case (perhaps two) of enhanced diffusion they consider to be due to cracks created during deformation. One case (and possibly two) of a measured enhancement is consistent with their analysis of pipe diffusion. One measured enhancement appears consistent with their analysis of the effect of rapid diffusion in migrating grain boundaries during deformation. One (and possibly two) measured set of enhancements they believe to be due to surface (interface) roughening produced by the deformation. The remaining sets of data showed no enhancement, and these results are consistent with their analyses of the conditions of these experiments.

In Russian work,[137] the self-diffusion coefficient of zirconium in the beta phase of Zircaloy-2 was found to be represented by

$$D = 6 \times 10^{-3} \exp(-40{,}000/RT)$$

This indicates that the activation energy for self-diffusion in Zircaloy-2 is appreciably higher than in pure zirconium.

(D. C. Carmichael)

Ceramic Technology

Investigators at Stanford Research Institute[138] are preparing single-crystal ZrO_2−2 wt.% CaO in an arc-image furnace, using a modified Verneuil method. The crystals are grown in air to sizes up to ⅛ in. in diameter and up to

$\frac{3}{4}$ in. long. They exhibited the cubic fluorite structure with $a = 5.118$ A. The direction of growth was consistently 8° off the [0 0 1] direction. When the crystals cracked, the fracture followed the (1 1 1) plane. The microhardness in the [0 0 1] direction was 2050 kg/mm^2. The crystals were highly strained and showed some substructure. Nonetheless they were relatively transparent (>40% transmission) over the wavelength range 0.37 to 6.7 μ.

Boules of polycrystalline pure monoclinic ZrO_2 were prepared in the arc-image furnace. These had average grain sizes ranging from 0.5 to 2 mm and showed extensive intergranular separation on cooling.

Vallecitos investigators[139] are studying some of the properties of selected rare-earth oxides and borates. M_2O_3 type oxides of samarium, europium, dysprosium, gadolinium, and erbium all have large, body-centered cubic structures, melting points exceeding 2000°C, and large negative free energies of formation. In addition, all have high absorption cross sections for thermal neutrons. This combination of properties makes the rare-earth oxides obvious candidates for control materials in high-temperature reactors, and General Electric has been looking into their suitability from the standpoints of corrosion resistance and radiation stability.

The oxides tend to hydrate even in room-temperature air. However, this can be remedied by small additions of TiO_2. Compatibility studies were made on the rare-earth oxides Eu_2O_3, Sm_2O_3, and Dy_2O_3 with the metals iron, nickel, type 304 stainless steel, Hastelloy B, Inconel X, molybdenum, tungsten, and niobium. Tests with the latter three metals were made at 1800 to 2000°C, and the remaining metals were tested at 1120 to 1200°C. The tests indicated that Eu_2O_3 was much more reactive than Sm_2O_3 and Dy_2O_3, the latter two reacting only with nickel. All three oxides were inert to molybdenum, tungsten, and niobium.

Rare-earth borates (MBO_3) also have potential as control materials. Materials of this class have melting points exceeding 1500°C. The borates studied in this work exhibited a phase transition to vaterite ($CaCO_3$) structure in the temperature range of 834 to 1041°C. The densities of the high-temperature forms were somewhat lower than those of the low-temperature forms. Borates of samarium, europium, gadolinium, dysprosium, and erbium are virtually inert to steam at 500°C and 1000 psi for 500 hr, and ErBO and $EuBO_3$ were shown to be inert with molybdenum and tungsten in 20-hr exposures at 1000°C.

Compacts of selected oxides and borates were irradiated in the General Electric Test Reactor at temperatures of 100 and 320°C and for exposure of 0.34 to 2.4×10^{21} nvt (thermal). The oxide specimen densities ranged from 89 to 97% of theoretical; the borates ranged from 42 to 66%. In almost every case, varying degrees of cracking or fragmenting occurred. The Sm_2O_3 and Eu_2O_3 specimens were softened by the irradiation, whereas Gd_2O_3 was hardened. Metallographic examinations of these three irradiated oxides showed no apparent structural changes. However, irradiated Eu_2O_3 exhibited no X-ray diffraction pattern, indicating gross structural damage.

These experiments indicate that rare-earth oxides and borates are of doubtful value for use as unsupported, monolithic control members. However, their use within a metal cladding, where cracking is less of a problem, remains a possibility. (A. K. Smalley)

References

1. Knolls Atomic Power Laboratory, Reactor Technology Report No. 22—Chemistry, USAEC Report KAPL-2000-19, September 1962.
2. J. P. Pemsler, Studies on the Oxygen Gradients in Corroding Zirconium Alloys, *J. Nucl. Mater.*, 7(1): 16-25 (September-October 1962).
3. D. W. Shannon, Electrical Properties of ZrO_2 Corrosion Films. Electrical Resistance Measurements. Interim Report No. 1, USAEC Report HW-75501, Hanford Atomic Products Operation, November 1962.
4. J. N. Wanklyn, C. F. Britton, D. R. Silvester, and N. J. M. Wilkins, The Corrosion of Zirconium and Its Alloys in High Temperature Steam. Part III. The Influence of the Environment on Oxidation, British Report AERE-R-4130, August 1962.
5. D. Weinstein and F. C. Holtz, Improved Zirconium Alloys. Quarterly Report, July 1–September 30, 1962, Report ARF-2198-34, Illinois Institute of Technology, Armour Research Foundation, Oct. 12, 1962.
6. E. Hillner and J. N. Chirigos, The Effect of Lithium Hydroxide and Related Solutions on the Corrosion Rate of Zircaloy in 680°F Water, USAEC Report WAPD-TM-307, Westinghouse Electric Corp., Bettis Atomic Power Laboratory, August 1962.

7. L. R. Lynam, E. F. Losco, G. J. Salvaggio, and J. G. Goodwin, Fabrication Defects Observed in PWR Core 1 Blanket Fuel Rods, USAEC Report WAPD-TM-321, Westinghouse Electric Corp., Bettis Atomic Power Laboratory, September 1962.
8. Atomic Energy of Canada, Ltd., 1962. (Unpublished)
9. Oak Ridge National Laboratory Status and Progress Report, September 1962, USAEC Report ORNL-3368, Oct. 5, 1962.
10. R. J. Lobsinger, Corrosion of X-8001 Aluminum and Zircaloy-2 Under Conditions of High Heat Transfer, USAEC Report HW-SA-2454, Hanford Atomic Products Operation, Apr. 27, 1962.
11. J. E. Draley, W. E. Ruther, and S. Greenberg, Aluminum Alloys with Improved High Temperature Aqueous Corrosion Resistance, *J. Nucl. Mater.*, 6(2): 157-171 (July 1962).
12. Hanford Atomic Products Operation, Research and Development Programs Executed for the Division of Reactor Development. Quarterly Progress Report, January–March 1962, USAEC Report HW-73915, Aug. 1, 1962.
13. C. R. Breden, Boiling Water Reactor Technology, Status of the Art Report, Volume II. Water Chemistry and Corrosion, USAEC Report ANL-6562. Argonne National Laboratory, February 1963.
14. S. Greenberg and W. E. Ruther, Effects of Oxygen and Surface Treatment on the Corrosion of Stainless Steels in Superheated Steam, USAEC Report ANL-FGF-381, Argonne National Laboratory, August 1962.
15. R. C. Ulmer, H. A. Grabowski, and R. C. Patterson, Water Treatment, Corrosion, and Internal Deposit Studies for Eddystone, *J. Eng. Power*, 82: 264-271 (1960).
16. A. E. Mravca (Comp.), Proceedings of the Nuclear Superheat Meeting No. 6, Windsor, Connecticut, March 7, 8, and 9, 1962, USAEC Report TID-7634, Mar. 30, 1962.
17. C. R. Bergen, Deposition and Release of Corrosion Products in SM-1, *Nucleonics*, 20(7): 70, 72, 74, 75 (July 1962).
18. C. B. Kenahan, D. Schlain, and W. L. Acherman, Chemical and Galvanic Corrosion Properties of High-Purity Vanadium, Report BM-RI-5990, Bureau of Mines, July 1961.
19. R. E. Clausing, Calculation of the Requirements for Operation of Refractory-Metal Components at High Temperature in Vacuum, USAEC Report ORNL-TM-334, Oak Ridge National Laboratory, Sept. 18, 1962.
20. J. A. DeMastry and A. A. Bauer, Development of Niobium-Base Alloys for Use in a Nuclear Superheater, Quarterly Progress Report—June 1962, USAEC-Euratom Report EURAEC-425 (BMI-X-10003), Battelle Memorial Institute, July 1, 1962.
21. P. Kofstad, Studies of Oxidation of Ta–10W at 700–1300°C. Technical Note No. 4, Norwegian Report ARL-62-377, March 1962.
22. E. A. Gulbransen, K. F. Andrew, F. A. Brassart, and P. E. Blackburn, Oxidation of Tungsten and Tungsten-Based Alloys, Report WADC-TR-59-575 (Part III), Westinghouse Electric Corporation, December 1961.
23. W. A. Gibeaut and J. J. English, DMIC Review—Oxidation-Resistant Coatings for Refractory Metals, DMIC Newsletter, Battelle Memorial Institute, Defense Metals Information Center, Nov. 2, 1962.
24. W. A. Gibeaut and J. J. English, DMIC Review—Oxidation-Resistant Coatings for Refractory Metals, DMIC Newsletter, Battelle Memorial Institute, Defense Metals Information Center, Jan. 25, 1963.
25. W. A. Gibeaut and D. J. Maykuth, Summary of the Sixth Meeting of the Refractory Composites Working Group, Report DMIC-175, Battelle Memorial Institute, Defense Metals Information Center, Sept. 24, 1962.
26. P. M. Arzhanyy, R. M. Volkova, and D. A. Prokoshkin, Kinetics of Oxidation of Niobium and Its Alloys, *Issled. po Zharoproch. Splavam. Akad. Nauk SSSR, Inst. Met.*,7: 214-220 (1961).
27. J. J. Rausch and F. C. Holtz, High-Temperature Oxidation Protective Coatings for Vanadium-Base Alloys, Report ARF-2227-6, Illinois Institute of Technology, Armour Research Foundation, Aug. 1, 1962.
28. J. B. Berkowitz, Kinetics of Oxidation in the Mo-Si System, Report ASD-TDR-62-203 (Pt. I), A. D. Little, Inc., March 1962.
29. C. Vanleugenghe, L. Kimczak-Mathieu, J. Meunier, and M. Pourbaix, The Behavior of Alloy Steels in Bicarbonate Solutions. The Effect of Chlorine and Oxidants, *Proceedings of the IAEA Conference on the Corrosion of Reactor Materials, Salzburg, Austria, June 4-8, 1962*, Vol. II, pp. 1-49, 1962.
30. Knolls Atomic Power Laboratory, Reactor Technology Report No. 22—Chemistry, USAEC Report KAPL-2000-19, September 1962.
31. R. L. Dillon, High Temperature Aqueous Corrosion in Nuclear Reactors, USAEC Report HW-SA-2745, Hanford Atomic Products Operation, Sept. 5, 1962.
32. Hanford Atomic Products Operation, Reactor and Fuels Laboratory, Monthly Report, January 1963, USAEC Report HW-76315A, Feb. 15, 1962. (Classified)
33. Hanford Atomic Products Operation, Reactor and Fuels Laboratory, Monthly Report, February 1963, USAEC Report HW-76596A, February 1963. (Classified)
34. Argonne National Laboratory, Reactor Development Program, Progress Report for February 1963, USAEC Report ANL-6698, Mar. 15, 1963.

35. Hanford Atomic Products Operation, Metallurgy Research Operation. Quarterly Progress Report, October–December, 1962, USAEC Report HW-76228, Jan. 15, 1963.
36. *Proceedings of the IAEA Conference on the Corrosion of Reactor Materials, Held at Salzburg, Austria, June 4-8, 1962.*
    a. J. R. Weeks and C. J. Klamut, Liquid Metal Corrosion Mechanisms, Vol. I, pp. 105-132.
    b. J. R. DiStefano and E. E. Hoffman, Relation Between Distribution and Corrosion in Some Refractory Metal-Lithium Systems, Vol. II, pp. 431-452.
    c. J. H. DeVan and R. B. Evans III, Corrosion Behavior of Reactor Materials in Fluoride Salt Mixtures, Vol. II, pp. 557-580.
    d. B. J. Thamer, Corrosion Tests With Molten Plutonium Fuels, Vol. II, pp. 285-318.
    e. W. E. Parkins, Corrosion Effects With Organic-Liquid Reactor Coolants, Vol. II, pp. 503-536.
    f. V. S. Lyashenko and B. A. Nevzorov, The Mechanism of Carbon Transfer in Liquid Sodium, Vol. II, pp. 373-408.
    g. V. S. Lyashenko, V. V. Zotov, and V. A. Ivanov, Resistance to Corrosion of Austenitic and Ferro-Perlitic Steels in a Stream of Liquid Sodium at Temperatures of 600°C and 700°C, Vol. I, pp. 297-315.
    h. Y. Imai, T. Ishizaki, K. Nishino, and T. Masumoto, Corrosion and Erosion of Ferritic Steels by Liquid Bismuth, Vol. II, pp. 51-65.
    i. G. Ito, Y. Shimizu, and F. Sawayanagi, Corrosion of Metallic Materials in Organic Reactor Coolants, Vol. II, pp. 335-344.
37. Atomics International, Annual Technical Progress Report, AEC Unclassified Programs, Fiscal Year 1962, USAEC Report NAA-SR-7400, Nov. 15, 1962.
38. Ames Laboratory, Annual Summary Research Report in Chemistry, Engineering, Metallurgy, and Physics, July 1, 1961–June 30, 1962, USAEC Report IS-500, September 1962.
39. E. M. Simons, Spur Program Phase II Subcontract, Final Technical Report Covering Period July 15, 1962, Through January 15, 1963, to AiResearch Manufacturing Co. of Arizona, Battelle Memorial Institute.
40. G. W. Wensch and B. E. Prince, AEC Division of Reactor Development, May 1962. (Unpublished)
41. Aerojet-General Nucleonics, Rubidium Corrosion and Solubility Study; Topical Report for Period February 1, 1961–July 31, 1962, USAEC Report AGN-8063.
42. MSA Research Corporation, Effect of 1200°F Sodium on Austenitic and Ferritic Steels. Physical Properties of Materials. Progress Report No. 25, September 1962, USAEC Report MSAR-62-126, Oct. 19, 1962.
43. P. E. Novak and J. M. Gerhart, Performance of Rejected Ceramic Fuel in Sodium, *Trans. Am. Nucl. Soc.*, 5(2): (November 1962).
44. H. J. Chick (Comp.), Bibliography on Corrosion by Liquid Metals (1957–September 1962), USAEC Report LAMS-2779, Los Alamos Scientific Laboratory, Oct. 12, 1962.
45. Argonne National Laboratory, Reactor Development Program Progress Report, October 1962, USAEC Report ANL-6635, Nov. 15, 1962.
46. Argonne National Laboratory, Reactor Development Program Progress Report, November 1962, USAEC Report ANL-6658, Dec. 15, 1962.
47. Argonne National Laboratory, Reactor Development Program Progress Report, December 1962, USAEC Report ANL-6672, Jan. 15, 1963.
48. Argonne National Laboratory, Reactor Development Program Progress Report, February 1963, USAEC Report ANL-6698, Mar. 15, 1963.
49. R. R. Coltman, Jr., C. E. Klabunde, D. L. McDonald, and J. K. Redman, Reactor Damage in Pure Metals, *J. Appl. Phys.*, 33: 3509-3525 (December 1962).
50. A. Sosin, Irradiation Pinning and Thermal Depinning of Dislocations, *Acta Met.*, 10: 390-396 (April 1962).
51. D. O. Thompson, A Thermally Activated Internal Friction Spectrum in Copper Following Neutron Irradiation, *Acta Met.*, 10: 327-331 (April 1962).
52. V. K. Pare and D. O. Thompson, Temperature Dependence from 250°K to 370°K of Dislocation Pinning in Copper Single Crystals by Radiation Defects, *Acta Met.*, 10: 382-389 (April 1962).
53. J. N. Lomer and D. H. Niblett, Some Effects of Electron Irradiation on the Internal Friction of Copper, *Phil. Mag.*, 7: 1211-1222 (July (1962).
54. A. I. Zakharov, The Problem of the Effect of Neutron Irradiation on the Modulus of Elasticity and the Damping Capacity of Copper, *Fiz. Metal. i Metalloved.*, 13: 241-247 (1962).
55. D. Gelli, T. Federighi, and F. Pieragostini, Neutron Irradiation Effects on Dislocation Damping in Cold-Worked Aluminum, *Phil. Mag.*, 7: 1791-1794 (1962).
56. B. L. Eyre, Direct Observations of Neutron Irradiation Damage in α-Iron, *Phil. Mag.*, 7: 2107-2113 (December (1962).
57. M. L. Swanson, G. R. Piercy, and D. J. Mackinnon, Effect of Plastic Deformation on Neutron Irradiation Damage in Copper and Aluminum at 1.8°K, *Phys. Rev. Letters*, 9: 418-421 (Nov. 15, 1962).
58. R. S. Nelson, M. W. Thompson, B. W. Farmery, and M. J. Hall, Evidence for Focused Recoil Trajectories from a High Energy Sputtering Experiment with Copper, *Phys. Letters*, 2: 124-126 (Sept. 1, 1962).
59. R. S. Nelson and B. W. Farmery, Focused Collision Sequences in Tungsten and Molybdenum, *Phil. Mag.*, 8: 693 (1963).
60. M. W. Thompson, R. S. Nelson, and B. W.

Farmery, Evidence for Heated Spikes in Bombarded Gold from the Energy Spectrum of Atoms Ejected by 43 kev A^+ and Xe^+ Ions, *Phil. Mag.*, 7(84): 2015-2026 (December (1962).

61. H. E. Kissinger, Diffraction Effects from Irradiated Aluminum Single Crystals, USAEC Report HW-SA-2538, Hanford Atomic Products Operation, July 31, 1962.
62. F. W. Young, Jr., Etch Pit Studies of Dislocations in Copper Crystals Deformed by Bending: I Annealed Crystals; II Irradiated Crystals, *J. Appl. Phys.*, 33: 3553-3564 (December 1962).
63. M. deJong and J. S. Koehler, Diffusion of Single Vacancies and Divacancies in Quenched Gold, *Phys. Rev.*, 129: 40-49 (Jan. 1, 1963).
64. M. deJong and J. S. Koehler, Annealing of Pure Gold Quenched from Above 800°C, *Phys. Rev.*, 129: 49-61 (Jan. 1, 1963).
65. R. P. Huebener and C. G. Homan, Pressure Effect on Vacancy Formation in Gold, *Phys. Rev.*, 129: 1162-1168 (Feb. 1, 1963).
66. P. DeFeo and G. Sacerdoti, Decay of Trapped Flux in a Superconducting Ring Subjected to Irradiation by α-Particles from a Po^{210} Source, *Phys. Letters*, 2: 264 (Oct. 15, 1962).
67. M. Nachman, G. Glanz, and L. Ribco, Oxidation of Silver Induced by Nuclear Radiation, *Rev. Phys., Acad. Rep. Populaire Roumaine*, 6: 403-409 (1961).
68. W. V. Cummings and W. I. Clark, Radiation Effects in Borides. Part III. Crystallographic Changes in Irradiated Borides, USAEC Report GEAP-3743 (Pt. III), Vallecitos Atomic Laboratory, May 31, 1962.
69. Atomic Energy of Canada, Ltd., 1962. (Unpublished)
70. F. E. Fujita and A. C. Damask, The Influence of Radiation-Produced Defects on the Precipitation of Carbon in Iron, USAEC Reports BNL-6248 and BNL-6333, Brookhaven National Laboratory, 1962. This paper was presented at the International Conference on Crystal Lattice Defects held in Kyoto, Japan, Sept. 7-12, 1962.
71. H. C. Claiborne, An Estimate of the Effect of Neutron-Energy Spectrum on Radiation Damage of Steel, USAEC Report ORNL-TM-299, Oak Ridge National Laboratory, July 27, 1962.
72. A. D. Rossin, Significance of Neutron Spectrum on Radiation Effects Studies, USAEC Report TID-17211, Argonne National Laboratory, August 1962.
73. J. H. W. Simmons, Atomic Energy Research Establishment, personal communication to R. E. Nightingale, Hanford Atomic Products Operation.
74. C. Baker and A. Kelly, Energy To Form and To Move Vacant Lattice Sites in Graphite, *Nature*, 193: 235 (1962).
75. D. G. Schweitzer, Activation Energy for Annealing Single Interstitials in Neutron-Irradiated Graphite and the Absolute Rate of Formation of Displaced Atoms, *Phys. Rev.*, 128: 556-559 (Oct. 15, 1962).
76. S. Weissmann, T. Imura, K. Nakajima, and S. E. Wisnewski, Lattice Defects of Quartz Induced by Fast Neutron Irradiation, Technical Report No. 1, USAEC Report NYO-10444, Rutgers University, September 1962.
77. S. Weissmann and K. Nakajima, Defect Structure and Density Decrease in Neutron-Irradiated Quartz, Technical Report No. 2, USAEC Report NYO-10445, Rutgers University, September 1962.
78. P. B. Price and R. M. Walker, Observations of Charged-Particle Tracks in Solids, *J. Appl. Phys.*, 33: 3400-3406 (December 1962).
79. P. B. Price and R. M. Walker, Chemical Etching of Charged-Particle Tracks in Solids, *J. Appl. Phys.*, 33: 3407-3412 (December 1962).
80. P. B. Price and R. M. Walker, A New Track Detector for Heavy Particle Studies, *Phys. Letters*, 3: 113-115 (Dec. 15, 1962).
81. J. J. Kelsch and O. F. Kammerer, Observation of the $Li^6(n,\alpha)H^3$ Reaction by Electron Microscopy of Li^6F Films, USAEC Report BNL-6082, Brookhaven National Laboratory, 1962.
82. C. B. Childs and L. Slifkin, Detection of Nuclear Disintegrations Produced by 1.55 Bev Protons in Silver Chloride Single Crystals, *Phys. Rev. Letters*, 9: 354-355 (Oct. 15, 1962).
83. C. B. Childs and L. M. Slifkin, Delineation of Tracks of Heavy Cosmic Rays and Nuclear Processes with Large Crystals of Silver Chloride, *Rev. Sci. Instr.*, 34: 101-104 (January 1963).
84. T. K. Bierlein and B. Mastel, Fission-Induced Vaporization of UO_2 from a Source and Subsequent Condensation on Collectors Exposed to Fission Fragment Bombardment, *J. Nucl. Mater.*, 7: 32-37 (1962).
85. M. D. Rogers and J. Adam, Ejection of Atoms from Uranium by Fission Fragments, *J. Nucl. Mater.*, 6: 182-189 (1962).
86. J. S. Nadeau, Color Centers and Flow Stress of LiF Single Crystals, *J. Appl. Phys.*, 33: 3480-3486 (December 1962).
87. P. W. Levy, Direct Measurement of the Vacancies Produced in Sodium Chloride by Fast Reactor Neutrons, *Phys. Rev.*, 129: 1076-1085 (Feb. 1, 1963).
88. T. Hibi and K. Yada, Direct Observation of Crystal Imperfections in KCl Single Crystals by Electron Microscope, *J. Appl. Phys.*, 33: 3530-3536 (December 1962).
89. M. Lambert, S. Lefebvre, and A. Guinier, Study, by X-Ray Diffraction, of Defects Formed in a Single Crystal of LiF Irradiated by Thermal Neutrons at −195°C, *Compt. Rend.*, 225(1): 97-99 (July 2, 1962).
90. H. B. Charman and R. M. Dell, Fast Neutron Damage at the Surface of Metal Oxides, *Phys. Chem. Solids*, 23: 1567-1570 (1962).
91. O. S. Oen and M. T. Robinson, The Effect of

Channeling on Displacement Casdade Theory, *Appl. Phys. Letters*, 2: 83-85 (Feb. 15, 1963).

92. D. G. Besco and J. R. Beeler, Jr., Computer Programs Describing Collision Cascades in Binary Materials. I. Square Planar Lattice, USAEC Report GEMP-192, General Electric Company, Flight Propulsion Laboratory Department, February 1963.
93. P. E. McElligott, K. R. Jordan, and R. J. Allio, The Effect of Anisotropic Neutron Scattering on Radiation Damage, USAEC Report TID-11164, Knolls Atomic Power Laboratory, Nov. 9, 1960.
94. B. N. Finkel'shtein and Yu. L. Khait, Theory of Defects Arising in Solids by Atomic Recoil from Gamma-Emission, *Dokl. Akad. Nauk. SSSR*, 114: 85-88 (May 1, 1962).
95. J. A. Baicker, H. Flicker, and J. Vilms, Proton Induced Lattice Displacements in Silicon, *Appl. Phys. Letters*, 2: 104-106 (Mar. 1, 1963).
96. B. N. Finkel'shtein and Yu. L. Khait, The Theory of Defects Formed in Solids by Recoil Atoms During Gamma Radiation, *Soviet Phys. "Doklady" (English Transl.)*, 7: 394-396 (November 1962).
97. P. Hoekstra and D. R. Behrendt, Energies of Two Interstitial Configurations in a Face-Centered Cubic Crystal, *Phys. Rev.*, 128: 560-561 (Oct. 15, 1962).
98. A. Corciovei, G. Ghika, and D. Grecu, The Distribution Function of Irradiation-Displaced Atoms in Solids, *Rev. Phys., Acad. Rep. Populaire Roumaine*, 7: 227 (1962).
99. B. Ya. Yur'kov, Concerning the Theory of Annealing of Radiation Defects, *Soviet Phys.—Solid State (English Transl.)*, 3: 2591-2596 (June 1962).
100. G. J. Dienes and A. C. Damask, Kinetics of Vacancy-Interstitial Annihilation III. Interstitial Migration to Sinks, *Phys. Rev.*, 128: 2542-2546 (Dec. 15, 1962).
101. B. Ya. Yur'kov, The Effect of Annealing on the Spatial Distribution of Radiation Defects in Silicon, *Soviet Phys.—Solid State (English Transl.)*, 4(4): 626-628 (October 1962).
102. R. L. Fleischer, Solution Hardening by Tetragonal Distortions: Application to Irradiation Hardening in F. C. C. Crystals, *Acta. Met.*, 10: 835-842 (1962).
103. A. H. Cottrell, Theoretical Aspects of Radiation Damage and Brittle Fracture in Steel Pressure Vessels, *Ing. Nucleare*, 4: 131-141 (July–August, 1962).
104. Effects of Neutron Irradiation in Nonfissionable Metals and Alloys, Austrian Report STI/PUB/21/6, 1962.
105. V. V. Pen'kovskii, *Deistvie Oblucheniya na Metally I Nekotorye Tuboblavkie Materialy*, Publishing House of the Academy of Science, Kiev, Ukrainian SSSR, 1962.
106. A. N. Goland, Atomic Displacements in Solids by Nuclear Radiation, *Ann. Rev. Nucl. Sci.*, 12: 243-284 (1962).
107. A. N. Goland, The Role of the Electron Microscope in the Observation of Radiation Damage, USAEC Report MRL-126, Watertown Arsenal, Materials Research Laboratory, November 1962.
108. F. Seitz, The Effects of Irradiation on Metals, *Rev. Mod. Phys.*, 34: 656-666 (1962).
109. F. Seitz, The Effects of Irradiation on Metals, *Science*, 138: 563-571 (Nov. 2, 1962).
110. A. Scharmann, Radiation Damage in Solids, *Kerntechnik*, 4: 159-161 (April 1962).
111. R. E. Nightingale, Radiation Effects in Graphite, USAEC Report HW-SA-2394, Hanford Atomic Products Operation, May 11, 1962.
112. J. J. Stobbs, Effects of Radiation on Metallic Corrosion, *Met. Rev.*, 7: 95-131 (1962).
113. Radiation Effects State of the Art, 1961-1962, Report REIC-24, Battelle Memorial Institute, Radiation Effects Information Center, June 30, 1962.
114. *Proceedings of the IAEA Symposium on Radiation Damage in Solid and Reactor Materials, Held at Venice, Italy, May 7-11, 1962.*
    a. J. LeMaire, E. Cibois, and M. Weisz, A Study of Neutron-Irradiation-Induced Embrittlement of Weldable Manganese-Molybdenum Steels, Vol. II, pp. 153-188.
    b. J. LeMaire, T. L. Bernard, E. Cibois, and M. Weisz, The Effects of Irradiation on the Mechanical Properties of Zircaloy-2, Vol. II, pp. 27-53.
115. J. J. Prislinger, Results of Tensile Tests Performed on Materials Exposed in the Homogeneous Reactor Experiment No. 2 Blanket and Low-Flux-Core Region, USAEC Report ORNL-TM-337, Oak Ridge National Laboratory, Oct. 2, 1962.
116. M. Grounes and H. P. Myers, Swedish Studies on Irradiation Effects in Structural Materials, Swedish Report AE-90, December 1962.
117. D. R. Harries, P. J. Barton, and S. B. Wright, The Effects of Neutron Spectrum and Dose Rate on Radiation Hardening and Embrittlement in Steels, British Report AERE-R-4222, December 1962.
118. D. R. Harries, G. H. Wooldridge, and I. H. McWilliam, The Effects of Neutron Irradiation at 250°C on the Tensile and Impact Properties of a 1% Cr: 0.5% Mo Pressure Vessel Steel, British Report AERE-R-4193, September 1962.
119. D. W. McLaughlin, Neutrons Embrittle Reactor Vessels of Carbon Steel, *Nucleonics*, 21(2): 36-41 (February 1963).
120. W. E. Murr, F. R. Shober, R. Lieberman, and R. F. Dickerson, Effects of Large Neutron Doses and Elevated Temperature on Type 347 Stainless, USAEC Report BMI-1609, Battelle Memorial Institute, Jan. 21, 1963.
121. W. E. Murr and F. R. Shober, Annealing Studies

of Irradiated Type 347 Stainless, USAEC Report BMI-1621, Battelle Memorial Institute, Mar. 6, 1963.

122. M. B. Reynolds, Slow Cycle Strain Fatigue in Thin Wall Tubing: Preliminary Report, USAEC Report GEAP-3983, Vallecitos Atomic Laboratory, July 19, 1962.
123. L. J. Defferding, Postirradiation Evaluation of Zircaloy-2 PRTR Pressure Tubes. Part I, USAEC Report HW-73698 (Rev.), Hanford Atomic Products Operation, November 1962.
124. D. Peckner, Refractory Metals Roundup, *Mater. Design Eng.*, 56(4): 131-146 (October 1962).
125. General Electric Company, Flight Propulsion Laboratory Department, High-Temperature Materials Program, Progress Report No. 17, Part A, USAEC Report GEMP-17A, Nov. 15, 1962.
126. A. G. Imgram, M. W. Mallett, B. G. Koehl, E. S. Bartlett, and H. R. Ogden, Notch Sensitivity of Refractory Metals, Report ASD-TR-61-474, Battelle Memorial Institute, January 1962.
127. P. J. Pankaskie, Creep Properties of Zircaloy for Design Application, USAEC Report HW-SA-2803, Hanford Atomic Products Operation, Oct. 10, 1962.
128. V. N. Svechnikov and A. Ts. Spektor, Verification of Fe-Zr Alloy Equilibrium Phase Diagrams, *Sb. Nauchn. Rabot Inst. Metallofiz. Akad. Nauk Ukr. SSR, No. 11*, 30-35 (1960).
129. V. A. Phillips, R. W. Guard, and J. D. Livingston, Research on Dispersion Hardening, Report ARL-62-357, Aeronautical Research Laboratories, May 1962.
130. R. R. Hasiguti, N. Igot, and G. Kamosheta, Internal Friction Peaks in Cold Worked Metals, *Acta Met.*, 10: 442-447 (April 1962).
131. L. P. Costas and R. P. Marshall, The Solubility of Lithium in Aluminum, *Trans. AIME*, 224: 970-974 (October 1962).
132. L. I. Van Torne, Yielding and Plastic Flow of Polycrystalline Niobium, USAEC Report UCRL-10356, University of California, Lawrence Radiation Laboratory, August 1962.
133. D. P. Gregory and G. H. Rowe, Mechanisms of Work Hardening in Body Centered Cubic Metals, USAEC Report PWAC-375, Pratt & Whitney Aircraft Division, July 12, 1962.
134. D. G. Evans, Some Preliminary Experiments in the Thermal Cycling of Zirconium and Zirconium Alloys, Canadian Report CRGM-1106, August 1962.
135. M. F. Berard, Diffusion in Ceramic Systems, A Selected Bibliography, USAEC Report IS-448, Ames Laboratory, May 1962.
136. R. W. Balluffi and A. L. Ruoff, On Enhanced Diffusion in Metals During Plastic Deformation, USAEC Report TID-16372, Aug. 7, 1962.
137. G. B. Fedorov and F. I. Zhomov, Self-Diffusion of Zirconium in the Beta-Phase of Zircaloy-2 (in Russian), *Met. i Metalloved. Chistykh Metal.*, (3): 43-45 (1961).
138. F. A. Halden and R. Sedlacek, Growth and Evaluation of Boron Suboxide and Zirconium Dioxide Single Crystals, Report ARL-63-2, Stanford Research Institute, October 1962.
139. E. W. Hoyt, W. V. Cummings, D. L. Zimmerman, and H. E. Perrine, Rare Earth Oxides and Rare Earth Borates—Corrosion, Compatibility, and Radiation Effects, USAEC Report GEAP-3909, Vallecitos Atomic Laboratory, April 1962.

Section V

Reactor Materials

Special Fabrication Techniques

Melting, Hot and Cold Working

The increased emphasis that is presently being placed on high-temperature materials is reflected in the number of laboratories concerned with the preparation and fabrication of the refractory metals. Nuclear Metals has reported[1] on the preparation of tungsten–2 at.% ruthenium and tantalum–2 at.% ruthenium alloy ingots, utilizing inert-gas tungsten-electrode arc-melting techniques. The elemental powders were blended, cold pressed, and then melted. The production of tungsten tubing by coextrusion techniques that utilize mild steel, stainless steel, and molybdenum as both can and core for the sintered tungsten powder is also being investigated. Densification of the tungsten was achieved by extruding it in a molybdenum can at 1800°C, using reduction ratios of 16 to 1.

Further reference to tungsten-alloy preparation and fabrication was noted in reports from Los Alamos,[2] Wah Chang,[3] and Westinghouse.[4] The research conducted at Los Alamos was concerned with the effects of up 25% of ultrafine powder mixed with commercial tungsten powders of 2-, 4.5-, and 6.8-μ average particle size. The highest density was achieved in the sintered material containing the largest addition of ultrafine powder to the 2-μ particle-size commercial powder. Wah Chang reported the successful extrusion of cast tungsten–3 wt.% molybdenum alloy into T-sections utilizing a die with an entry angle of 130°, a billet temperature of 3100 to 3200°F, and a reduction ratio of 18 to 1. The Westinghouse research was initially conducted on the tungsten–6 wt.% molybdenum–2 wt.% niobium alloy. It was stated that the latter alloy could not be melted satisfactorily owing to thermal cracking of the ingot but that this difficulty was alleviated by reducing the niobium content from 6 to 2 wt.%. It was also stated that, owing to meltback and disintegration of the electrode, banding occurred in the ingots. This difficulty can often be overcome by redesign of the electrode to inhibit the flow of the low-melting-point constituent prior to the melting of the adjacent material.

Nuclear Metals is engaged in a study[5] designed to relate the properties of various binary refractory alloys to their phase diagrams, microstructure, and thermal history. All the alloys were prepared by nonconsumable arc-melting techniques, followed by extrusion in molybdenum cans.

An interesting technique was used in the preparation of F-48 sheet by General Electric.[6] Investigators employed hot pressing to consolidate relatively low-cost hydrided powder to yield material that was approximately 90% as strong and equally as ductile as arc-cast material made from high-cost electron-beam-melted niobium.

The fabrication of iodide chromium and chromium containing up to 200 ppm nitrogen is being studied at Iowa State University.[7] The materials, encapsulated in mild steel, were swaged at 750°C, and ample time to reach this temperature was permitted between passes. The same technique proved satisfactory for rolling materials that contained up to 50 ppm nitrogen, but this proved inadequate for materials with higher nitrogen concentrations. The materials that contained greater than 50 ppm nitrogen were jacketed in stainless steel and then rolled at 800 to 850°C to sheet of excellent quality.

Results of investigations concerned with the preparation, fabrication, and evaluation of fuel materials for reactor applications are reported by numerous sites. The National Lead Co. of

Ohio[8] continues its efforts to utilize uranium scrap for remelt stock and to find less costly and more satisfactory fabrication techniques. The latest evaluations were concerned with the use of pickled drip crops as remelt feed stock. The results of the investigations showed that this material was deleterious to the quality of the uranium fuel cores and should not be used as remelt feed for the production of reactor-grade uranium ingots. National Lead has also issued a report[9] that details studies of the feasibility of rotary-piercing reactor-grade uranium in the high-alpha temperature range. From these studies reliable data were obtained for establishing limits for the preheat temperature, deformation rates, and roll-pass designs for future tests. Bridgeport Brass[10] has also studied the feasibility of rotary-piercing uranium. All attempts by Bridgeport to fabricate in the alpha region failed, but it was demonstrated that fabrication might be accomplished in the gamma region.

Nuclear Metals[1] and Phillips[11] are investigating a number of uranium-alloy fuels. The study at Nuclear Metals has just been initiated, and an attempt will be made to improve the resistance to swelling during irradiation by dispersing fine metallic powders in the uranium. This study will be interesting to follow, not only in relation to the properties that may be imparted to the uranium but also with respect to the distribution of the additives in the melt. Nuclear Metals[12] is also conducting a program concerned with developing an improved uranium-alloy fuel. Of particular interest are additions of aluminum, silicon, iron, and chromium on the order of 150 to 500 ppm. Latest indications are that an alloy of uranium–350 ppm iron–450 ppm aluminum–350 ppm silicon–150 ppm chromium possesses an extrusion constant approximating 27 tsi. This is much higher than the extrusion constant of unalloyed uranium and indicates that this composition possesses relatively high strength at the extrusion temperature.

Hanford[13] is continuing its research on thorium-base alloys that contain uranium. Twenty-four-pound thorium–25 wt.% uranium and thorium–2.5 wt.% uranium–1 wt.% zirconium ingots have been made by double consumable-electrode arc-melting techniques. The zirconium addition improved the surface appearance of the ingot. Apparently it increases the fluidity of the melt and lowers the melting point of the alloy slightly. It was also noted that zirconium lowered the room-temperature hardness of the alloy from 94 to 72 BHN, but it had no significant effect on the extrusion force at the 760°C preheat temperature.

(N. E. Daniel)

Cladding

Cladding by Rolling and Swaging

Bloomster and Nelson at Hanford have been investigating the roll cladding of a plutonium–15 wt.% zirconium alloy with zirconium.[14,15] Aluminum foil previously used in these studies as a barrier material was eliminated in the most recent packs. The formation of brittle compounds at the core-to-cladding interface ceased to be a problem. A tentative roll-bonding process was proposed for fabricating these fuel elements. The core alloy is cold rolled to thickness and sheared to size. The core is then assembled into a zirconium picture frame and canned in a mild-steel pack. Hot rolling is done at 840°C to a 12-to-1 reduction in thickness. A total of 14 to 17 passes are used. The fuel plate is then stripped from the pack and finally sized. Apparently zirconium self-bonding occurs between 90 and 93% reduction.

Battelle[16] issued a final report concerning the roll-form bonding of a tube joint that is used in NPD-2 and CANDU reactor design. The objective of the study was to form a cold weld between Zircaloy-2 and type 410 stainless-steel tubular members. The first part of the study dealt with cold-roll bonding of flat-plate samples. Bonding was achieved at reductions as low as 34% in one pass. When the program was expanded to the tubular configuration, it was found that the roll-forming equipment was not capable of producing the reductions necessary. However, pressure-tight joints were achieved with a soft silver-alloy inlay in the joint interface.

Cummings, Lewis, and Blood at General Electric examined type 304 stainless-steel cladding for UO_2 fuel in the as-received condition and also after it was cold swaged and tandem rolled.[17] Metallographic examination of the cladding showed an expected cold-work texture with a limited amount of UO_2 penetration of the cladding inside diameter. At a symposium on powder-packed UO_2 fuel elements,[18] the inves-

tigators agreed that the use of high-particle-density low-surface-activity powder was preferable for swaging.

General agreement was also reached on the following:

1. With increasing reduction in area, the density increased until a maximum was reached.
2. The maximum density was different for different tube diameters and types of UO_2 powders.
3. For a given starting density and swaging reduction, lower densities were obtained for larger tube diameters.
4. The variation in local density along the length of the rod was usually within ± 1%; values as low as ± 0.5% were attained.

Several other reports appeared on the swage cladding and densification of UO_2. Although most of the data reported are not significantly new, some of the more detailed reports are listed for the interested reader.[19–22]

(H. D. Hanes and R. J. Diersing)

Pressure Bonding

Mixtures of oxides were developed[23] to provide high-density green cores that were "active" during the pressure-bonding cycle. Green densities up to 86% of theoretical were attained by pressing at 50 tsi. Cores containing 30 to 60 wt.% ceramic oxide in a fused oxide demonstrated the most promise. Rod, flat plate, and tubular fuel geometries were studied in which type 304 stainless steel was used as the cladding material. Bonding conditions of 3 hr at 2100°F and 10,000 psi were found to yield optimum properties for the stainless-steel bonds and also produced final oxide densities of up to 99.5% of theoretical. Helium permeability and thermal-conductivity measurements yielded values consistent with those reported for pressed-and-sintered oxides of equivalent density.

Diffusion Bonding

An interesting study of the diffusion bonding of various dissimilar alloys has been continued by General Electric.[24] The tensile shear strengths of lap joints diffusion bonded between (1) niobium–1 wt.% zirconium and type 316 stainless steel, (2) niobium–1 wt.% zirconium and copper, and (3) copper and type 316 stainless steel were determined. These combinations are not amenable to joining by welding or brazing due to their great differences in melting point and/or thermal conductivity. During diffusion bonding at 1800°F, the niobium-to-stainless-steel joint forms an intermetallic at the interface, the niobium-to-copper joint exhibits neither intermetallic formation nor extensive interdiffusion, and the copper-to-stainless-steel joint forms a rather wide, ductile diffusion zone at the interface. In the strength tests at room temperature, the two couples in which copper is a component exhibited high bond strength that is attributed to solution strengthening and the absence of brittle intermetallics at the interface. In the niobium–stainless-steel system, however, the hard intermetallic layer that is formed led to failure of the bond interface.

Investigations have also been conducted on the diffusion bonding of beryllium to type 316 stainless steel, using a bonding temperature of 1800°F for 4 hr. The diffusion bond formed was extremely brittle and fractured during cooling or metallographic preparation. Also, cracks originated from microhardness indentations in the stainelss-steel zone into which beryllium had diffused.

Experiments by the investigators at General Electric have, in the past, shown that brittle intermetallic layers are formed between molybdenum–0.5 wt.% titanium and a cobalt-base (L-605) or a nickel-base (René 41) alloy. The effect of a chromium barrier at these interfaces has therefore been investigated. A 1-mil-thick layer of electroplated chromium was found to be an effective barrier in limiting the intermetallic formation and the attendant brittleness in a bond with the nickel-base alloy formed at 1800°F for 4 hr. In a molybdenum–0.5 wt.% titanium–chromium–L-605 specimen, however, fracture of the joint occurred near the chromium–L-605 interface. It has not yet been ascertained whether the poor bond is due to poor quality of the chromium plating or to the formation of a chromium-rich carbide layer.

In a separate study at General Electric,[25] the diffusion bonding of a variety of refractory metals and alloys is being investigated. The process consists of placing the surfaces of the metals together and heating to 1370 to 2200°C in a vacuum of 2×10^{-5} mm Hg. An applied pressure of 5 psia is used on the specimen. Recrystallization is not a limiting factor in fabricating refractory metals by diffusion bond-

Table V-1 REQUIRED TEMPERATURES REPORTED BY GENERAL ELECTRIC[25] FOR SOLID-STATE DIFFUSION BONDING OF REFRACTORY METALS

Bonded material	Temperature, °C								
	W	W–26 Re	Re	Ta	Ta–10 W	Mo	Mo–50 Re	Nb	V
W	1930	1930	1630	1930	2200	1640	2200*	1640	1370
W–26 Re	1930	1930	2200	1930	2200	1640	2200*	1640	1370
Re	1630	2200	2200	2200	1930	1930	2200*	1640	
Ta	1930	1930	2200	1930	2200	1640	2200*	1640	1370
Ta–10 W	2200	2200	1930	2200	1930	1930	2200*	1640	
Mo	1640	1640	1930	1640	1930	1640	2200*	1640	1370
Mo–50 Re	2200*	2200*	2200*	2200*	2200*	2200*	2200*		
Nb	1640	1640	1640	1640	1640	1640		1640	1370
V	1370	1370		1370		1370		1370	1370

*Only bonding temperature was surveyed.

ing for the space applications of interest, because the anticipated service temperatures are several hundred degrees above bonding temperatures. The investigators have determined the temperatures required to initiate bonding between various refractory metals, and these temperatures are shown in Table V-1. Stress-rupture tests at 2200 to 2600°C of self-bonds of tantalum, tantalum–10 wt.% tungsten, molybdenum, and molybdenum–50 wt.% rhenium are reported to have given good results. (D. C. Carmichael)

Coextrusion

Coextrusion techniques are being developed[13] for cladding thorium–2.5 wt.% uranium alloy cores with Zircaloy-2. Initial pilot runs were aimed at producing 0.875-in.-OD by 0.495-in.-ID tubes at an extrusion ratio of 17.4 to 1 based on the tooling dimensions. The billets were designed to simulate the extrusion of the final 1.75-in.-OD Zircaloy-2-clad thorium-uranium alloy tubes. The pilot billets were vacuum sealed in copper cans, lubricated with Ficks 604 and graphite, and preheated at 760°C for 4 hr prior to extrusion. Evaluation of the extruded half-size Zircaloy-clad thorium–uranium alloy tubes indicated that cladding uniformity was extremely good. Variation in cladding thickness was about ±0.0005 in., indicating that as-cast machined billets may be used without primary working. Cladding-core interfaces were clean, and bonding was complete. Additions of 1 wt.% zirconium to the thorium–2.5 wt.% uranium alloy core material did not show a significant effect on the extrusion force at 760°C preheat temperature.

In later efforts at Hanford,[26] the pilot runs on 0.875-in.-OD tubes were scaled up to the full size of 1.75-in.-OD by 1.05-in.-ID tubes. Preliminary information indicates that coextrusion of the full-size Zircaloy-2-clad thorium–2.5 wt.% uranium–1 wt.% zirconium alloy tubes was successful.

In work on the development of the Dynapak extrusion technique at Argonne,[27] the high degree of wall rippling in a series of 15 extrusions was greatly reduced by placing a metal core in the extrusion billet, with the gap between the core and the billet wall filled with a metal powder. Extrusions of the modified billets have included copper jackets with copper cores, and Zircaloy-2 jackets with copper, Armco iron, and Zircaloy-2 cores.

Canning

A method for compacting a powder in a metal container is described in a recent patent.[28] The container is vibrated above and below its resonant frequency, and the frequency of vibration is cycled several times through the resonant frequency. It is claimed that this compensates for the change in resonant frequency caused by densification of the powder in the container and permits higher densities to be achieved.

Progress in vibratory compaction of UO_2 fuel elements was reported by Du Pont.[29] Arc-fused UO_2 was vibrationally compacted to as high as 93.4% density inside a stainless-steel sheath tube. Selected particle sizes were used, and the assembly was vibrated axially in the frequency range of 300 to 1500 cps. The same blend of UO_2 particle sizes was compacted to 87.5% density within the annulus between two

concentric stainless-steel sheath tubes. The effects of particle-size distribution, compaction procedure, sheath thickness, and fuel-element shape on the maximum obtainable density were investigated.

Vibratory-compaction experiments have continued to show good results with regard to powder densification and process reproducibility in recent studies at Combustion Engineering.[30] Stainless-steel tubes filled with fused depleted UO_2 were vibratory compacted to densities of 85 to 88% and subsequently cold swaged from 6 to 12%. Visual examination after swaging revealed neither wrinkles, fins, nor cracks in the cladding.

Progress in the vibrational compaction of UO_2-PuO_2 fuel rods has been reported by Hanford.[31] Densities of from 85 to 90% were achieved. An incremental loading device was used to control the PuO_2 dispersion to within ±5% of the nominal composition. It was found that rods loaded with 140 increments of coarse, medium, and fine particles have much more uniform PuO_2 distribution than rods loaded with 80 increments.

Studies at General Electric[32] have indicated that high-density UO_2 powder particles, such as are obtained from arc-fused powder, have been consistently packed to 88 ± 1% of theoretical density using vibratory-compaction techniques. It is necessary to use certain rules of powder particle-size combinations to achieve optimum results. In general, at least three sizes of particles, 60 wt.% coarse, 20 wt.% medium, and 20 wt.% fine, are required. The particle-size ratios are roughly in the order of 64:8:1.

Recently released reports[18,33] that cover the symposium on powder-packed uranium dioxide fuel elements discuss the present status of vibrational-compaction techniques. Process variables are discussed as to their influence on maximum density and uniformity of density over an extended length.

A method was described in a recent British patent[34] for producing canned reactor-fuel elements with a molten heat-transfer metal between the can and fuel sections. The method requires loading the fuel sections with interposed solid disks of the heat-transfer metal into the can and heating the can from bottom to top. To assure that the air escapes from the can during melting, the can is vibrated while a reduced pressure is maintained inside.

(E. G. Smith)

Nonelectrolytic Chemical-Plating Techniques

The categories of information covered in this review include chemical transport of materials, preparation of solid materials in bulk form and as thin films, overlay coatings, and diffusion coatings.

Three imporant publications[35–37] outlined current theories regarding the vapor transport of solids. Study of these publications should be helpful to those utilizing chemical vapor deposition as a process tool.

A paper[38] that contains an extensive review and a report of experimental work on the use of the van Arkel–de Boer method of preparing high-purity metals in massive form was published. Exploratory studies[39] were made of the utility of anhydrous ammonia, water vapor, oxygen, and hydrogen sulfide as catalysts in the deposition of nickel from thermally decomposed nickel carbonyl. Mixtures that contain hydrogen sulfide and water vapor or oxygen were found most effective. Small samples of isotopic titanium and zirconium in the form of ductile rods 1 in. long and weighing 1 to 2 g each were prepared by a two-step iodide-refining process.[40] The source materials were prepared by calcium reduction of the separated oxides of Ti^{46}, Ti^{47}, Ti^{48}, Ti^{49}, Ti^{50}, Zr^{90}, Zr^{91}, Zr^{92}, and Zr^{94}. Thin foils of a large number of elements for use as nuclear particle targets were prepared by chemical vapor deposition.[41]

Overlay chemical vapor-deposited coatings of chromium were laid down on copper rods and nickel tubes by thermal decompostion of chromium dicumene. Argon and hydrogen were used as carrier gases.[42]

Reviews of current methods of producing diffusion type coatings were presented,[43,44] and a study of the mechanism of siliciding was reported.[45] Pack methods received the greatest amount of attention. A diffusion coating process for metals of the group molybdenum, niobium, tungsten, rhenium, vanadium, and tantalum, and their mixtures and alloys, was patented.[46] Investigations were reported for pack cementation of tantalum-base alloys,[47] composite metal-silicide coatings on tungsten sheet,[48] and a two-cycle cementation process for a special substrate.[49] The general problems of evaluating silicide-coated specimens were discussed.[50] Analysis of the effects of processing variables on the frequency of occurrence of microcracks in silicide coatings was made.[51] In general,

pack-deposited silicon does not fill in microcrack fissures. Evaluation of the effect of stepwise, isothermal pack coating on composite reliability is under way. Molybdenum-alloy parts up to 36 by 48 by 72 in. are being coated in a pack-cementation process.[52]

(E. M. Sherwood)

Ceramic Coatings

A method for protecting graphite, molybdenum, and molybdenum alloys for use at high temperature is claimed in a British patent.[53] A first coat of one or more oxides of beryllium, chromium, zirconium, titanium, or nickel is flame sprayed on the substrate. One of these metals is then sprayed on, and the coated piece is heated at a high temperature to fuse the metal and produce an impermeable layer. A third coating that has the same composition as the first may then be applied. (B. W. King)

Welding and Brazing

The users of stainless-steel tubing who usually prefer the seamless type because of the nonuniform properties of welded tubing should now be encouraged by a newly developed technique. Davies and Steer[54] eliminate the differences between the structural and mechanical properties of butt welds and the parent metal by a carefully controlled combination of cold work and heat-treatment. Seamed, titanium-stabilized, type 18-8 stainelss-steel tubing with a wall thickness of 0.032 in., which showed no signs of the weld, was made by being cold reduced between 15 and 32%, annealed at 1920°F for 15 min, and then quenched in oil.

A method of producing SAP aluminum products that have improved weldability and greater elevated-temperature stability is reported.[55] Vacuum-pressing techniques that permit the reduction of the hydrogen content from 50 ppm to 1 to 2 ppm are responsible. Also reported is a new hot-pressure-welding method for SAP.

If friction welding continues to receive the attention given it by Hazlett,[56] this welding method should soon become useful to the fabricators of reactor components. Narrow weld and heat-affected zones are obtained by the utilization of high rotation speeds and lower axial pressures than reported by Russian investigators. For this reason, the method is attractive for welding dissimilar metals. Hazlett has determined the welding parameters for joining 0.25-in.-diameter rods of the dissimilar combinations: zirconium to mild steel, zirconium to stainless steel, and nickel to magnesium. The order of welding difficulty increases as the hot strength of one of the two metals increases.

Some concern has been shown when electron-beam welds in nickel-free Zircaloy-2 had a greater as-welded weight gain on testing than the normal unwelded material. Bettis[57] has begun a study of the problem. Early results indicate that an anneal at 1400°F helps the situation. Annealing removes beta needles (Widmanstätten) from the microstructure and produces an all-alpha structure. Isakoff and Hood[58] at Savannah River have shown that the strength of welded Zircaloy fuel rods is not adversely affected by irradiation. The rupture load was actually increased. No comment on properties such as ductility was made, however.

The Bureau of Mines[59] found the alloy systems niobium-titanium-vanadium, niobium-chromium-aluminum-titanium, and niobium-vanadium suitable for joining niobium and niobium alloys.

Aerojet-General[60] has published a final report that includes a description of the joining of tungsten to graphite by the diffusion brazing technique. A 50 wt.% chromium–5 wt.% nickel brazing-alloy powder was employed to braze joints at 2500°F, which, after a diffusion treatment, did not remelt at 5000°F. Pure nickel, 62 wt.% palladium–38 wt.% chromium, and a system of interleaved nickel and tantalum foils also were studied, but the remelt temperatures obtained were not encouraging.

Experiences in the spot welding and fusion welding of the niobium alloys F-48 and FS-82 were reported by McDonnell Aircraft.[61] They were not able to obtain ductile fusion welds in the F-48, but the FS-82 was successfully welded. Inert atmospheres of 99.995% purity and −65°F maximum dew point were required. Acceptable welds were annealed (10^{-4} mm Hg at 2200°F) to provide stress relief and better ductility.

When F-48 sheets were spot welded in thicknesses between 0.012 and 0.080 in., welding procedures that provided a diffusion recrystallization type joint gave better properties than did the cast-nugget type. The tensile strengths of recrystallized spot welds were 30% higher than those of cast-nugget welds. Preheating and low pressures were used to

minimize cracking. Nonuniform surface conditions and other material variables greatly influenced the spot-welding procedure. Specifications for both spot welding and fusion welding of niobium alloys are reported, as are schedules for resistance welding of F-48.

Work on the development of high-temperature sandwich structures is in progress by several organizations. Lockheed will use pure molybdenum for the facings and Inconel 702 for the core. They expect to braze, initially, with palladium-gold alloys. Northrup will use quartz-lamp radiant-heat brazing to produce all-molybdenum and all-niobium structures. Northrup reports successful diffusion bonding of TZM molybdenum alloy with titanium foil as an intermediate. On D-36 niobium alloy, zirconium foil was used. The diffusion temperature was 1500°F. The niobium alloy was also successfully brazed with titanium–13 wt.% vanadium–11 wt.% chromium–3 wt.% aluminum alloy as the filler metal.

Solar Aircraft is beginning experimentation on the joining of refractory-metal foils. The niobium alloys D-36 and B-66 and the TZM molybdenum alloy are included in this study. The objective is to develop joints that are compatible with protective coatings.

Titanium–13 wt.% vanadium–11 wt.% chromium–3 wt.% aluminum was chosen in preference to commercially pure titanium by Martin-Marietta for brazing the D-36 niobium alloy. The alloy produced better fillets with fewer voids in the joints of honeycomb structures than did pure titanium. Resistance spot welding is being used to fabricate experimental D-36 niobium-alloy honeycomb cores; electron-beam welding is used to make TZM cores.

(R. M. Evans)

Explosive Forming

High-energy impaction refers to a process for producing ultrahigh-density fuel particles from UO_2 and other refractory nuclear materials by (1) impaction to ultrahigh density and (2) impaction followed by heat-treating.

A 12 wt.% cobalt–88 wt.% tungsten carbide punch was used by Hanford[62] to compact UO_2 under impact pressures in the range of 100,000 to 300,000 psi. As-compacted UO_2 densities in the 100,000- to 300,000-psi range varied from 8.4 to 10.6 g/cm^3. Subsequent sintering of these samples, however, increased the density to 10.8 g/cm^3 in all cases.

A vertical model 1220B Dynapak machine was used to compact 4-in.-diameter by 6-in.-long stainless-steel cans that contained 10 lb of UO_2 at 1100°C and 150,000 psi; an energy release of 145,000 ft-lb was used. After cans were impacted, crushed to –4 mesh, and heated at 1700°C for 12 hr, a density of >99% of theoretical was achieved.

Micronized $UO_{2.09}$ was directly impacted at 1100 to 1200°C in evacuated type 310 stainless-steel cans at 250,000 to 400,000 psi with the use of a 25 wt.% cobalt–bonded tungsten carbide die. The as-compacted oxygen-to-uranium ratio was 2.03 to 2.04; however, this was reduced by hydrogen treatment at 1000°C to <2.01.

The diameter of the specimen container, which can be compacted by the high-energy modified Bridgman anvil technique at 1100°C and 500,000 psi, has been successfully increased from 1 to 2 in.[63] Several types of powder mixtures, UN, UO_2, UO_2–40 mole % ZrO_2, and UO_2-uranium have been compacted by high-energy impaction to 14.25 g/cm^3 (99.5% of the theoretical density), 10.92 g/cm^3 (94.4% of the theoretical density), and 10.86 g/cm^3, respectively.

Tungsten carbide dies have been very useful in high-energy impaction of powders, since they can withstand higher pressures than conventional tool-steel dies. It has been found that a 12 wt.% cobalt–bonded tungsten carbide punch was capable of withstanding impact pressures of 300,000 to 350,000 psi; however, it failed at 390,000 psi. A 25 wt.% cobalt–bonded tungsten carbide punch has been used successfully to compact UO_2 at 408,000 psi to a particle density of 10.78 g/cm^3. The use of the cobalt-bonded tungsten carbide makes it possible to compact UO_2 by high-energy impaction to ultrahigh density without subsequent sintering, as required when tool-steel dies are used, and without using expendable die parts such as are required when using the Bridgman anvil technique.

Yttrium oxide powder has also been compacted by high-energy impaction at 1100°C and 200,000 psi to a density of 4.36 g/cm^3 (90% of the theoretical density).

The high-energy compaction of UO_2 has continued at Hanford.[64] Electrodeposited –20-mesh $UO_{2.015}$ (10.17 g/cm^3 particle density) has been

consolidated in 3-lb batches at 1200°C and 325,000-psi impact pressure. The compacted material showed a density of 10.84 g/cm^3 and an oxygen-to-uranium ratio of 2.006.

Sintered UO_2 scrap has also been converted to a dense solid (10.80 g/cm^3). Two high-energy-rate techniques were used. The first technique consisted in crushing, ball milling for 48 hr, and compacting at 1200°C and 380,000 psi. The second consisted in crushing to −20 mesh, roasting for 16 hr at 140°C, compacting at 900°C and 200,000 psi, and sintering for 12 hr at 1700°C.

The effects of temperature, heating rate, and soaking time on UO_2 that has a density of 10.17 g/cm^3 have been investigated. It was found that a reduction in the heating rate from 225 to 75°C/hr, an increase in sintering temperature from 1400 to 1750°C, and an increase in soaking time from 1 to 12 hr resulted in an increase in density. Further densification of this type of UO_2 can be accomplished by using a heating rate of 100°C/hr to 1750°C and holding for 4 hr at that temperature.

A 50 wt.% −325-mesh tungsten−50 wt.% −65-mesh UO_2 mixture has also been compacted by high-energy techniques to 13.44 g/cm^3 (96% of the theoretical density). The blended and evacuated mixture was compacted at 1100°C and 250,000-psi impact pressure. The resulting cermet possessed a continuous tungsten phase.

A method of high-speed stereophotography has been developed in which the basic principles of contour mapping by aerial photography are used.[65] This technique can be used to study the explosive forming of metal parts. An actual operation, the explosive free-forming of an aluminum plate, is discussed. The data obtained establish the feasibility of the processes; however, these data have not been analyzed in terms of actual operations. This type of analysis will form the basis for future reports.

A book covering the proceedings of a technical conference concerning the response of metals to high-velocity deformation has been published by the American Institute of Mining, Metallurgical, and Petroleum Engineers.[66] Primary emphasis is directed toward the deformation mechanism that results from high-pressure shock waves. The techniques and equipment used in analyzing deformation are also discussed. The major problems impeding understanding of these effects and experimental results are analyzed. (C. C. Simons)

Nondestructive Testing

Ultrasonic Techniques

Potentially one of the most useful ultrasonic image-conversion systems is one known as charge scanning. This system has been investigated rather extensively over the past 15 years. In work with units of this type at Northwestern University, the image is displayed by means of a 729-line interlaced closed-circuit television system at a rate[67] of 30 frames/sec.

Argonne[27,68] is assembling an ultrasonic imaging system patterned after the system now in use at Northwestern. A life test on one sealed-off ultrasonic pickup tube that has a 2-in.-diameter, 2-Mc quartz target has exceeded 1000 hr. In a second life test, another tube is reported to have good electron emission and shows no signs of excess gassing.

(D. Ensminger)

NDT Techniques Other Than Ultrasonic

Hanford[69] has worked out an eddy-current method to measure the annular spacing between a fuel-channel process tube and its surrounding shroud tube in the Plutonium Recycle Test Reactor. Direct access to the annulus is not possible, and the measurement is made by traversing the inside of the inner Zircaloy-2 tube with a sensing probe. Eddy currents are coupled inductively through the relatively thick-walled Zircaloy tube to sense displacements of the outer aluminum tube. The probe has four sensing coils mounted at 90° to one another. This probe has been operated successfully in the radiation environment inside the reactor during shutdown. Tube-to-tube displacements can be measured to an accuracy of ±0.0002 in. throughout the 0.550-in. range. This requires, of course, that the inner wall thickness be constant. Under ideal conditions it is reported that displacements as small as 0.0005 in. can be detected.

The high-speed 3000 Polaroid film has an emulsion speed comparable with the conventional medium-speed X-ray films. It is possible to obtain a finished radiograph in a matter of seconds after exposure. Argonne indicated[70] that Polaroid film was tested to determine exposure charts, emulsion characteristic curves, resolution, and sensitivity, although no data were

given. This information made it possible for Argonne to use this film for rapid inspections. (C. Seale)

References

1. Nuclear Metals, Inc., Fundamental and Applied Research and Development in Metallurgy, USAEC Report NMI-2109, Oct. 29, 1962.
2. P. R. Mundinger, H. H. Hausner, and W. H. Lenz, The Application of Ultra-fine Particles in Tungsten Powder Metallurgy, USAEC Report LAMS-2736, Los Alamos Scientific Laboratory, July 1962.
3. A. E. Riesen, Tungsten Extrusion Development Program, Interim Technical Engineering Report, April 20–June 20, 1962, Report ASD-TR-7-793 (IV), Wah Chang Corporation.
4. G. A. Reimann, Vacuum Arc Melting of a Tungsten Alloy (Tungsten-Molybdenum-Columbium), Report ASD-TDR-62-781, Westinghouse Electric Corp., July 1962.
5. Nuclear Metals, Inc., Fundamental and Applied Research and Development in Metallurgy, USAEC Report NMI-2107, July 31, 1962.
6. T. L. Robertshaw, M. A. Levinstein, and J. Pugh, Powder Metallurgy of Columbium, Report ASD-TR-61-559, General Electric Company, Flight Propulsion Laboratory Department, November 1961.
7. Ames Laboratory, Annual Summary Research Report in Chemistry, Engineering, Metallurgy and Physics, July 1, 1961–June 30, 1962, USAEC Report IS-500, September 1962.
8. R. Burgett (Ed.), Summary Technical Report (on Feed Materials) for the Period July 1–September 30, 1962, USAEC Report NLCO-860, National Lead Co. of Ohio, Oct. 31, 1962.
9. H. Davis and J. F. Schiltz, Three-Roll Rotary-Piercing Operation for the Fabrication of Uranium Tubes, USAEC Report NLCO-857, National Lead Co. of Ohio, Oct. 5, 1962.
10. Bridgeport Brass Company, Process Development Summary, January–December, 1961, USAEC Report BRB-68, Sept. 18, 1962. (Classified)
11. G. W. Gibson and W. C. Francis, Annual Progress Report on Fuel Element Development for Fiscal Year 1962, USAEC Report IDO-16799, Phillips Petroleum Co., Aug. 15, 1962.
12. S. Isserow, R. W. Anderson, D. M. Davis, W. L. Larson, and A. B. Bremer, Power Reactor Program, Progress Report to Savannah River Operations Office, USAEC for the Period November 1–November 30, 1962, USAEC Report NMI-7257, Nuclear Metals, Inc., Dec. 27, 1962.
13. Hanford Atomic Products Operation, Fuels Development Operation Quarterly Progress Report, July–September 1962, USAEC Report HW-74378, Oct. 15, 1962. (Classified)
14. Hanford Atomic Products Operation, Plutonium Metallurgy Operation Quarterly Progress Report, April–June 1962, USAEC Report HW-74162, July 16, 1962. (Classified)
15. Hanford Atomic Products Operation, Plutonium Metallurgy Operation Quarterly Progress Report, July–September 1962, USAEC Report HW-74718, Oct. 15, 1962. (Classified)
16. S. J. Paprocki and S. W. Porembka (Eds.), Joining Zircaloy–Stainless Steel and SAP Alloys by Friction, Rolling, and Explosive Techniques, USAEC Report BMI-1594, Battelle Memorial Institute, Sept. 4, 1962.
17. W. V. Cummings, D. R. Lewis, and R. E. Blood, Examination of 304 Stainless Steel Cladding from Cold-Swaged and Rolled Fuel Rods, USAEC Report GEAP-3997, Vallecitos Atomic Laboratory, July 1962.
18. Combustion Engineering, Inc., Symposium on Powder Packed Uranium Dioxide Fuel Elements, November 30–December 1, 1961, Vol. 1, USAEC Report CEND-153 (Vol. I).
19. H. Bairiot, UO_2 Compaction by Swaging, USAEC-EURATOM Report EURAEC-281, Centre d'Étude de l'Energie Nucléaire and Société Belge pour l'Industrie Nucléaire, Brussels, Nov. 30, 1961.
20. Swaging of Uranium Dioxide. Quarterly Progress Report No. 7. January 1–March 31, 1962, USAEC-EURATOM Report EURAEC-310, FIAT. Sezione Energia Nucleare, Turin, Apr. 30, 1962.
21. C. M. Ryer, Powder Fuel Processing by Two-Pass Swaging. The Effect of Particle Size and Distribution, USAEC Report GEAP-3891, Vallecitos Atomic Laboratory, Apr. 10, 1962.
22. B. E. Murtha and W. P. Chernock, The Development and Testing of UO_2 Fuel Systems for Water Reactor Applications. Quarterly Report No. 2, October–December 1961, USAEC Report CEND-152, Combustion Engineering, Inc., January 1962.
23. Nuclear Fuels and Materials Development, USAEC Report TID-11295 (2nd ed.), September 1962.
24. W. R. Young and J. W. Clark, Investigation of the Physical Metallurgy of Joining Tungsten and Columbium, Quarterly Progress Report No. 6, May 1, 1962–August 1, 1962, Report NP-12144, General Electric Company, Flight Propulsion Laboratory Department, Aug. 31, 1962.
25. General Electric Company, Flight Propulsion Laboratory Department, High-Temperature Materials Program Progress Report No. 15, Part A, USAEC Report GEMP-15A, Sept. 14, 1962.
26. Hanford Atomic Products Operation, Reactor and Fuels Laboratory Monthly Report, February 1963, USAEC Report HW-76596A, Mar. 15, 1963. (Classified)
27. Argonne National Laboratory, Reactor Development Program Progress Report, USAEC Report ANL-6698, February 1963.
28. J. J. Hauth, *Vibration Compaction*, U. S. Patent 3,042,594 (to USAEC), July 3, 1962.

29. H. G. Marsh, Fabrication of UO_2 Fuel Elements by Vibrational Compaction, USAEC Report DP-681, E. I. du Pont de Nemours & Co., Inc., February 1962.
30. Combustion Engineering, Inc., The Development and Testing of the UO_2 Fuel Element System. Quarterly Report, December 1, 1960–February 28, 1961, USAEC Report CEND-122, March 1961.
31. Hanford Atomic Products Operation, Research and Development Programs Executed for the Division of Reactor Development, Quarterly Progress Report, April–June 1962, USAEC Report HW-74761, Nov. 15, 1962.
32. W. R. DeHollander, Vibrational Compaction of Uranium Dioxide, USAEC Report GEAP-4032, Vallecitos Atomic Laboratory, Mar. 1, 1962.
33. Combustion Engineering, Inc., Symposium on Powder Packed Uranium Dioxide Fuel Elements, November 30–December 1, 1961, USAEC Report CEND-153 (Vol. II), November 1962.
34. A. C. Winter and O. Erikson, *Methods of Producing Canned Fuel Elements for Nuclear Reactors*, British Patent 908,857, Oct. 24, 1962.
35. R. Lever, Multiple Reaction Vapor Transport of Solids, *J. Chem. Phys.*, 37(5): 1078-1081 (Sept. 1, 1962).
36. R. Lever, Transport of Solids Through the Gas Phase Using a Single Heterogeneous Equilibrium, *J. Chem. Phys.*, 37(6): 1174-1176 (Sept. 15, 1962).
37. G. Mandel, Multiple Reaction Vapor Transport of Solids, *J. Chem. Phys.*, 37(6): 1177-1180 (Sept. 15, 1962).
38. M. L. Rodriguez and J. T. Martorell, New Contribution to the Method of Van Arkel for the Purification of Metals on Incandescent Filaments, Spanish Report JEN 102–DMe/I-9, 1962.
39. W. E. Tewes, T. E. Zava, and T. B. Hoover, Catalytic Gas Plating with Nickel Carbonyl, USAEC Report K-1533, Oak Ridge Gaseous Diffusion Plant, Nov. 23, 1962.
40. N. Veigel and J. M. Blocher, Jr., Preparation of Small Samples of Ductile Titanium and Zirconium from the Isotopic Oxides by Iodide Refining, *J. Electrochem. Soc.*, 109(7): 647-648 (July 1, 1962).
41. L. D. F. Allen, Preparation of Foils for Nuclear Particle Targets, USAEC Report LA-2769, Los Alamos Scientific Laboratory, September 1962.
42. W. H. Metzger, Jr., Chromium Plating by Thermal Decomposition of Chromium Dicumene, *Plating*, 49(1): 1176 (November 1962).
43. R. B. Puyear, High-Temperature Metallic Coatings, *Machine Design*, 34: 176-184 (July 19, 1962).
44. P. King, Protecting Refractory Metals with Diffusion Coating, *Prod. Eng.*, 33: 63-67 (June 25, 1962).
45. V. K. Titov and E. F. Makarov, Mechanism of Metal Siliconization, *Dopovidi Akad. Nauk Ukr. RSR*, (1): 50-53 (1961).
46. R. L. Wachtell, *Diffusion Coating of Nonferrous Metals*, U. S. Patent 3,037,833 (to Chromalloy Corporation), June 5, 1962.
47. L. Sama, High-Temperature Oxidation-Resistant Coatings for Tantalum Base Alloys, Third Quarterly Progress Report, May 1, 1962–July 31, 1962, Report NP-11990, General Telephone and Electronics Laboratories, Inc., Aug. 20, 1962.
48. H. Nolting, Oxidation Resistant High Temperature Protective Coatings for Tungsten, Sixth Quarterly Progress Report, August 1, 1962 to October 31, 1962, Report TM-3543-67, Thompson Ramo Wooldridge, Inc., Nov. 15, 1962.
49. University of California, Lawrence Radiation Laboratory, Oct. 4, 1962. (Unpublished)
50. R. Perkins, L. Riedinger, and S. Sokolsky, Problems in the Oxidation Protection of Refractory Metals in Aerospace Applications, *Trans. 7th Symp. on Ballistic Missile Space Technol.*, 1: 429-450 (Oct. 30, 1962).
51. Pratt & Whitney Aircraft Division, Jan. 31, 1963. (Unpublished)
52. G. J. Dormer and P. J. Chao, Manufacturing Methods for High-Temperature Coating of Large Molybdenum Parts, Interim Engineering Report, July 1–October 1, 1962, The Pfaudler Co., A Division of Pfaudler Permutit, Inc.
53. W. E. Stanton, *Improved Method of Protecting Graphite, Molybdenum or Molybdenum Alloy Articles from Oxidation Deterioration and Corrosion*, British Patent 908,181, Oct. 17, 1962.
54. J. M. Davies and C. Steer, Butt Welded Seamed Tubes as a Material for Reactor Components, British Report AERE-M-1125, November 1962.
55. D. Gualaudi and T. Jehenson, Improvements in the Technology of SAP Production for Nuclear Applications, *Met. Ital.*, 54: 291-299 (July 1962).
56. T. H. Hazlett, Properties of Friction Welds Between Dissimilar Metals, *Welding J. (N. Y.)*, 41: 448s-450s (October 1962).
57. Westinghouse Electric Corp., Bettis Atomic Power Laboratory, Pressurized Water Reactor (PWR) Project, Technical Progress Report, October 24–December 23, 1962, USAEC Report WAPD-MRP-101.
58. E. I. du Pont de Nemours & Co., Inc., Heavy Water Moderated Power Reactors. Progress Report, November 1962, USAEC Report DP-805, December 1962.
59. Bureau of Mines, Metallurgical Quarterly Progress Report Number 16 for the Period July 1–September 30, 1962, USAEC Report USBM-U-978.
60. G. K. Hickox, Diffusion Bonding of Tungsten Alloys, Tech. Rep. WAL TR 465.54/4, Final Report No. 0433-01F, for Watertown Arsenal (August 1, 1961–July 31, 1962), Aerojet General Corporation, Nov. 15, 1962.
61. C. W. Neff and R. G. Frank, Refractory Metals Structural Development Program: Structural

Component Design and Fabrication, Vol. IV, Report ASD-TR-61-392 (Vol. IV), McDonnel Aircraft Corp. and General Electric Company, Flight Propulsion Laboratory Department, August 1962.

62. Hanford Atomic Products Operation, August 1962. (Unpublished)
63. Hanford Atomic Products Operation, Reactor and Fuels Research and Development Operation Monthly Report, July 1962, USAEC Report HW-74522A, Aug. 15, 1962. (Classified)
64. Hanford Atomic Products Operation, Reactor and Fuels Research and Development Operation Monthly Report, September 1962, USAEC Report HW-75127A, Oct. 15, 1962. (Classified)
65. R. Gallup and J. Pearson, The Use of High Speed Stereophotography in Explosive Metal Forming, Report NOTS-TP-2698, Naval Ordnance Test Station, July 21, 1961.
66. P. G. Shewmon and V. F. Zackay (Eds.), *Response of Metals to High Velocity Deformation*, Metallurgical Society Conferences, Vol. 9, Interscience Publishers, New York, 1961.
67. J. E. Jacobs, Ultrasonic Image Converters and Cinesonography in Nondestructive Testing, pp. 59-81, *Proceedings of the Symposium on Physics and Nondestructive Testing, Oct. 2-4, 1962.*
68. Argonne National Laboratory, Reactor Development Program Progress Report, January 1963, USAEC Report ANL-6683, Feb. 15, 1963.
69. Hanford Atomic Products Operation, Research and Development Programs Executed for the Division of Reactor Development, Quarterly Progress Report, October–December 1961, USAEC Report HW-73100, May 1, 1962.
70. Argonne National Laboratory, Metallurgy Division Annual Report for 1961, USAEC Report ANL-6516.

LEGAL NOTICE

This document was prepared under the sponsorship of the U. S. Atomic Energy Commission. Neither the United States, nor the Commission, nor any person acting on behalf of the Commission:

A. Makes any warranty or representation, expressed or implied, with respect to the accuracy, completeness, or usefulness of the information contained in this report, or that the use of any information, apparatus, method, or process disclosed in this report may not infringe privately owned rights; or

B. Assumes any liabilities with respect to the use of, or for damages resulting from the use of any information, apparatus, method, or process disclosed in this report.

As used in the above, "person acting on behalf of the Commission" includes any employee or contractor of the Commission, or employee of such contractor, to the extent that such employee or contractor of the Commission, or employee of such contractor prepares, disseminates, or provides access to, any information pursuant to his employment or contract with the Commission, or his employment with such contractor.

* U. S. Government Printing Office: 1963 0-702339 (1)